IFT - UNESP
INSTITUTO DE FÍSICA TEÓRICA

MASTER'S DISSERTATION IFT–D.003/21

Quantum Entanglement in the QCD Dynamical Chiral Symmetry Breaking

Bruno Lopes da Costa

Advisor

Prof. Gastão Inácio Krein

September, 2021

C838q
Costa, Bruno Lopes da
Quantum entanglement in the QCD dynamical chiral symmetry breaking / Bruno Lopes da Costa. – São Paulo, 2021
96 f.

Dissertação (mestrado) – Universidade Estadual Paulista (Unesp), Instituto de Física Teórica (IFT), São Paulo
Orientador: Gastão Inácio Krein

1. Simetria quebrada (Física). 2. Cromodinâmica quântica. 3. Teoria quântica da campos. 4. Informação quântica. I. Título

Sistema de geração automática de fichas catalográficas da Unesp. Biblioteca do Instituto de Física Teórica (IFT), São Paulo. Dados fornecidos pelo autor(a).

To all the people who value academic research

Acknowledgments

To my mom, who gave me all the support that I needed even though I'm very distant, I always feel more confident because of her, and without her I could never start this journey.

To my friends from the undergrad times, especially Isabella and Paulo that are like a second family to me. With you, I know I am never alone and will never be. You made my life better and gave me the strength to continue, thank you!

To my friends from IFT, especially Isabela and Gabriel who are with me since the beginning. It's always good to have people in the same boat to overcome difficulties, and you helped me a lot with that. I will never forget our time together, especially during Advanced Quantum Mechanics.

To my research group: Bárbara, João, Matheus, Pedro, and more recently Eduardo, it's nice to have people to talk about the research all the way through the night sometimes, and you made it possible.

To all the professors that I crossed paths, especially Rodrigo, who taught me the very basic foundations and beleived I could go very far, and CARocha, my first advisor who made it possible for me to enter the academic world.

To my advisor, Gastão, that helped me all the way through since undergrad times. I loved all the patience you had with me and the care you took. I learned a lot from you, you're really my hero and will always be!

To CAPES, that funded the scholarship during my master's degree and made it possible.

"The life that I could still live, I should live, and the thoughts that I could still think, I should think."

Carl G. Jung, *The Red Book: Liber Novus*

Resumo

Conceitos de informação quântica podem trazer novas perpectivas a respeito de fenômenos envolvendo quebra de simetrias. Nesta dissertação, usamos emaranhamento quântico para estudar caracteríticas da quebra dinâmica da simetria quiral (DCSB) na cromodinâmica quântica (QCD). Entre outros efeitos, a DCSB implica na existência de um condensado no vácuo, formado por pares de quarks e antiquarks correlacionados em momentum. Construímos um formalismo baseado na representação de estados coerentes para calcular matrizes densidade e definir medidas de emaranhamento sobre partições do espaço de Fock. Empregamos o formalismo em dois modelos para o vácuo da QCD: o renomado modelo de Nambu–Jona-Lasinio e um modelo que apresenta um função de massa dos quarks dependente do momento, confinamento de cor e liberdade assintótica. Calculamos a entropia de emaranhamento associada aos pares quark-antiquark com momentos correlacionados no vácuo. Encontramos que essa entropia de emaranhamento é finita para uma interação assintoticamente livre, aumenta com a intensidade da DCSB e adquire uma dependência de escala determinada pelo comportamento ultravioleta de função de massa. Os resultados obtidos no contexto de modelos encorajam o uso de conceitos de teoria da informação no estudo da DCSB na QCD.

Palavras Chaves: Emaranhamento Quântico; Quebra de Simetria Quiral; Cromodiâmica Quântica; Modelos de Quark.

Áreas do conhecimento: Física; Mecânica Quântica; Teoria Quântica de Campos; Informação Quântica.

Abstract

Quantum information concepts can bring new perspectives on symmetry-breaking phenomena. In this dissertation, we used quantum entanglement to study features of the dynamical chiral symmetry breaking (DCSB) in quantum chromodynamics (QCD). Among other effects, DCSB entails a condensate in the vacuum, formed by momentum-correlated quark-antiquark pairs. We have set up a formalism based on the coherent state representation to compute density matrices and define entanglement measures over partitions of the Fock space. We used the formalism within two models for the QCD vacuum: the well-known Nambu–Jona-Lasinio (NJL) model and a model featuring a momentum-running quark mass function, color confinement and asymptotic freedom. We computed the entanglement entropy associated with the momentum-correlated quark-antiquark pairs in the vacuum. We found that this entanglement entropy is finite for an asymptotically free interaction, increases with the strength of the DCSB, and acquires a scale dependence determined by the ultraviolet running of the quark mass function. Our results for the models encourage the use of information-theoretic approaches to study DCSB in QCD.

Keywords: Quantum Entanglement; Chiral Symmetry Breaking; Quantum Chromodynamics; Quark Models.

Areas: Physics; Quantum Mechanics; Quantum Field Theory; Quantum Information.

Contents

Chapter 1

Introduction

Unlike classical physics, in quantum mechanics we can have strong correlations between degrees of freedom so that we cannot separate them, meaning that measuring one impacts the other, which we call quantum entanglement. There are many theoretical tools that allow us to quantify entanglement, the most common ones are based on the density matrix formalism, such as the Schmidt entanglement parameter (or Schmidt number) [1] and the entanglement entropy [2]. In fact, the classical and entanglement entropies, at first sight, seem to be the same, but they are much different conceptually: the former is a probabilistic description of an ensemble of many particles that we can't keep track of, and the latter is a measure of the lack of information for a system for which there is no definite state.

Quantum entanglement has been studied in a variety of research fields over the last decades, from quantum computing to quantum field theory. In quantum computing, quantum entanglement can be used to perform computational tasks that in classical information theory seem to be impossible, a feature called quantum supremacy [3], which apparently has been realized recently with a Google processor with programmable superconducting qubits [4]. Quantum entanglement can be used as well in cryptography and teleportation [5, 6, 7]. Among the theoretical and phenomenological applications, it was shown that entanglement measures can be used to identify critical phenomena in, e.g., spin-chain systems, which ends up being analogous to the behavior of entanglement between regions of space in a conformal field theory [8]. Quantum entanglement has also been proved useful to get insight into a variety of many-body problems. An interesting example, closely related to the problem we study in this dissertation, is that quantum entanglement was used to quantify the degree of compositeness of a particle, with a correlation between the deviation from the bosonic canonical commutation relations and the Schmidt entanglement parameter [9, 10]. Recently, a conjecture of quantum systems being restricted to the ones that extremize entanglement is becoming popular. It has been shown that maximizing the entanglement between helicities generated in electromagnetic scattering processes can be seen as constraining the gauge structure of the theory [11]. It was also shown that restricting the S-matrix of a two-fermion scattering process to minimally entangling operators, we can enlarge the flavor symmetry space of fermions [12, 13]. In this dissertation, we focus on entanglement measures to get new perspectives into the phenomenon of dynamical chiral symmetry breaking in Quantum Chromodynamics (QCD).

QCD is the theory of the strong force. It describes the strongly interacting matter making up atomic nuclei and the interior of superdense stars. This matter, at its most fundamental level, consists of quarks and gluons. Quarks and gluons are not observed as free particles, they are permanently confined in the interior of hadrons. Hadrons are a class of subatomic particles that interact via the strong force, like the proton, neutron, and π meson. Presently, six types (or flavors) of quarks are known. Two of them, *up* (u) and *down* (d), have masses of a few MeV and are the main components of the ordinary matter composed of protons and neutrons. The other quark flavors are much heavier than the u and d quarks, they are the *strange* (s), *charm* (c), *bottom* (b), and *top* (t). They are produced in high energy particle collisions and existed in the early universe, they are short-lived and decay into the u and d due to the weak force. QCD is a quantum gauge field theory, with the local gauge group being the $SU(3)$ group [14]. The corresponding gauge field is the gluon field, it carries $SU(3)$ charge in the adjoint (or regular) representation and couples to the quarks, which carry color charge in the fundamental representation of the group.

Presently, there are no discrepancies between QCD predictions and experiments of strongly interacting processes at high energy particle collisions. Such collisions probe quarks and gluons at short relative distances [15]. The predictions come mainly from detailed analytical calculations supported by the asymptotic freedom of QCD [16, 17]. Asymptotic freedom is the property that the coupling among quarks and gluons becomes weak as one probes them at short distances, or large momentum transfers. Asymptotic freedom is due to the gluon self-interactions, that happen due to the non-Abelian nature of the theory. Because the interaction becomes weak at short distances, one can study high-energy processes employing the well known perturbation theory based on an expansion in the coupling constant. On the other hand, for low-energy phenomena, one cannot employ weak-coupling expansions because the coupling among quarks and gluons is not weak in these phenomena. Prominent low energy phenomena are hadron formation and hadron mass generation. The present dissertation concerns the latter.

Hadron mass generation is of particular interest to the problem of understanding the origin of the masses of the protons and neutrons, which comprise most of the visible matter in the universe. The quarks composing the proton and the neutron are the u and d quarks, their masses are of the order of 5 MeV, whereas the mass of the proton is approximately 938 MeV and of the neutron 940 MeV. The minimum quark content of the proton is uud and of the neutron is ddu[1]. Given these facts, how do protons and neutrons acquire their masses from massless gluons and essentially massless quarks? An answer to this question is the phenomenon of dynamical chiral symmetry breaking (DCSB), which we will review in Chapter 4. Chiral symmetry is an approximate symmetry of the QCD Lagrangian in the light u and d quark sector: if the u and d quark massess were exactly zero (and those of the heavier quarks infinitely heavy), the QCD Hamiltonian (or Lagrangian) would be invariant under $SU(2)_L \times SU(2)_R$ transformations of the quark field operators, where R and L refer to left-handed and right-handed. DCSB refers to the phenomenon that the ground state of the theory, the vacuum, does not share with the Hamiltonian the $SU(2)_L \times SU(2)_R$ symmetry. As we explain in Chapter 4, a consequence of this vacuum symmetry breaking is the existence of a *chiral condensate*, given by a correlation function of the scalar quark density in the vacuum state. Such a condensate leads to a picture of the vacuum as a state populated by momentum-correlated quark-antiquark pairs, as we detail in Chapter 5. In addition, quarks moving within such a vacuum are massive and hence break the symmetry of the Hamiltonian. As a result of the symmetry breaking of the vacuum, the π meson (*pion*) arises as Goldstone boson—in the physical world, in which the symmetry is explicitly broken by the small masses of the u and d quarks, the pion is not massless and one refers to it as being a pseudo Goldstone boson, in that its mass is much smaller than the masses of any of the other hadrons composed by the u and d quarks.

This symmetry breaking mass generation mechanism is a lot similar to the spontaneous symmetry breaking mechanism that leads to the phenomenon of

[1] In quantum field theory, properties of bound states as their masses and sizes are obtained from correlation functions of field operators of the constituents. Minimum quark content of a hadron is given by the minimum number of quark and gluon field operators required to define the hadron's quantum numbers.

superconductivity in metals. The possibility that such a mechanism would exist in the strong interactions was first pointed out by Nambu in 1960 [18] and explicitly demonstrated with a relativistic quantum field theory model in the subsequent year [19, 20]. The QCD condensate is akin to the superconducting condensate of Cooper pairs, momentum-correlated electron pairs bound by lattice vibrations (phonons) [21], but the analogy stops here, as in metal superconductivity the Goldstone boson from the spontaneous symmetry breaking combines with the electromagnetic gauge field to produce a massive vector boson, the Anderson plasmon [22].

Confidence that hadron mass generation happens in QCD through Nambu's mechanism comes from a variety of sources [23]. However, the question is not yet fully settled, as the properties of the chiral condensate and the (pseudo) Goldstone bosons (the pions) internal structure are still under scrutiny [24]. The difficulty in settling the question is due to the fact that such a symmetry-breaking mechanism is a nonperturbative phenomenon. The only known first-principles methods to deal with nonpertubative QCD phenomena are lattice QCD [25, 26] and functional methods [27, 28, 29, 30]. Lattice QCD is a numerical method, in which the path integral representation of the generating functional of Euclidean space correlation functions is discretized on a spacetime lattice. The lattice numerical methods are based on large scale Monte Carlo simulations that require the use of supercomputers. Functional methods are formulated in the continuum of spacetime, normally also formulated in Euclidean space and require truncation strategies to break the infinite chain of equations relating the different quark and gluon field correlation functions. These methods also require numerical simulations, albeit much lighter than those used in lattice simulations. On the other hand, much of our present physical understanding of this mass generation mechanism comes from effective field theories, effective models, and approximations in functional methods. Our study is conducted within effective models.

Our study is a first attempt to quantify the amount of entanglement in the quark-antiquark momentum correlations induced by DCSB in the vacuum. More specifically, within a model for the symmetry breaking vacuum, we explore the interrelationship between the strength of the DCSB and the amount of entanglement between quarks and antiquarks. The momentum-correlated quark-antiquark pairs form a natural bipartite system, in that the quark and the antiquark in a pair have opposite momenta and opposite spin projections. As such, one can quantify the amount of entanglement by computing the entanglement entropy obtained from a reduced density matrix of the symmetry-broken vacuum state. The reduced density matrix is obtained from the symmetry-broken vacuum density matrix by a partial trace taken over antiquark momenta and spin. We compute the partial traces employing the coherent state representation of the vacuum density matrix [31]. We employ two effective models to conduct this study: the Nambu–Jona-Lasinio (NJL) model and a chiral quark model defined by a microscopic Hamiltonian inspired in the QCD Hamiltonian in Coulomb gauge [32]—we refer to this model by the acronym CGQH, standing for Coulomb Gauge Quark Hamiltonian. The NJL model is based on a four-fermion contact interaction. The version of the model we use is the transcription to QCD of the pre-QCD model [19, 20]. In the $SU(2)_L \times SU(2)_R$ version of the model, for example, the protons and neutrons of the original model are replaced by the u and d quarks. Since the 1980's the model has been used continuously up to present time to study a variety of low-energy QCD properties; Refs. [33, 34, 35, 36] are thorough reviews on the uses of the model in different QCD problems. The CGQH model is based on a Hamiltonian in that gluonic effects are represented by finite-range interactions that depend only on quark fields. The model Hamiltonian includes an infrared divergent interaction that models the full non-Abelian color Coulomb kernel in QCD. This interaction, in addition to contributing to DCSB, also confines the quarks and antiquarks into color singlet hadronic states. The model Hamiltonian also contains an infrared finite interaction that models transverse-gluon interactions which, among other effects, leads to asymptotic freedom, hyperfine splittings of hadrons masses [37, 38], and plays an important role in hadron-hadron interactions [39, 40].

This dissertation is organized in seven chapters and two appendices, as follows: in Chapter 2, we present the basic quantum information concepts, in particular quantum entanglement, using a simple spin system as an example. Then, we describe methods to quantify entanglement based on the density matrix description of quantum systems, using some of the most common entanglement measures in the literature. Finally we calculate such measures for a system of two bosonic oscillators.

In Chapter 3, we introduce the coherent states description of Fock spaces for both bosonic and fermionic systems. We build up a formalism to perform calculations of entanglement between modes in second-quantized systems that are solvable with a BCS-like[2] variational method. We apply the technique to simple examples of coupled oscillators, as well as analyze the behavior of the entanglement measures we obtain as we change some parameters.

Chapter 4 is dedicated to Quantum Chromodynamics (QCD) and its phenomenology. There, we present aspects of hadronic spectroscopy that motivated the introduction of quark models and then QCD itself based on symmetries. We also discuss the asymptotic freedom at high energies and the non-perturbative regime at low energies, as well as the non-perturbative phenomena of confinement and dynamical chiral symmetry breaking.

In Chapter 5, we detail the NJL model and the CGQH model. For both cases, we use a BCS-like approach to diagonalize the corresponding Hamiltonians and obtain the ground state and the constituent quark masses. This approach allows us to treat the DCSB phenomenon in terms of an explicit construction of the vacuum state in terms of a quark-antiquark condensate, in a way that it becomes possible to obtain entanglement measures between momentum modes using the formalism from Chapter 3.

Chapter 6 contains calculations of entanglement between quark-antiquark momentum modes in the vaccum of the NJL and CGQH models. We use the the NJL model to set up the coherent state formalism of Chapter 3 to compute density matrices of vacuum states populated by momentum-correlated quark-antiquark pairs. We compute partial traces to obtain reduced density matrices and expressions for the Rényi entanglement entropies. We compute the constitutent-quark mass dependence of those entropies and introduce a new criterion for determining the physical vacuum state based on the entropy to energy ratio. Then, we apply the methods developed for the NJL model to the CGQH model. We study the effect of a momentum dependent quark-mass function on the entanglement entropy. We also obtain the entanglement entropy between quark-antiquark momentum modes for the different quark flavors. We study the role played by the current-quark mass explicit symmetry breaking on the entanglement entropy.

In chapter 7, we summarize the results we have obtained and assess their significance. We also discuss prospects for possible future studies based on the same formalism we have built. Finally, Appendix A contains the notations and conventions we have used during the dissertation, whilst Appendix B shows

[2]BCS stands for the Nobel laureates J. Bardeen, L. Cooper and J.R. Schriefer, who presented the first microscopic theory for the phenomenon of superconductivity in metals [41].

results for very recurrent types of Gaussian integrals.

Chapter 2

Short Review on Quantum Entanglement

In quantum systems, correlations between degrees of freedom can be manifested in a different way than the classical ones. The stronger correlations – quantum entanglement – have been used to make quantum computing and to characterize quantum phase transitions and symmetries. In this chapter, we present a brief review on quantum entanglement and some mathematical tools to quantify it. We focus on the most relevant aspects for the present study.

2.1 The Concept of Entanglement

We represent the state of a closed quantum mechanical system by a vector $|\Psi\rangle$ defined in a Hilbert space $\mathcal{H}$. The vector $|\Psi\rangle$ contains all available information on the system and can be used to compute the possible outcomes of measurements of physical observables, the latter being represented by operators in $\mathcal{H}$. We call such a state, that can be represented by a vector $|\Psi\rangle$, a *pure state*. In contrast, it is not always possible to use such a vector to represent the state of an open quantum system, i.e. a system in contact with an environment. In this case, one says that the state of the system is a *mixed state*, or, as we shall see, a state entangled with its environment. Such a situation may also happen when a closed quantum system, associated with a Hilbert space $\mathcal{H}$, is separated into two parts, A and B, to which one associates separate Hilbert spaces, $\mathcal{H}_A$ and $\mathcal{H}_B$, such that :

$$\mathcal{H} = \mathcal{H}_A \otimes \mathcal{H}_B. \tag{2.1}$$

In general, it may not be possible to represent the state of subpart A (or B) by a vector in the subspace $\mathcal{H}_A$ (or $\mathcal{H}_B$). If that is the case, it is a manifestation of what we call quantum entanglement: there's no definite state for the subsystem A a priori, and a measure of an observable defined only in A also affects the subsystem in B.

To illustrate such an effect, take as an example a system of two spin-1/2 particles. A separable state is defined as a state vector in $\mathcal{H}$ that can be constructed by a tensor product of a state in $\mathcal{H}_A$ and another one in $\mathcal{H}_B$. If we use the basis of the projection in the z axis of the spin of each particle to describe our Hilbert subspaces, such state can be written in the general form:

$$|\psi\rangle = (a_1|\uparrow\rangle_A + a_2|\downarrow\rangle_A) \otimes (b_1|\uparrow\rangle_B + b_2|\downarrow\rangle_B)\,, \tag{2.2}$$

where the arrows indicate whether the spin is pointing up or down. Note that a measurement in the spin of the particle A, in this case, does not affect the particle B as, for example:

$$_A\langle\uparrow|\psi\rangle = a_1\,(b_1|\uparrow\rangle_B + b_2|\downarrow\rangle_B)\,. \tag{2.3}$$

However, a state vector of a general two particle spin system can be written as:

$$|\Psi\rangle = c_1|\uparrow\uparrow\rangle + c_2|\uparrow\downarrow\rangle + c_3|\downarrow\uparrow\rangle + c_4|\downarrow\downarrow\rangle, \tag{2.4}$$

where $|\uparrow\uparrow\rangle \equiv |\uparrow\rangle_A \otimes |\uparrow\rangle_B$. The state $|\Psi\rangle$ can only be written in the form of $|\psi\rangle$ in Eq. (2.2) if we have the condition:

$$c_1c_4 = c_2c_3, \tag{2.5}$$

which is not always satisfied. In fact, if we take, e.g., the singlet state (the one with zero total spin), we get that it can't be written as a product:

$$|0,0\rangle = \frac{1}{\sqrt{2}}\,(|\uparrow\downarrow\rangle - |\downarrow\uparrow\rangle) \neq |\psi\rangle\ \forall\{a_1, b_1, a_2, b_2\}. \tag{2.6}$$

where we have the first entry as the total spin and the second as the projection in the z axis. Note that a measurement of particle A's spin in such state affects the B, as we have, for example:

$$_A\langle\uparrow|0,0\rangle = \frac{1}{\sqrt{2}}|\downarrow\rangle_B \tag{2.7}$$

So, after measuring spin up in particle A, the particle B collapses to spin down. Therefore, there is entanglement between the projection in the z axis of the spins of the two particles. We again emphasize that entanglement depends on how we choose the subsystems A and B—to further details on how different choices may result in entanglement or not, one can check, e.g., Ref. [42], still for spin systems, or see Section 2.3 for a different example.

To conclude, we note that there are many possible distributions for the c_i coefficients in the general state of Eq. (2.4) that can't be written as product states in the same Hilbert space partition, and some are closer to separable states than others. In the next section, we're going to present a way to quantify how entangled a quantum system is to its environment, which can also be used to quantify how close a state vector is to a product state.

2.1.1 Density Matrix Description

As we have stated in the previous section, if a system is entangled with its environment (a mixture), we can't write a state vector for it. However, we can still write a mathematical object called density matrix (sometimes called state operator [7]) that contains information on the probabilities to find the system in each possible state. For a general quantum system of D dimensions, the density matrix is defined as:

$$\rho = \sum_{i=1}^{D} \Lambda_i |\psi_i\rangle\langle\psi_i|, \tag{2.8}$$

with the states $|\psi_i\rangle$ formimg a basis to the Hilbert space $\mathcal{H}$. The eigenvalues Λ_i are the probabilities of the system to be found on the states $|\psi_i\rangle$, so they are real numbers and we have the conditions:

$$\sum_{i=1}^{D} \Lambda_i = 1, \quad \Lambda_i \geq 0. \tag{2.9}$$

Then, if the system is in a pure state, we have that:

$$\rho_{pure} = |\psi_i\rangle\langle\psi_i| \tag{2.10}$$

for a given i, which corresponds to $\Lambda_i = 1$ and $\Lambda_j = 0$ for $j \neq i$.

Next, define two Hilbert subspaces $\mathcal{H}_A$ and $\mathcal{H}_B$ such that $\mathcal{H} = \mathcal{H}_A \otimes \mathcal{H}_B$, as in the previous section. We can write a density matrix only for the $\mathcal{H}_A$ subspace by defining the partial trace:

$$\rho_A = \mathrm{Tr}_B \rho = \sum_{i \in B} \langle i|\rho|i\rangle. \tag{2.11}$$

Note that ρ_A depends on how we choose the subsystems A and B, but it doesn't depend on the choice of the basis $|i\rangle$. In order to write down a specific represantation for ρ_A, we then use the Schmidt decomposition: if the overall system is in a pure state, it is always possible [1] to decompose it in separable states for any choice of A and B as:

$$|\Psi\rangle = \sum_{i=1}^{d_s} \sqrt{\lambda_i}|\phi_i\rangle_A \otimes |\phi_i\rangle_B \tag{2.12}$$

where d_S is the dimension of the smaller of the two Hilbert subspaces, called Schmidt number, the number of possible Schmidt modes $|\phi_i\rangle_A \otimes |\phi_i\rangle_B$. This corresponds to diagonalize the reduced density matrix ρ_A, as we can choose the $|\phi_i\rangle_B$ basis to take the partial trace and obtain:

$$\rho_A = \mathrm{diag}(\lambda_1, \ldots, \lambda_{d_S}), \tag{2.13}$$

where the set of eiganvalues λ_i forms a distribution of probabilities that characterizes ρ_A as a density matrix. Then, we can look at ρ_A and see whether it describes a pure state or a mixture. If ρ_A describes a mixture whilst ρ describes a pure state, we then conclude that there's entanglement between the subsystems. If both density matrices describe pure states, then the overall state vector $|\Psi\rangle \in \mathcal{H}$ is separable.

As an example, consider again the singlet state of the previous section. Its total density matrix is given by:

$$\rho = |0,0\rangle\langle 0,0| = \frac{1}{2}\left(|\uparrow\downarrow\rangle\langle\uparrow\downarrow| - |\uparrow\downarrow\rangle\langle\downarrow\uparrow| - |\downarrow\uparrow\rangle\langle\uparrow\downarrow| + |\downarrow\uparrow\rangle\langle\downarrow\uparrow|\right) \tag{2.14}$$

then, if we separate the Hilbert space using the projection in the z axis of the spins, we obtain:

$$\rho_A = {}_B\langle\uparrow|\rho|\uparrow\rangle_B + {}_B\langle\downarrow|\rho|\downarrow\rangle_B = \frac{1}{2}\left(|\uparrow\rangle_{AA}\langle\uparrow| + |\downarrow\rangle_{AA}\langle\downarrow|\right) \tag{2.15}$$

so we end up with a mixture with both probabilities being $1/2$, which does not tell much about the system: it is what we call a maximally entangled state—in the next section, we are going to present ways to quantify it.

2.2 Entanglement Measures

Looking at the set of eigenvalues of a (reduced) density matrix of a system, it is possible to quantify how entangled it is with its compliment. The simplest way to do it is by defining the purity:

$$P = \text{Tr}\rho_A^2 = \sum_{i=1}^{d_S} \lambda_i^2 \leq 1, \tag{2.16}$$

which is equal to 1 if the density matrix ρ_A describes a pure state, and has the minimum value of $1/d_S$ for a flat distribution $\lambda_i = 1/d_S \ \forall i$, which describes a maximally entangled system. We can also define the Schmidt entanglement parameter $\mathcal{K}$ [1], sometimes called just Schmidt number (e.g., in Ref. [9]) that gives, roughly, the number of Schmidt modes that contribute in a non negligible way as:

$$\mathcal{K} = \frac{1}{P}, \tag{2.17}$$

so that, for a system with only one contributing Schmidt mode (pure state), we have $\mathcal{K} = 1$, whilst for a maximally entangled system where λ_i is a constant for all i, we have $\mathcal{K} = d_S$. For the rest of this dissertation, we will refer to this measure as the Schmidt number.

The next relevant entanglement measure is the entanglement entropy, defined as:

$$S_E = -\,\text{Tr}[\rho_A \log \rho_A] = -\sum_{i=1}^{d_S} \lambda_i \log \lambda_i, \tag{2.18}$$

such that it has the same form as the classical Shannon entropy [2]. It has its minimum for a pure state, with $S_E = 0$, and the maximum is for a maximally entangled system, with $S_E = \log d_S$. The relevance of the entanglement entropy is in the fact that it shares some mathematical properties with the classical one, despite conceptually different. In fact, the Shannon entropy can be seen as a measure of how much information we have about the system described in terms of its probabilities, which is, in a sense, similar to what the entanglement entropy is measuring—the difference lies in the fact that, in quantum systems, there's no definite state a priori in a mixture, whilst in the classical we talk about probabilities in an ensamble of many particles that we can't keep track of.

A way to generalize the entanglement entropy is to define the Rényi entropies [43]:

$$S_n = \frac{1}{1-n} \log \text{Tr}\, \rho_A^n, \tag{2.19}$$

which was originally proposed in the 1960's [44] as an extrapolation of the Shannon entropy, but as the entanglement entropy has the same mathematical form, it also works for the latter. Note that, if we take the limit of $n \to 1$, we recover S_E as:

$$\begin{aligned} \lim_{n\to 1} S_n &= -\lim_{n\to 1} \frac{\partial}{\partial n} \log \sum_{i=1}^{d_S} \lambda_i^n \\ &= -\sum_{i=1}^{d_S} \lambda_i \log \lambda_i. \end{aligned} \tag{2.20}$$

This procedure is called the replica trick: in a sense, we work with n copies of the system, ρ_A^n, and then go back to the original. Another property of the Rényi entropies is that higher orders always have smaller absolute values, as:

$$\frac{\partial}{\partial n} S_n \leq 0. \tag{2.21}$$

Moreover, as we have the dependence on the probability distribution through λ_i^n and $n \geq 1$, we have that a change in the set of λ_i that increases any of the Rényi entropies also increases all other S_n, which makes all of them equivalent in terms of comparing how entangled a state is in relation to another, as we shall see next in a simple example.

2.3 A Simple System: Two Bosonic Oscillators

Now we are going to apply the quantum information concepts we have seen to a simple physical system of two interacting bosonic oscillators as in, e.g., Ref. [45], with a Hamiltonian of the kind:

$$H = \frac{1}{2}\left[p_1^2 + p_2^2 + k(x_1^2 + x_2^2) + \lambda(x_1 - x_2)^2\right], \tag{2.22}$$

where, for simplicity, we set the respective masses of the oscillators 1 and 2 as $m_1 = m_2 = 1$ and treat it in 1 spatial dimension. We then note that the transformation

$$x_\pm = (x_1 \pm x_2)/\sqrt{2} \tag{2.23}$$

decouples the Hamiltonian of Eq. (2.22), i.e., it can be written as:

$$H = H_+ + H_-, \tag{2.24}$$

where $H_\pm$ only depends on $x_\pm$ and their conjugate momenta $p_\pm$. As a consequence, the ground state becomes separable in the new variables:

$$\langle x_+ x_- | \Psi_0 \rangle \equiv \Psi_0(x_+, x_-) = \psi_+(x_+)\psi_-(x_-). \tag{2.25}$$

This fact shows that there's no entanglement between the coordinates x_+ and x_-. However, we can proceed to calculate entanglement between the original coordinates x_1 and x_2 and emphasize that it depends on how we separate the Hilbert space. As the Hamiltonian is quadratic in x_+ and x_-, we have the ground state as a double Gaussian:

$$\psi_\pm(x_\pm) = \mathcal{N}_\pm e^{-x_\pm^2/\sigma_\pm^2}, \tag{2.26}$$

in which $\mathcal{N}_\pm$ is a normalization constant which is not important for now and the width of the Gaussians are given in terms of the parameters of the Hamiltonian as:

$$\begin{aligned} \sigma_+^2 &= \frac{2}{\sqrt{k}}, \\ \sigma_-^2 &= \frac{2}{\sqrt{k+2\lambda}}. \end{aligned} \tag{2.27}$$

Having the ground state, we can rewrite it in terms of the original coordinates x_1 and x_2 and get the total density matrix:

$$\rho(x_1, x_2; x_1', x_2') = \langle x_1 x_2 | \Psi_0 \rangle \langle \Psi_0 | x_1' x_2' \rangle = \Psi_0(x_1, x_2)\Psi_0^*(x_1', x_2'), \tag{2.28}$$

with:

$$\Psi_0(x_1, x_2) = \mathcal{N} E(x_1) E(x_2) \, \exp\left[-(\sigma_+^2 - \sigma_-^2) x_1 x_2 / \sigma_+^2 \sigma_-^2\right], \tag{2.29}$$

where we have defined:

$$E(x) \equiv \exp\left[-(\sigma_+^2 + \sigma_-^2) x^2 / 2\sigma_+^2 \sigma_-^2\right]. \tag{2.30}$$

Then, we separate the Hilbert space as $\mathcal{H} = \mathcal{H}_1 \otimes \mathcal{H}_2$, $\mathcal{H}_i$ being the subspace of the position of oscillator i, so we can trace out one of them and write a reduced density matrix for the other:

$$\begin{aligned}\rho_1(x_1,x_1') &= \int_{-\infty}^{+\infty} dx_2\, \rho(x_1,x_2;x_1',x_2) \\ &= \mathcal{N}' E(x_1)E(x_1') \int_{-\infty}^{+\infty} dx_2\, f(x_1,x_1',x_2),\end{aligned} \tag{2.31}$$

with:

$$f(x_1,x_1',x_2) = \exp\left[-(\sigma_+^2+\sigma_-^2)x_2^2/\sigma_+^2\sigma_-^2 + (\sigma_-^2-\sigma_+^2)(x_1+x_1')x_2/\sigma_+^2\sigma_-^2\right]. \tag{2.32}$$

Performing the Gaussian integral, we obtain:

$$\rho_1(x_1,x_1') = \mathcal{N}'' \exp\left[-\alpha(x_1^2+x_1'^2)+\beta x_1 x_1'\right], \tag{2.33}$$

with:

$$\begin{aligned}\alpha &= \frac{1}{4}\Big(\frac{1}{\sigma_+^2}+\frac{1}{\sigma_-^2}+\frac{4}{\sigma_+^2+\sigma_-^2}\Big) \\ \beta &= \frac{1}{2}\Big(\frac{1}{\sigma_+^2}+\frac{1}{\sigma_-^2}-\frac{4}{\sigma_+^2+\sigma_-^2}\Big).\end{aligned} \tag{2.34}$$

To calculate an entanglement measure, we need to find the eigenvalues of the reduced density matrix, that is, the set $\{c_n\}$ such that:

$$\int_{-\infty}^{+\infty} dx_1'\, \rho_1(x_1,x_1') f_n(x_1') = c_n f_n(x_1). \tag{2.35}$$

In general, this is a hard problem and can't be done analytically. However, in this simpler case with a double Gaussian, there's an analytical solution: the eigenfunctions are given in terms of the Hermite polynomials, as in Ref. [46]:

$$f_n(x) = H_n(ax)\, e^{-a^2x^2/2}, \qquad a = \sqrt{\frac{2}{\sigma_+\sigma_-}}, \tag{2.36}$$

with the definition:

$$H_n(x) = (-1)^n e^{x^2}\frac{d^n}{dx^n}e^{-x^2}. \tag{2.37}$$

The corresponding eigenvalues are given by:

$$c_n = (1-z)z^n \tag{2.38}$$

with:

$$z = \left(\frac{\sigma_+ - \sigma_-}{\sigma_+ + \sigma_-}\right)^2. \tag{2.39}$$

Having the eigenvalues of the reduced density matrix, we can easily calculate the Schmidt number as an entenglement measure:

$$\mathcal{K} = \frac{1}{\sum_n c_n^2} = \frac{1}{(1-z)^2 \sum_n z^{2n}} = \frac{1+z}{1-z}, \tag{2.40}$$

which is represented graphically in Fig. 2.1.

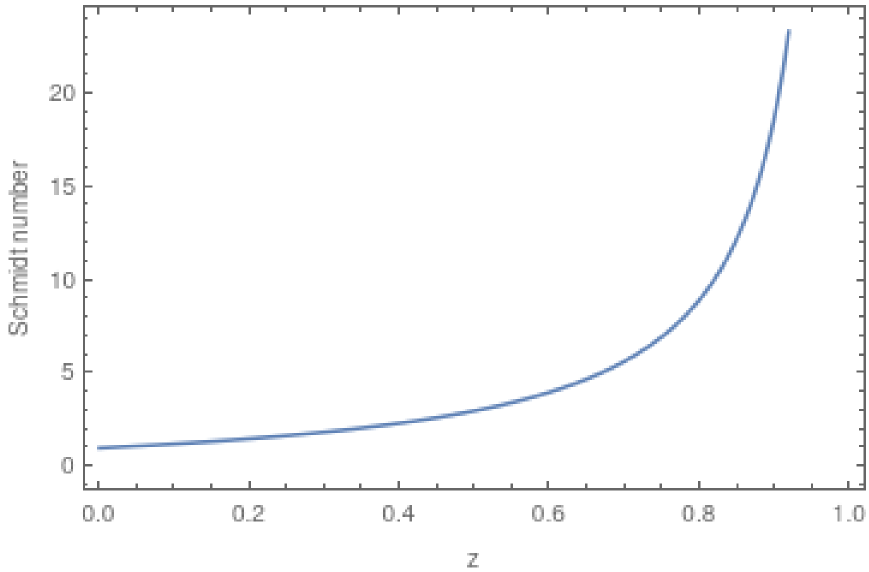

Figure 2.1: Schmidt number for the entanglement between the two oscillators

We notice that, as we turn off the interaction between the oscillators, that is, as we make $\lambda \to 0$, getting $\sigma_+ \to \sigma_-$ and $z \to 0$, we obtain $\mathcal{K} \to 1$, describing a pure state. As we increase λ (keeping k fixed), z grows monotonously to 1 and $\mathcal{K}$ gets arbitrarily high, so the ground state gets more entangled. From that, we see the fact that interaction generates entanglement between the particles in the position space. Further studies, such as Refs. [9] and [10] (the latter for more general systems), use this result to investigate how a system of two particles behaves as an elementary boson depending on how entangled they are with each other. For our study, it suffices to apply the method and concepts.

Another thing that we can easily do for this simple model of two oscillators, as we have the eigenvalues of the reduced density matrix, is to calculate the higher order Rényi entropies and the entanglement entropy. The Rényi entropies are given by:

$$S_n = \frac{1}{1-n} \log \sum_m (1-z)^n (z^n)^m, \tag{2.41}$$

which again is a convergent geometric series that gives:

$$S_n = \frac{1}{1-n} \left[n \log(1-z) - \log(1-z^n) \right]. \tag{2.42}$$

The entanglement entropy can be obtained either directly or by doing the limit:

$$S_E = \lim_{n \to 1} S_n \tag{2.43}$$

which gives $0/0$, so we can use L'Hospital's rule and take the derivative with respect to n to obtain:

$$S_E = -\log(1-z) - \frac{z \log z}{1-z}. \tag{2.44}$$

We then compare the entropies graphically in Fig. 2.2. As we have stated earlier, we see that they are equivalent in the sense that all of them grow as we increase the interaction. We also notice that the entanglement entropy is always higher than the higher order Rényi entropies—we can use this as a consistency check.

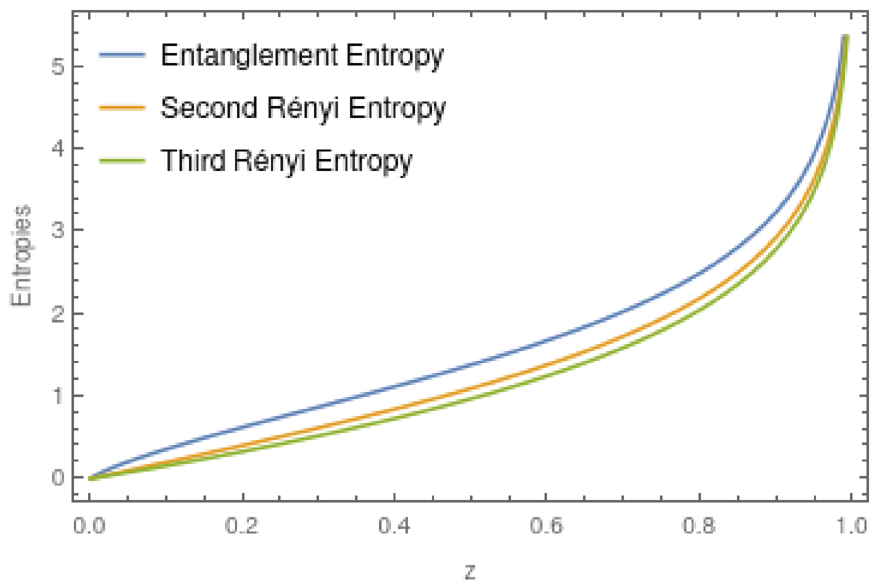

Figure 2.2: Rényi and entanglement entropies as functions of the parameter z

For now, we only see that interaction can generate entanglement. In the next chapters, we are going to present more realistic systems in which we will perform similar calculations and see how such measures can have deeper physical consequences.

Chapter 3

Entanglement Calculations with Coherent States

In order to calculate entanglement measures for the models that we will explore later in this dissertation, we need a different mathematical treatment as there are many degrees of freedom to work with. In this chapter, we will present a handy representation of the Fock space that makes such calculations possible and use it to construct the operations we need, as well as apply it to simple systems.

In the next two sections, we will build up the formalism to describe Fock Spaces using coherent states for bosonic and fermionic systems. Then, in Section 3.3 we apply the formalism to a two-fermion system and in Section 3.4 to a two-boson system

3.1 Bosonic Systems

Suppose we have a system described by creation and annihilation operators $a_k^\dagger$ and a_k such that:

$$[a_k, a_{k'}^\dagger] = \delta_{kk'}, \quad [a_k, a_{k'}] = [a_k^\dagger, a_{k'}^\dagger] = 0, \tag{3.1}$$

where the indices k take value from 1 to N (not necessarily finite). We then define the number operators as:

$$n_k \equiv a_k^\dagger a_k. \tag{3.2}$$

The eigenstates of the n_k are given by:

$$|n_k\rangle = \frac{\left(a_k^\dagger\right)^n}{\sqrt{n!}}|0_k\rangle \tag{3.3}$$

with $|0_k\rangle$ being the eigenstate of n_k with eigenvalue zero, which can be obtained by:

$$a_k|0_k\rangle = 0 \ \forall k, \tag{3.4}$$

and we also define:

$$|0\rangle \equiv \bigotimes_{k=0}^{N} |0_k\rangle. \tag{3.5}$$

With these definitions, we have that the $|n_k\rangle$ are normalized and their eigenvalues are just integer numbers given by n in Eq. (3.3). As all n_k are hermitian operators, the eigenstates of each n_k form a complete set and their span forms a Hilbert space $\mathcal{H}_k$. The Fock space is defined as the direct sum of all these Hilbert spaces, that is:

$$\mathcal{F} \equiv \bigoplus_{k=1}^{N} \mathcal{H}_k, \tag{3.6}$$

with:

$$\mathcal{H}_k = \mathrm{Span}\{|n_k\rangle\}. \tag{3.7}$$

We then define the coherent states as the eigenstates of the annihilation operators, i.e.:

$$a_k|z\rangle = z_k|z\rangle, \tag{3.8}$$

where $|z\rangle$ is a vector living in the Fock space defined as a product of vectors of the Hilbert subspaces:

$$|z\rangle \equiv \bigotimes_{k=1}^{N} |z_k\rangle. \tag{3.9}$$

Such states can be constructed by acting with a function of the creation operators on $|0\rangle$. In order to do that, we note that, for a particular k, we have:

$$[a_k, f(a_k^\dagger)] = \frac{\partial}{\partial a_k^\dagger} f(a_k^\dagger), \tag{3.10}$$

and therefore:

$$a_k f(a_k^\dagger)|0_k\rangle = \frac{\partial}{\partial a_k^\dagger} f(a_k^\dagger)|0_k\rangle. \tag{3.11}$$

With that in hand, the coherent states are given by, up to a normalization constant:

$$|z_k\rangle = e^{z_k a_k^\dagger}|0_k\rangle, \tag{3.12}$$

as we have:

$$\frac{\partial}{\partial a_k^\dagger} e^{z_k a_k^\dagger} = z_k e^{z_k a_k^\dagger}. \tag{3.13}$$

Then, we can construct a resolution of the identity in the Fock space using the states we have just defined as:

$$\mathbb{1} = \int Dz^* Dz \, e^{-z^* \cdot z} |z\rangle\langle z^*|, \tag{3.14}$$

with the notation:

$$z^* \cdot z \equiv \sum_{k=1}^{N} z_k^* z_k, \tag{3.15}$$

and we also have defined the integration measure as:

$$Dz^* Dz \equiv \prod_{k=1}^{N} \left(\frac{dz_k^* dz_k}{2\pi i} \right). \tag{3.16}$$

One can show explicitly [31] that, by integrating over all possible values of z_k^* and z_k, we get, indeed:

$$\int \frac{dz_k^* dz_k}{2\pi i} \, e^{-z_k^* z_k} |z_k\rangle\langle z_k^*| = \sum_{n_k} |n_k\rangle\langle n_k| \tag{3.17}$$

and, as the $|n_k\rangle$ are the eigenstates of an hermitian operator n_k, it is a resolution of the identity in the Hilbert space $\mathcal{H}_k$, and then Eq. (3.14) is indeed the identity in the whole Fock space $\mathcal{F}$.

Defining $|n\rangle$ as a basis to the Fock space, we can take the trace of an operator $\mathcal{O}$ as:

$$\mathrm{Tr}\, \mathcal{O} = \sum_n \langle n|\mathcal{O}|n\rangle. \tag{3.18}$$

As a remark, there's no necessary relation between this basis $|n\rangle$ and the one for the Hilbert subspaces constructed with the eigenstates of the number operators n_k we have just seen. Next, we insert the identity from Eq. (3.14) and obtain:

$$\mathrm{Tr}\, \mathcal{O} = \sum_n \int Dz^* Dz \, e^{-z^* \cdot z} \langle n|z\rangle\langle z^*|\mathcal{O}|n\rangle. \tag{3.19}$$

The matrix elements within the integral are just c-numbers, so we can just commute them to get the combination $\sum_n |n\rangle\langle n|$, which is another resolution of the identity, so we can remove it without changing the result. Therefore, we have an expression to take traces in the coherent states representation:

$$\mathrm{Tr}\,\mathcal{O} = \int Dz^* Dz\, e^{-z^* \cdot z} \mathcal{O}(z^*, z), \tag{3.20}$$

where we have defined:

$$\mathcal{O}(z^*, z') \equiv \langle z^* | \mathcal{O} | z' \rangle. \tag{3.21}$$

This shows that it becomes a lot easier to use the coherent states than trying to construct the same operation with eigenstates of number operators in the Fock space as we increase the number of Hilbert subspaces, as we can see, e.g., in Ref. [47] (there it's done for fermions).

As an extension, one can use this coherent states representation to take partial traces as:

$$\mathrm{Tr}_A \mathcal{O} = \int \prod_{k \in A} \left(\frac{dz_k^* dz_k}{2\pi i} \right) e^{-\sum_{k \in A} z_k^* z_k} {}_A\langle z^* | \mathcal{O} | z \rangle_A, \tag{3.22}$$

where A is an arbitrary subspace of the total Fock space and:

$$|z\rangle_A \equiv \bigotimes_{k \in A} |z_k\rangle. \tag{3.23}$$

The Eq. (3.22) is the important result we are going to use multiple times during calculations, but there are other possibilities in this representation, such as well defined path integrals [31, 48]. Next, we are going to point out the differences when trying to do the same for fermionic systems.

3.2 Fermionic Systems

Now suppose we have a fermionic system described by the creation and annihilation operators that follow the anticommutation relations:

$$\{a_k, a_{k'}^\dagger\} = \delta_{kk'}, \quad \{a_k, a_{k'}\} = \{a_k^\dagger, a_{k'}^\dagger\} = 0. \tag{3.24}$$

As in the bosonic case, we can define the number operators $n_k \equiv a_k^\dagger a_k$ and describe the Hilbert subspaces with their eigenvectors. However, because of the Pauli principle, for fermions, the number operators obey the equation:

$$n_k(1 - n_k) = 0, \tag{3.25}$$

which can be easily checked by noting that $(a_k^\dagger)^2 = 0$. As a consequence, their eigenvalues follow the same equation, which has the solutions $n = \{0, 1\}$, and we have:

$$a_k|0_k\rangle = 0, \quad a_k^\dagger|1_k\rangle = 0, \quad a_k^\dagger|0_k\rangle = |1_k\rangle, \tag{3.26}$$

in a way that one could just exchange a_k with $a_k^\dagger$ and $|0_k\rangle$ with $|1_k\rangle$ and the algebra would be the same.

We can proceed with the same steps as the bosonic case to define the coherent states as:

$$a_k|\xi_k\rangle = \xi_k|\xi_k\rangle. \tag{3.27}$$

However, for this case, the objects ξ_k are not commuting c-numbers anymore, they are anticommuting Grassmann numbers [31]. One can obtain the kind of algebra they obey by first noting that:

$$\{a_k, f(a_k^\dagger)\} = \frac{\partial}{\partial a_k^\dagger} f(a_k^\dagger), \tag{3.28}$$

so the coherent states are constructed in the same way as the bosonic case:

$$|\xi_k\rangle = e^{\xi_k a_k^\dagger}|0_k\rangle. \tag{3.29}$$

One can check [31] that we can make translations to the creation and annihilation operators as:

$$\begin{aligned} e^{-\xi_k a_k^\dagger} a_k e^{\xi_k a_k^\dagger} &= a_k + \xi_k, \\ e^{-\xi_k^* a_k} a_k^\dagger e^{\xi_k^* a_k} &= a_k^\dagger + \xi_k^*. \end{aligned} \tag{3.30}$$

By performing such translations on $\{a_k, a_{k'}^\dagger\}$ from Eq. (3.24), it follows that:

$$\{a_k, a_{k'}^\dagger\} = \{a_k + \xi_k, a_{k'}^\dagger + \xi_{k'}^*\} = \delta_{kk'}, \tag{3.31}$$

which implies:

$$\{\xi_k, a_{k'}^\dagger\} + \{a_k, \xi_{k'}^*\} + \{\xi_k, \xi_{k'}^*\} = 0. \tag{3.32}$$

This is consistent if the numbers ξ_k and ξ_k^* satisfy the following algebra:

$$\{\xi_k, \xi_{k'}\} = \{\xi_k^*, \xi_{k'}^*\} = \{\xi_k, \xi_{k'}^*\} = 0 \tag{3.33}$$

$$\{\xi_k, a_{k'}^\dagger\} = \{\xi_k^*, a_{k'}^\dagger\} = \{\xi_k, a_{k'}\} = \{\xi_k^*, a_{k'}\} = 0. \tag{3.34}$$

Now, to write matrix elements of fermionic operators in a fashion similar to those for bosonic operators, it is convenient to work with Grassmann numbers that commute with the creation and annihilation operators. This can be achieved by defining the operator:

$$\zeta_3 \equiv \prod_{k=1}^{N} [a_k, a_k^\dagger], \tag{3.35}$$

which has the property $\zeta_3^2 = 1$ and anticommutes with all the other objects of the algebra, namely:

$$\{\zeta_3, a_k\} = \{\zeta_3, a_k^\dagger\} = 0, \ \forall k. \tag{3.36}$$

The desired Grassmann numbers, which we denote z_k and z_k^*, are given by

$$\xi_k = \zeta_3 z_k \quad \text{and} \quad \xi_k^* = \zeta_3 z_k^*. \tag{3.37}$$

It is easy to show that the z_k and z_k^* indeed anticommute with themselves:

$$\{z_k, z_{k'}^*\} = \{z_k, z_{k'}\} = \{z_{k'}^*, z_k^*\} = 0, \tag{3.38}$$

and commute with the creation and annihilation operators:

$$[z_k, a_{k'}^\dagger] = [z_k, a_{k'}] = [z_k, a_{k'}^\dagger] = [z_k, a_{k'}] = 0. \tag{3.39}$$

We note that the coherent states are also eigenstates of the operator ζ_3:

$$\zeta_3 |\xi_k\rangle = |\xi_k\rangle. \tag{3.40}$$

With this in hand, we can work only with the z_k Grassmann numbers. We also relabel the coherent states:

$$|\xi_k\rangle \equiv |z_k\rangle \tag{3.41}$$

and note that their conjugate is given by:

$$\left(|z_k\rangle\right)^\dagger = \langle z_k^*|, \tag{3.42}$$

which are the eigenstates of the creation operators. We also define the Fock space vector:

$$|z\rangle \equiv \bigotimes_{k=1}^{N} |z_k\rangle. \tag{3.43}$$

Next, we postulate the Grassmann integration as [31]:

$$\int dz = 0, \quad \int dz\, z = 1. \tag{3.44}$$

These two definitions are enough to integrate any analytic function of Grassmanian numbers, as, if we expand it in power series, there will be only contributions up to the first order on them:

$$f(z) = c_0 + c_1 z + \mathcal{O}(z^2), \; z^2 = 0. \tag{3.45}$$

In particular, the integrals:

$$\int dz_k^* dz_k \, e^{-z_k^* z_k} = 1, \tag{3.46}$$

$$\int dz_k^* dz_k \; z_k \; e^{-z_k^* z_k} = \int dz_k^* dz_k \; z_k^* \; e^{-z_k^* z_k} = 0, \tag{3.47}$$

$$\int dz_k^* dz_k \; z_k z_k^* \; e^{-z_k^* z_k} = 1 \tag{3.48}$$

will be very useful because of the representation of the coherent states in the basis of the number operator eigenstates for a particular Hilbert subspace:

$$|z_k\rangle\langle z_k^*| = |0_k\rangle\langle 0_k| + z_k|1_k\rangle\langle 0_k| + z_k^*|0_k\rangle\langle 1_k| + z_k z_k^*|1_k\rangle\langle 1_k|. \tag{3.49}$$

Therefore, by multiplying with $e^{-z_k^* z_k}$ and integrating over, we obtain:

$$\int dz_k^* dz_k \; e^{-z_k^* z_k} |z\rangle\langle z^*| = \sum_{n=0}^{1} |n_k\rangle\langle n_k| = \mathbb{1}_k, \tag{3.50}$$

so we can write, finally, the realization of the identity in the coherent states representation for a fermionic Fock space:

$$\mathbb{1} = \bigotimes_{k=1}^{N} \mathbb{1}_k = \int Dz^* Dz \; e^{-z^* \cdot z}, \tag{3.51}$$

where we have used the same dot product notation as in the bosonic case and with the integration measure being defined as:

$$Dz^* Dz \equiv \prod_{k=1}^{N} dz_k^* dz_k. \tag{3.52}$$

Now that we have the identity in the coherent states representation, we can proceed to how to take traces using it. As in the bosonic case, we define a basis $\{|n\rangle\}$ to the Fock space, so that the trace is given by:

$$\mathrm{Tr}\,\mathcal{O} = \sum_n \langle n|\mathcal{O}|n\rangle, \tag{3.53}$$

and then we insert the identity, ending up with:

$$\mathrm{Tr}\,\mathcal{O} = \sum_n \int Dz^* Dz\, e^{-z^*\cdot z} \langle n|z\rangle\langle z^*|\mathcal{O}|n\rangle. \tag{3.54}$$

However, the matrix elements within the integral are not necessarily commuting c-numbers (only the product of them must be). If each of them contains an odd number of Grassmann numbers, then they anticommute and we get an overall minus sign when trying to remove the identity $\sum_n |n\rangle\langle n|$. In order to fix it, we note that, under the integral:

$$\langle n|z\rangle\langle z^*|\mathcal{O}|n\rangle = \langle z^*|\mathcal{O}|n\rangle\langle n|-z\rangle, \tag{3.55}$$

which is true because, if $\langle n|$ is constructed by acting with annihilation operators on the state $\langle 0|$, we have that:

$$\langle n|z\rangle = \langle 0|\prod_{k\in A} a_k|z\rangle = \prod_{k\in A} z_k, \tag{3.56}$$

where A is a subset of the possible values of k, the index that denote the corresponding Hilbert subspace. If the subset A contains K elements, then we get a factor of $(-1)^K$ when changing $z_k \to -z_k$. Then, within the integral, the other matrix element must have the corresponding z_k^* factors, or else it would not contribute as we can see by looking at the definitions of Grassmann integration of Eq. (3.44). This means that, when commuting the matrix elements within the integral of Eq. (3.54), we get another factor of $(-1)^K$ canceling out the one that we already had. Therefore, in order to commute the matrix elements, we just need to flip the sign of z, finally getting the expression:

$$\mathrm{Tr}\,\mathcal{O} = \int Dz^* Dz\, e^{-z^*\cdot z}\mathcal{O}(z^*, -z) = \int Dz^* Dz\, e^{-z^*\cdot z}\mathcal{O}(-z^*, z) \tag{3.57}$$

in which the last equality is obtained by noting that the only term that contributes to the integral is the one containing all the pairs $z_k^* z_k$, therefore if we flip both signs it does not change the result. Furthermore, we can also define partial traces for the fermionic case in the same way:

$$\mathrm{Tr}_A \mathcal{O} = \int \prod_{k\in A} dz_k^* dz_k \, e^{-\sum_{k\in A} z_k^* z_k} {}_A\langle -z^* | \mathcal{O} | z \rangle_A, \tag{3.58}$$

where again A is an arbitraty subspace of the total Fock space.

As now we know how to take traces in the coherent states representation, we can proceed to the calculations of entanglement measures using it. Next, we will see how it can be applied to systems of two harmonic oscillators as an example.

3.3 Two Fermionic Oscillators

Consider a system similar to the one from Ref. [49], described by the Hamiltonian:

$$H = \omega \left(a_1^\dagger a_1 + a_2^\dagger a_2 \right) + \lambda \left(a_1^\dagger a_2^\dagger - a_1 a_2 \right), \tag{3.59}$$

where the a operators respect the fermionic anticommutation relations:

$$\{a_i, a_j\} = \{a_i^\dagger, a_j^\dagger\} = 0, \quad \{a_i, a_j^\dagger\} = \delta_{ij}, \tag{3.60}$$

and the relative minus sign in the interaction part is necessary for the total Hamiltonian to be hermitian. Now define the b operators related to the a's via:

$$a_1 = u b_1 + v b_2^\dagger, \quad a_2 = u b_2 - v b_1^\dagger. \tag{3.61}$$

In order for the b operators to obey the same anticommutation relations as the a's, we need to have:

$$u^2 + v^2 = 1, \tag{3.62}$$

which means we can parametrize the transformation with an angle θ, namely:

$$u = \cos\theta, \quad v = \sin\theta. \tag{3.63}$$

Transformations of the type in Eq. (3.61) are known as Bogoliubov-Valatin transofrmations. We now are able write the Hamiltonian in terms of the b operators and the parameter θ:

$$\begin{aligned} H &= (\omega\cos 2\theta - \lambda\sin 2\theta)\,(b_1^\dagger b_1 + b_2^\dagger b_2) \\ &+ (\omega\sin 2\theta + \lambda\cos 2\theta)\,(b_1^\dagger b_2^\dagger - b_1 b_2) + \text{const.} \end{aligned} \tag{3.64}$$

and note that, if we have:

$$\tan 2\theta = -\frac{\lambda}{\omega}, \tag{3.65}$$

the interaction part vanishes and H is diagonalized. In this situation, we can build a variational vacuum, defined as:

$$b_1|\Omega\rangle = b_2|\Omega\rangle = 0 \tag{3.66}$$

which is written in terms of the a operators as:

$$(ua_1 - va_2^\dagger)|\Omega\rangle = (ua_2 + va_1^\dagger)|\Omega\rangle = 0. \tag{3.67}$$

We can construct such relations by imposing:

$$a_1|\Omega\rangle = a_2^\dagger \tan\theta|\Omega\rangle, \;\; a_2|\Omega\rangle = -a_1^\dagger \tan\theta|\Omega\rangle, \tag{3.68}$$

that are satisfied if:

$$|\Omega\rangle = \exp\left\{a_1^\dagger a_2^\dagger \tan\theta\right\}|0\rangle, \tag{3.69}$$

with $|0\rangle$ being defined such that:

$$a_1|0\rangle = a_2|0\rangle = 0. \tag{3.70}$$

Now that we have the variational vacuum, we can write the total density matrix as:

$$\rho = \mathcal{N}|\Omega\rangle\langle\Omega|, \tag{3.71}$$

and then we trace out the a_2 modes using the coherent states representation, namely:

$$\rho_1 = \mathcal{N}\int dz_2^* dz_2\; e^{-z_2^* z_2}\langle -z_2^*|\Omega\rangle\langle\Omega|z_2\rangle \tag{3.72}$$

where z_2 is the eigenvalue of a_2, which is a Grassmann number as we have seen in the previous section. The matrix elemtents of ρ_1 in the coherent states representation are, then, given by:

$$\begin{aligned} \rho_1(z_1^*, z_1') &\equiv \langle z_1^*|\rho_1|z_1'\rangle \\ &= \mathcal{N} \int dz_2^* dz_2 \ \exp\left(-z_2^* z_2 - z_1^* z_2^* \tan\theta + z_2 z_1' \tan\theta\right). \end{aligned} \tag{3.73}$$

Performing the Gaussian integral as in Appendix B, it becomes:

$$\rho_1(z_1^*, z_1') = \mathcal{N} \exp\left\{z_1^* z_1' \tan^2\theta\right\}. \tag{3.74}$$

The normalization constant can then be obtained by setting $\mathrm{Tr}\rho_1 = 1$, that is:

$$\int dz_1^* dz_1 e^{-z_1^* z_1} \rho_1(-z_1^*, z_1) = 1, \tag{3.75}$$

which implies:

$$\mathcal{N} = \left(1 + \tan^2\theta\right)^{-1} \tag{3.76}$$

Next, we proceed to calculate an entanglement measure. For simplicity, in this model we will be calculating only the second Rényi entropy. First, we note that:

$$\rho_1^2(z_1^*, z_1') = \langle z_1^*|\rho_1 \cdot \mathbb{1} \cdot \rho_1|z_1'\rangle \tag{3.77}$$

and we write the resolution of the identity as:

$$\mathbb{1} = \int d\bar{z}_1^* d\bar{z}_1 e^{-\bar{z}_1^* \bar{z}_1} |\bar{z}_1\rangle\langle\bar{z}_1^*|, \tag{3.78}$$

obtaining:

$$\rho_1^2(z_1^*, z_1') = \int d\bar{z}_1^* d\bar{z}_1 e^{-\bar{z}_1^* \bar{z}_1} \rho_1(z_1^*, \bar{z}_1)\rho_1(\bar{z}_1^*, z_1'), \tag{3.79}$$

which results in:

$$\rho_1^2(z_1^*, z_1') = \mathcal{N}^2 \exp\left\{z_1^* z_1' \tan^4\theta\right\}. \tag{3.80}$$

With that in hand, the second Rényi entropy is given by:

$$\begin{aligned} S_2 &= -\log \mathrm{Tr}\rho_1^2 \\ &= -\log\left(\mathcal{N}^2 \int dz_1^* dz_1 e^{-z_1^* z_1} e^{-z_1^* z_1 \tan^4\theta}\right) \\ &= 2\log\left(1 + \tan^2\theta\right) - \log\left(1 + \tan^4\theta\right). \end{aligned} \tag{3.81}$$

Graphically, keeping $\omega = 1$, we can analyze the behavior of the second Rényi entropy as we vary the interaction strength λ (the higher order Rényi entropies and the entanglement entropy would have a similar behavior).

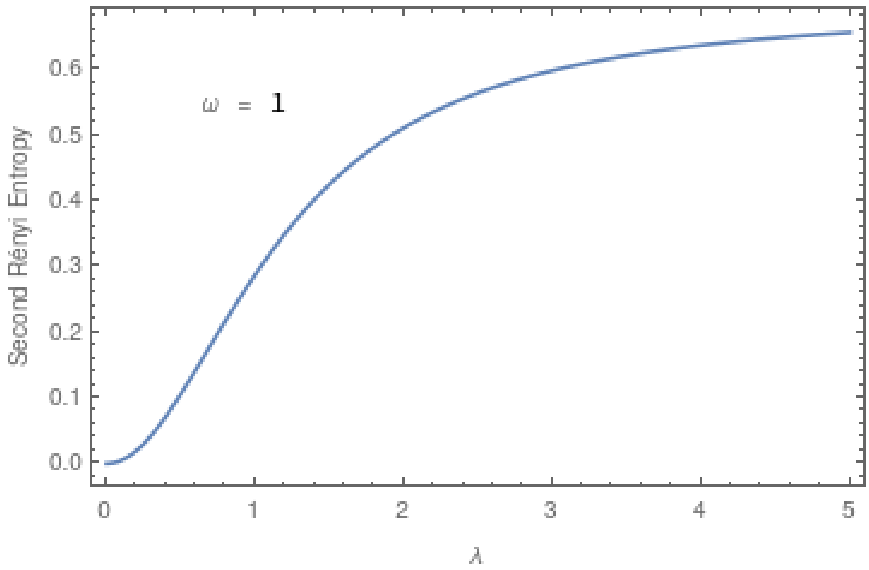

Figure 3.1: Second Rényi entropy as a function of the interaction strength

We also see an asymptotic behavior as we have, still keeping $\omega = 1$:

$$\lim_{\lambda \to \infty} S_2(\lambda) \approx 0.69. \tag{3.82}$$

Another interesting feature we can explore with this simple model is to compute the energy of this variational state and see how an increase in it affects entanglement. In order to do that, we first calculate the energy as:

$$E_0 = \frac{\langle \Omega | H | \Omega \rangle}{\langle \Omega | \Omega \rangle}, \tag{3.83}$$

which is a function of the parameters of the Hamiltonian and the angle θ, given by the constant in Eq. (3.64):

$$E_0(\theta, \omega, \lambda) = 2\omega \sin^2 \theta + \lambda \sin 2\theta. \tag{3.84}$$

As θ is fixed by Eq. (3.65), the vacuum energy can be expressed by a function only of the parameters of the Hamiltonian:

$$E_0(\omega, \lambda) = \omega \left(1 - \frac{\omega}{\sqrt{\omega^2 + \lambda^2}}\right) - \frac{\lambda^2}{\sqrt{\lambda^2 + \omega^2}} \tag{3.85}$$

Keeping ω fixed, we note that the modulus of E_0 is an increasing function of λ. The result is that, as we increase the variational vacuum energy gap, we generate entanglement up to a saturation value that has to do with the parameters of the model.

A generalization of this procedure can be applied to field theories in the BCS mean field approximation, as we will see in the next chapters. Altough we will only deal with fermionic field theories, it is interesting to note that this formalism also applies to bosons, so, in the next section, we will perform a similar calculation for bosonic oscillators and see how it goes.

3.4 Two Bosonic Oscillators

Now consider a system of two bosonic oscillators similar to the fermionic one from Sec. 3.3, described by the Hamiltonian:

$$H = \omega \left(a_1^\dagger a_1 + a_2^\dagger a_2\right) + \lambda \left(a_1 a_2 + a_1^\dagger a_2^\dagger\right), \tag{3.86}$$

where we the creation and annihilation operators obey the commutation relations:

$$[a_i, a_j] = [a_i^\dagger, a_j^\dagger] = 0, \;\; [a_i, a_j^\dagger] = \delta_{ij}. \tag{3.87}$$

In order to diagonalize the system, we change basis to the b operators related to the a ones as:

$$a_1 = ub_1 + vb_2^\dagger, \;\; a_2 = vb_1^\dagger + ub_2. \tag{3.88}$$

For the b modes to obey the same commutation relations as the a, we have the constraint:

$$u^2 - v^2 = 1, \tag{3.89}$$

so that we can parametrize the transformation with a hyperbolic angle θ, defiend such that:

$$u = \cosh\theta, \;\; v = \sinh\theta. \tag{3.90}$$

Then, we can write the Hamiltonian in terms of the b operators. It becomes:

$$\begin{aligned} H &= (\omega \cosh 2\theta + \lambda \sinh 2\theta)\,(b_1^\dagger b_1 + b_2^\dagger b_2) \\ &+ (\lambda \cosh 2\theta + \omega \sinh 2\theta)\,(b_1^\dagger b_2^\dagger + b_1 b_2) + \text{const.} \end{aligned} \tag{3.91}$$

To find the ground state, we impose that the Hamiltonian in Eq. (3.91) must be diagonal, which implies the relation:

$$\tanh 2\theta = -\frac{\lambda}{\omega}. \tag{3.92}$$

Then, the ground state $|\Omega\rangle$ is such that $b_{1(2)}|\Omega\rangle = 0$. Defining the trivial vacuum as $|0\rangle$ such that $a_{1(2)}|0\rangle = 0$, we obtain, up to a normalization constant:

$$|\Omega\rangle = e^{\alpha a_1^\dagger a_2^\dagger}|0\rangle \tag{3.93}$$

with α being a real parameter given in terms of the angle θ defined earlier as:

$$\alpha = \tanh\theta \tag{3.94}$$

Having the ground state, we can write down the density matrix of the system as:

$$\rho = \mathcal{N} e^{\alpha a_1^\dagger a_2^\dagger}|0\rangle\langle 0| e^{\alpha a_1 a_2}. \tag{3.95}$$

Then, in order to calculate the entanglement in the ground state between the a_1 and a_2 modes, we can use again the coherent states representation. Using the Eq. (3.22) to take the partial trace and the notation of Eq. (3.21), it becomes:

$$\begin{aligned} \rho_1(z_1^*, z_1') &= \mathcal{N} \int \frac{dz_2^* dz_2}{2\pi i}\; e^{-z_2^* z_2}\; e^{\alpha z_1^* z_2^*}\; e^{\alpha z_1' z_2} \\ &= \mathcal{N} e^{\alpha^2 z_1^* z_1'}, \end{aligned} \tag{3.96}$$

where we have used that the integral is of the type of Eq. (B.14) with:

$$M = \mathbb{1}, \quad \bar{J} = \alpha z_1^*, \quad J = \alpha z_1'. \tag{3.97}$$

Also, we can easily calculate the normalization constant with an integral of the same kind (with zero sources) by imposing $\mathrm{Tr}\,\rho_1 = 1$, which gives:

$$\mathcal{N} = 1 - \alpha^2. \tag{3.98}$$

We can then proceed to calculate ρ_1^2 in the coherent states representation as we did for fermions in Eq. (3.77) with the resolution of the identity from Eq. (3.14), evaluating an integral of the same kind as the previous:

$$\begin{aligned} \rho_1^2(z_1^*, z_1') &= \int \frac{d\bar{z}_1^* d\bar{z}_1}{2\pi i}\, e^{-\bar{z}_1 \bar{z}_1} \rho_1(z_1^* \bar{z}_1) \rho_1(\bar{z}_1^* z_1') \\ &= (1-\alpha^2)^2\, e^{\alpha^4 z_1^* z_1'}. \end{aligned} \tag{3.99}$$

We take the trace to get an entanglement measure as:

$$\mathrm{Tr}\,\rho_1^2 = (1-\alpha^2)^2 \int \frac{dz_1^* dz_1}{2\pi i}\, e^{-z_1^* z_1}\, e^{\alpha^4 z_1^* z_1} = \frac{(1-\alpha^2)^2}{1+\alpha^4}. \tag{3.100}$$

For higher powers of ρ_1, it turns out that we get chained Gaussian integrals as:

$$\rho_1^n(z_1^*, z_1') = \int \prod_{k=2}^{n} \left(\frac{d\bar{z}_k^* d\bar{z}_k}{2\pi i}\, e^{-\bar{z}_k \bar{z}_k} \right) \rho_1(z_1^* \bar{z}_2) \rho_1(\bar{z}_2^* \bar{z}_3) \cdots \rho_1(\bar{z}_n^* z_1'), \tag{3.101}$$

each integral raising the power of the numerator and of α in the denominator of Eq. (3.100) by 2, so that we obtain:

$$\mathrm{Tr}\,\rho_1^n = \frac{(1-\alpha^2)^n}{1-\alpha^{2n}}, \tag{3.102}$$

and from that, the n-th Rényi entropy:

$$S_n = \frac{1}{1-n} \left[n \log(1-\alpha^2) - \log(1-\alpha^{2n}) \right], \tag{3.103}$$

so that we can take the limit as $n \to 1$ and get the entanglement entropy:

$$S_E = \lim_{n \to 1} S_n = -\frac{\alpha^2 \log \alpha^2}{1-\alpha^2} - \log(1-\alpha^2), \tag{3.104}$$

which depends on the parameters of the Hamiltonian through Eqs. (3.94) and (3.92). Note that Eq. (3.92) only has a solution to the BCS angle for $\lambda < \omega$. Within this range, we note that, fixing a value for ω and increasing λ, the entanglement entropy increases with interaction, as we should expect. However, unlike the fermionic case, the entanglement entropy does not saturate—we get that S_E diverges as $\lambda \to \omega$.

As we did for the fermionic case, we can relate the entanglement entropy to the corresponding energy, that is given in terms of the BCS angle as:

$$E = \frac{\langle \Omega | H | \Omega \rangle}{\langle \Omega | \Omega \rangle} = 2\omega \sinh^2 \theta + \lambda \sinh 2\theta. \tag{3.105}$$

The energy gap $E[0] - E[\theta]$ is an increasing function of the interaction strength λ as we keep ω fixed. The behavior of the ratio between the entropy and the energy is shown in Fig. (3.2) for $\omega = 1$ (note that the energy is negative, as the zero point is the trivial vacuum).

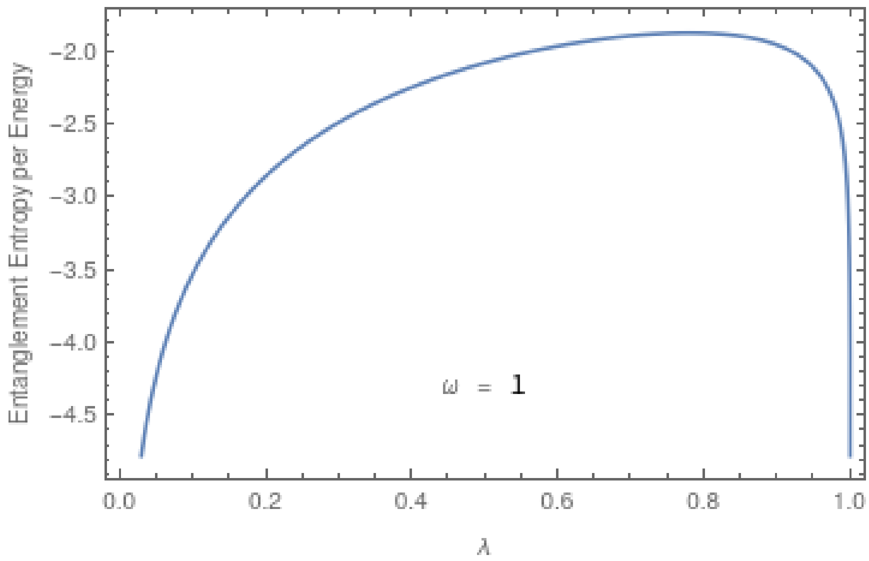

Figure 3.2: Ratio between entanglement entropy and energy for the variational vacuum as a function of the interaction strength

We note that there's a maximum for such ratio for $\lambda \approx 0.78$, meaning that there's a point in which the entanglement starts growing faster than the energy gap, which can be potentially interesting. Further analysis for bosons is left to a future study.

Although we have dealt with toy models so far, mainly for the purpose of illustrating the use of the coherent states representation to compute entanglement measures, the exercises pave the way to our study of interest in Chapter 6.

Chapter 4

General Aspects of Quantum Chromodynamics

In this chapter, we present a brief overview of Quantum Chromodynamics (QCD). As mentioned in the Introduction, QCD is the theory describing the strong force. The strong force is the predominant interaction inside the atomic nucleus, it is responsible for holding protons and neutrons together. It is also resposible for the properties of superdense stellar objects, such as neutron stars. We will make a quick review on the hadronic spetroscopy and the facts that led to the construction of QCD. Then, we present the theory itself and finally detail some of its nonperturbative phenomena, especially the chiral symmetry breaking.

4.1 Hadron Spectroscopy

Since the early 1930's with, e.g., the speculation about the existence of a neutron by Chadwick [50], a lot of effort has been done in order to describe a theory of the strong interactions that hold the atomic nucleus together. Shortly after Chadwick's conjecture, Heisenberg [51] introduced the isospin symmetry, in which the proton and the neutron would be different states of the same particle, the nucleon, in order to explain the difference of mass between them being so small. Then, in 1935, Yukawa [52] proposed that the strong interactions could be explained by the exchange of a massive boson, which turned out to be the pion, that was detected in 1947 [53].

In the following years, with the development of particle accelerators, many new particles were observed, which formed some multiplets if categorized by spin and parity. In 1961, Gell-Mann [54] and Ne'eman [55] extended the isospin symmetry and described such multiplets in terms of representations of an $SU(3)$ group, in what was called "The Eightfold Way". They have grouped the baryons with spin $J = 1/2$ in an octet that includes the proton, the neutron and the Σ, Λ and Ξ hyperions, whilst the $J = 3/2$ baryons (Δ's, Σ^*'s and Ξ^*'s) could not be grouped into an octet, so they have predicted the existence of the Ω^- hyperion, that was measured in 1964 [56], in order to make a decuplet. Fig. (4.1) shows the decuplet and the octet according to their strangeness S, which is a property of some particles that was postulated due to discrepancy in decay rates, and their isospin component I_3 with indicated spin and parity J^P:

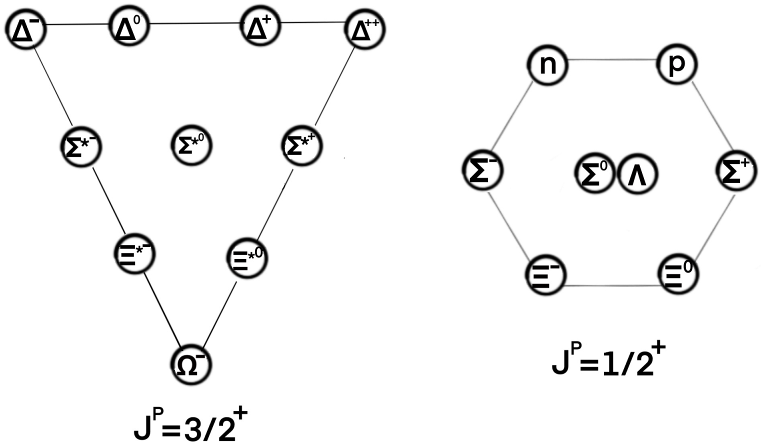

Figure 4.1: Baryon multiplets with spin 3/2 and 1/2 with positive parity in the $S - I_3$ plane

For mesons, they could make an octet for the pseudoscalar ones (or nonet, if one considers the η', that is in a singlet state) and another octet for the vectorial ones. These octets are represented in Fig. (4.2).

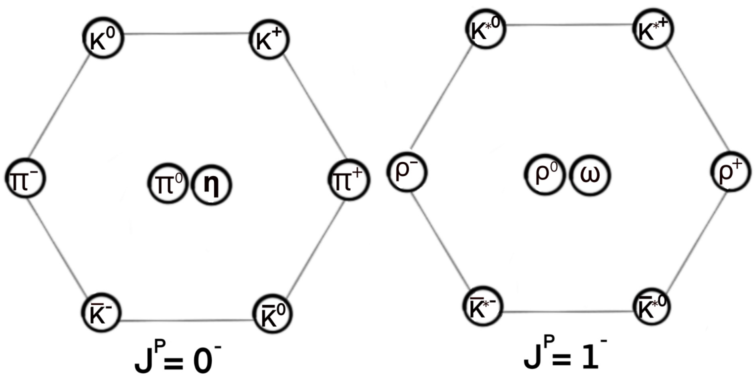

Figure 4.2: Meson octets with spin 0 and 1 with negative parity in the $S - I_3$ plane

Then, Gell-Mann proposed that the octets and decuplets that were observed could be written as products of a fundamental representation of an $SU(3)$ group, composed by particles that he called quarks [57], that come in three different flavors named *up* (u), *down* (d) and *strange* (s), and have fractionary electric charge (2/3, $-1/3$ and $-1/3$ units of the elementary charge, respectively). In this context, baryons were formed by combining three quarks (e.g., the proton is made by two up and one down quarks). Following the conventions of Appendix A for denoting representations of a group, the baryon multiplets can be written as the product:

$$\mathbf{3} \otimes \mathbf{3} \otimes \mathbf{3} = \mathbf{10} \oplus \mathbf{8} \oplus \mathbf{8} \oplus \mathbf{1}. \tag{4.1}$$

For mesons, the multiplets can be constructed by a product of the fundamental and the antifundamental representations, that is, they are composed by a quark and an antiquark:

$$\mathbf{3} \otimes \bar{\mathbf{3}} = \mathbf{8} \oplus \mathbf{1}. \tag{4.2}$$

After that, some dynamical models using the quarks as fundamental degrees of freedom were proposed (the so called quark models), which will be detailed in the next section. Furthermore, in the following years, with accelerators achieving higher energies, heavier particles were detected, and the theory was extended to 6 flavors, named, from the lightest to the heaviest:

$$u\,(\text{up}),\ d\,(\text{down}),\ s\,(\text{strange}),\ c\,(\text{charm}),\ b\,(\text{bottom}),\ t\,(\text{top}).$$

4.1.1 Quark Models

By exploring hadronic spectroscopy and thereof inferring that there is a fundamental representation of the flavor symmetry group, one can make dynamical models (see, e.g., Ref. [58]) with these degrees of freedom in order to reproduce the spectrum. To account for the unobservability of the fundamental degrees of freedom, it was natural to introduce an attractive potential of an harmonic oscillator, by writing a Hamiltonian of the form:

$$H = \sum_i \left(\frac{\mathbf{p}_i^2}{2M_i} + M_i \right) + \sum_{i>j} V_{ij} |\mathbf{r_i} - \mathbf{r_j}|^2, \tag{4.3}$$

where i and j are flavor indices, and M_i are the quark masses. As we shall see further ahead, these masses are not the quark masses that appear in the QCD Lagrangian in Eq. (4.7), they are effective masses generated by the QCD interactions. One could argue, for example, that the masses of the hadrons depend on spin, as we can see by looking at the octets from Fig. (4.2). Then, one can add a spin-dependent interaction in order to produce such an effect as:

$$H \to \tilde{H} = H + \sum_{i>j} S_{ij}(\mathbf{r_i}, \mathbf{r_j})\boldsymbol{\sigma}_i \cdot \boldsymbol{\sigma}_j, \tag{4.4}$$

where $\boldsymbol{\sigma}_i$ is the vector of Pauli matrices in the spin space of the particle i—this way, the strength of the interaction $S_{ij}(\mathbf{r_i}, \mathbf{r_j})$ would depend on the total spin. Many models using different kind of interactions were proposed in the 70's and 80's (see, e.g., Refs. [59], [60] and [61]).

The ground state wave function of a baryon in this kind of model, ignoring the entanglement caused by possible terms that mix the spaces, can be written as:

$$\Psi = \Psi_{space} \otimes \Psi_{spin} \otimes \Psi_{flavor}. \tag{4.5}$$

Due to the Pauli principle, one needs the overall quark wave function Ψ to be antisymmetric. However, in the hadronic spectrum, one has, for example, the Δ^{++} hyperion that is in the light quark decuplet of Fig. 4.1 and has zero strageness, electrical charge $2e$ and spin $3/2$. As such, it can only be formed by the quarks (uuu) with all spins up, which makes the wave function in both spin and flavor spaces symmetric, so Ψ_{space} should be antisymmetric. However, for ground states, one expects the wave function to be an s-wave. A possible solution for this problem, without giving up the Pauli Principle, was [62] to introduce a new symmetry, which was named color and forms an $SU(N_c)$ group, so that the wave function is extended as:

$$\Psi \to \Psi' = \Psi \otimes \Psi_{color}. \tag{4.6}$$

However, as there is no observed color charged particle, all the hadrons should be color singlets, which make them antisymmetric in the color space and the Pauli principle is mantained. Moreover, one has experimental evidence, such as the ratio between the cross sections of electron-positron pairs to annihilate into hadrons and into muons (see, e.g., Chapter 52 in Ref. [63]) that imply $N_c = 3$.

Making quark models in this way has its shortcomings: for example, it is difficult to explain why the bound states are always either a quark and an antiquark or three quarks, or the fact that the models are not relativistic. Another way to make quark models that deals with such difficulties is to use interacting quantum fields. Some examples of this kind are discussed in Chapter 5 and, nowadays, are treated as effective models to describe some of the phenomena predicted by Quantum Chromodynamics (QCD), which is described next.

4.2 QCD and its Symmetries

QCD is a theory that is obtained by imposing the symmetries discussed above in the context of quark models to a fundamental fermionic field and promoting the color symmetry to a local gauge one, coupling the quark field to a Yang-Mills field, the gluon. Denoting the quark field by ψ, one associates one ψ for each quark flavor, ψ^f, with $f = u, d, s, c, t, b$. Each quark flavor field ψ^f has three color components, ψ^f_c, with $c = 1, 2, 3$, indices of the fundamental representation. To have an $SU(3)$ gauge invariant Lagrangian, one needs eight gauge fields, commonly denoted A^a_μ, with $a = 1, \ldots, 8$, indices of the adjoint representation. In Minkowski space, using the conventions of Appendix A, the QCD Lagrangian density can be written as [23]:

$$\mathcal{L}_{QCD} = \bar{\psi}(i\not{D} - M)\psi - \frac{1}{4}F^a_{\mu\nu}F^{\mu\nu}_a. \tag{4.7}$$

Here, $\not{D} = \gamma^\mu D_\mu$ is the gauge covariant derivative, where D_μ is the matrix with elements in color space:

$$(D_\mu)_{cc'} = \delta_{cc'}\partial_\mu - ig(T^a)_{cc'}A^a_\mu, \tag{4.8}$$

with g being the coupling constant and $T^a = \lambda_a/2$, where λ_a are the $SU(3)$ Gell-Mann matrices in the color space. The color matrices T^a are normalized as (sum over repeated indices) $T^aT^a = 4/3$ and satisfy the algebra $[T^a, T^b] = if^{abc}T^c$, where f^{abc} are the structure constants of the $SU(3)$ group. In addition, M in Eq. (4.7) is a diagonal matrix in flavor space with the corresponding eigenvalues being the quark masses, $m_f = m_u$, m_d,m_s, m_c, m_b, m_t. Finally, $F^a_{\mu\nu}$ is the gluon field strength tensor, defined in terms of the gluon field A^a_μ as:

$$F^a_{\mu\nu} = \partial_\mu A^a_\nu - \partial_\nu A^a_\mu + gf_{abc}A^b_\mu A^c_\nu. \tag{4.9}$$

For completeness, let us mention that the local $SU(3)$ gauge transformation is defined by the 3×3 matrix in the color space:

$$U(\theta) \equiv \exp\left(i\theta^a T^a\right) \tag{4.10}$$

with θ^a being spacetime dependent parameters, which act on the quark field as:

$$\psi \rightarrow \psi' = U(\theta)\psi. \tag{4.11}$$

Then, to have the local gauge symmetry of the Lagrangian, the gluon field must transform as:

$$A_\mu \rightarrow A'_\mu = U(\theta)A_\mu U^{-1}(\theta) + \frac{i}{g}U(\theta)\partial_\mu U^{-1}(\theta), \tag{4.12}$$

where we have defined $A_\mu \equiv A^a_\mu T^a$ as it appears in the covariant derivative.

Let us now discuss transformations involving the flavor indices. A global flavor transformation on the quark fields is defined by:

$$\psi \rightarrow \exp\left(i\alpha^a t^a\right)\psi, \tag{4.13}$$

where t^a are the generators of the $SU(N_f)$ group for a theory with N_f flavors. Global flavor transformation means that the parameters α^a are spacetime independent. If such a transformation were to leave the Lagrangian invariant, the corresponding divergence of the Noether current would be given by:

$$\partial^\mu j^a_\mu = i\bar{\psi}[t^a, M]\psi. \tag{4.14}$$

That is, for the symmetry to be exact, M should be proportional to the identity in the flavor space, which corresponds to the masses of the different quark flavors to be the same.

Another global flavor transformation that one could make on the quark fields is the axial version of Eq. (4.13), given by:

$$\psi \rightarrow \exp\left\{i\gamma_5\alpha^a_5 t^a\right\}\psi, \tag{4.15}$$

with γ_5 being the Dirac matrix associated with chirality of a massless quark—the generator of the transformation inverts parity. If the QCD Lagrangian was to be invariant under such a transformation, the divergence of the corresponding Noether current would be given by:

$$\partial^\mu j^a_{5\mu} = i\bar{\psi}\{\gamma_5 t^a, M\}\psi. \tag{4.16}$$

That is, conservation of $j^a_{5\mu}$ requires vanishing quark masses.

Since quarks are confined, quark masses are measured indirectly through their influence on hadronic properties. This is an important distinction with the masses of, e.g., the electron or muon, which are observed as physical particles in particle detectors. Therefore, when one looks up quark mass values in the Particle Data Group [64], one must keep in mind that those numbers refer to a particular theoretical framework used to define them. This is so because the QCD Lagrangian needs regularization and subsequent renormalization due to the ultraviolet divergences that appear when computing correlation functions of quark and gluon fields. Renormalization is an essential step to obtain definite predictions for physical quantities, such as hadron masses and scattering amplitudes. In general terms, renormalization is a procedure that renders correlation functions finite through a subtraction scheme. There are different schemes to implement such a procedure, but all schemes invariably require the introduction of a dimensionful scale parameter, commonly denoted μ. A consequence of this fact is that the values of the coupling constant and of the quark masses refer to a particular renormalization scheme and are μ-dependent. To make these issues less abstract, in the next section we summarize the main steps of the renormalization process.

4.2.1 Renormalization, Perturbative and Nonperturbative QCD

Here we follow the presentation logic of Ref. [65] to discuss the QCD Lagrangian renormalization procedure. That logic suits our aim of clarifying how quark mass values are defined. In addition, it also allows us define in more concrete terms the meaning of perturbative and nonpertubative coupling constant.

To set up a renormalization procedure, in general, one starts defining a regularization method to obtain finite amplitudes, through which an ultraviolet dimensionful cutoff enters the theory. This parameter can be a lattice spacing or a momentum cutoff. In dimensional regularization, the spacetime dimension is changed from 4 to $4 - 2\varepsilon$ (the factor 2 is for convenience) and a mass parameter μ is needed to keep the coupling dimensionless. The parameter ε plays the role of the ultraviolet cutoff in that it controls ultraviolet divergences. One labels the quark and gluon fields, the mass parameters and the coupling in the QCD Lagrangian with the index (0), to identify them as unrenormalized (or bare) quantities. One defines renormalized fields through *wave-function renormalization* factors, $\psi^{(0)} = Z_2^{1/2}\psi$ and $A^{(0)} = Z_3^{1/2}A_\mu$. Then, one rewrites the original Lagrangian, defined by the unrenormalized quantities, in terms of the renormalized fields, so that one can identify relationships between the unrenormalized and renormalized parameters of the Lagrangian, $(m_f^{(0)}, g^{(0)})$ and (m_f, g). These relationships are not universal, they depend upon the regularization and gauge fixing methods. For our purposes here, we can follow Ref. [66], the standard reference on perturbative QCD; that reference uses dimensional regularization and linear convariant gauges (as the Feynman and Landau gauges). The Lagrangian density of QCD can then be written in terms of either unrenormalized or renormalized quantities as follows:

$$\begin{aligned}\mathcal{L}_{QCD} &= \bar{\psi}^{(0)}\left(i\gamma^\mu\partial_\mu + g^{(0)}\gamma^\mu A_\mu^{(0)} - M^{(0)}\right)\psi^{(0)} - \frac{1}{4}F^{a(0)}_{\mu\nu}F^{a(0)\mu\nu} + \mathcal{L}^{(0)}_{\text{g.f.}} \\ &= \bar{\psi}\left(i\gamma^\mu\partial_\mu + g\gamma^\mu A_\mu - M\right)\psi - \frac{1}{4}F^a_{\mu\nu}F^{a\mu\nu} + \mathcal{L}_{\text{g.f.}} + \mathcal{L}_{\text{c.t.}}. \end{aligned} \tag{4.17}$$

Here, $\mathcal{L}^{(0)}_{\text{g.f.}}$ and $\mathcal{L}_{\text{g.f.}}$ contain gauge-fixing terms depending on $A_\mu^{(0)}$ and A_μ, respectively, and depend also on gauge fixing parameters (different values for different gauges, but observables are independent of such parameters). $\mathcal{L}_{\text{c.t.}}$ refers to the counterterm Lagrangian density; it has the same structure as the other three terms in the second line of Eq. (4.17) and contains the renormalization factors Z_2 and Z_3. In a perturbative calculation, $\mathcal{L}_{\text{c.t.}}$ is treated as part of the interaction and the renormalization factors absorb the ultraviolet divergent terms.

In an explicit calculation, one needs to use experimental values of a few observables to fix the parameters of the theory. In the calculation, one fixes the ultraviolet regularization parameter, ε in dimensional regularization, holds the bare parameters $m_f^{(0)}$ and $g^{(0)}$ and varies the mass scale μ, so that one can relate the masses m_f and coupling constant $\alpha_s = g^2/4\pi$ at different values of μ through renormalization group (RG) equations. That is, the RG equations for $m_f(\mu)$ and $g(\mu)$ ensure that observables are μ-independent. The form of those RG equations depends on how one chooses to separate finite and divergent terms to define the renormalization factors Z_2 and Z_3. Different ways of choosing such a separation lead to different renormalization schemes. One of the most commonly used schemes is the modified subtraction scheme, denoted $\overline{\text{MS}}$. In that scheme, the RG equation for $m_f(\mu)$ at the one-loop order is given by [64]:

$$\mu^2\frac{dm_f(\mu)}{d\mu^2} = \left[-\frac{\alpha_s(\mu)}{\pi} + \mathcal{O}(\alpha_s^2)\right]m_f(\mu), \tag{4.18}$$

whereas that for $\alpha_s(\mu)$ is given by:

$$\mu^2 \frac{d\alpha_s(\mu)}{d\mu^2} = \beta(\alpha_s) = -b_0\,\alpha_s^2 + \mathcal{O}(\alpha_s^3), \quad \text{where} \quad b_0 = \frac{33 - 2N_f}{12\pi}, \tag{4.19}$$

with N_f being the number of light flavors with masses smaller than the scale μ. Integrating this last equation from μ_0 to μ, one obtains:

$$\frac{1}{\alpha_s(\mu)} = \frac{1}{\alpha_s(\mu_0)} + b_0 \ln\left(\frac{\mu^2}{\mu_0^2}\right). \tag{4.20}$$

This can be rewritten in terms of a μ-independent mass scale Λ_{QCD} as

$$\frac{1}{\alpha_s(\mu)} - b_0 \ln\left(\frac{\mu^2}{\Lambda_{QCD}^2}\right) = \frac{1}{\alpha_s(\mu_0)} - b_0 \ln\left(\frac{\mu_0^2}{\Lambda_{QCD}^2}\right). \tag{4.21}$$

The equality implies that Λ_{QCD} is given by:

$$\Lambda_{QCD} = \mu\, e^{-1/[2b_0\alpha_s(\mu)]}, \tag{4.22}$$

which implies that $\alpha_s(\mu)$ runs with μ as:

$$\alpha_s(\mu) = \frac{1}{b_0 \ln(\mu^2/\Lambda_{QCD}^2)} = \frac{12\pi}{(33 - 2N_f)\, \ln(\mu^2/\Lambda_{QCD}^2)}. \tag{4.23}$$

This last result encapsulates the *asymptotic freedom* of QCD [16, 17], alluded in the Introduction. In a perturbative calculation of a process, it turns out that, in order for the calculation to be valid, the scale μ must be chosen commensurate with the typical momenta driving the process [66]. That is, perturbation theory is applicable for processes involving large momentum transfers, since for those processes α_s can be small. On the other hand, one observes that for $\mu \sim \Lambda_{QCD}$, the coupling increases substantially. That is, Λ_{QCD} is the scale at which QCD becomes nonperturbative. Phenomena like quark confinement and hadron formation happen at such a scale.

The 2020 edition of the PDG [64] does not quote a value of Λ_{QCD} for different flavors, it only quotes the values of α_s at a given scale. Extractions from different observables show that α_s decreases with μ, varying from $\alpha_s \simeq 0.08$ at $\mu = 1000$ GeV to $\alpha_s \simeq 0.4$ at $\mu = 2$ GeV. In the 2016 edition of the PDG, the values of Λ_{QCD} in the $\overline{MS}$ scheme for different flavor numbers N_f are, in MeV [65]:

$$\Lambda_{QCD} = \begin{cases} 332 & \text{for} \quad N_f = 3 \\ 292 & \qquad\quad\;\; = 4 \\ 210 & \qquad\quad\;\; = 5 \\ 89 & \qquad\quad\;\; = 6 \end{cases} \tag{4.24}$$

Since one knows $\alpha_s(\mu)$, one can solve the RG equation for the quark masses $m_f(\mu)$ at the one loop order. As today, solutions of the RG equations for α_s are known to much higher orders [64]. The PDG quotes quark values obtained by combining different approaches: lattice QCD, chiral perturbation theory, sum rules and heavy-quark effective field theories. Below we list the quark masses values in the $\overline{\text{MS}}$ scheme compiled by the PDG [64]; the renormalization scale for the (u, d, s) quarks is $\mu = 2$ GeV and for the (c, b, t) quarks μ is equal to the mass itself, i.e. $m_Q(\mu = m_Q)$. The values are (approximate central values):

$$\begin{aligned} m_u \approx 2.16\,\text{MeV}, \quad m_d \approx 4.67\,\text{MeV}, \quad m_s \approx 93\,\text{MeV}, \\ m_c \approx 1.27\,\text{GeV}, \quad m_b \approx 4.18\,\text{GeV}, \quad m_t \approx 170\,\text{GeV}. \end{aligned} \tag{4.25}$$

4.2.2 Dynamical Chiral Symmetry Breaking

The mass hierarchy in Eq. (4.25) is evident, with the light-quark masses being much smaller than Λ_{QCD}. As mentioned previously, one computes hadron properties by studying correlation functions of hadron interpolating fields, i.e., gauge invariant products of quark and gluon field operators with the quantum numbers of the hadron of interest. The isolated poles in hadron correlation functions give the mass spectrum of the hadron. When studying light hadron properties, like protons and neutrons, although the relevant interpolators contain gluon and light-flavor quark fields only, the heavy quark fields do contribute to a correlation function through quantum fluctuations. However, the Appelquist-Carrazone theorem [67] (a.k.a. decoupling theorem) asserts that heavy-quark quantum fluctuations in light-hadron correlation function are suppressed by inverse powers of the heavy-quark masses or are eliminated through renormalization of the light-quark parameters. Therefore, it makes perfect sense to analyse the light-quark part of the QCD Langrangian ignoring the heavy quarks when studying light hadrons at low energy scales.

The light-quark masses being much smaller than Λ_{QCD} motivates the analysis of light-quark sector of the QCD Lagrangian with $m_f = 0$ as as a zeroth order approximation and eventually perform perturbation theory in m_f. For $m_f = 0$, one can write the light-quark part of the QCD Lagrangian as (we use the index l to denote light quarks)

$$\mathcal{L}^l_{QCD}(\psi) = \mathcal{L}^l_{QCD}(\psi_L) + \mathcal{L}^l_{QCD}(\psi_R), \tag{4.26}$$

where L and R refer to left-handed and right-handed, with ψ_L and ψ_R corresponding to spinors describing quarks and antiquarks with definite helicity:

$$\psi_L = \frac{1}{2}\left(1-\gamma_5\right)\psi \quad \text{and} \quad \psi_R = \frac{1}{2}\left(1+\gamma_5\right)\psi. \tag{4.27}$$

Each part of the Lagrangian is invariant under the transformations in the flavor indices discussed above, that is, the Lagrangian has an $SU(3)_L \otimes SU(3)_R$ chiral symmetry (considering u, d and s as the light quarks). One can show that the corresponding conserved charges Q^a_L and Q^a_R are related to the ones of the vector Q^a and axial Q^a_5 transformations of Eqs. (4.13) and (4.15) as:

$$\begin{aligned} Q^a_L(t) &= \frac{1}{2}\left(Q^a(t) - Q_{5a}(t)\right), \\ Q^a_R(t) &= \frac{1}{2}\left(Q^a(t) + Q_{5a}(t)\right). \end{aligned} \tag{4.28}$$

Therefore, we have the equivalence:

$$SU(3)_L \otimes SU(3)_R = SU(3)_V \otimes SU(3)_A. \tag{4.29}$$

It is important, however, to note that, although the left and right handed charges obey separate algebras, this is not true in the case of of the axial charges. To make this explicit, one has the equal-time commutation relations

$$\left[Q^a_L(t), Q^b_L(t)\right] = i f^{abc} Q^c_L(t), \tag{4.30}$$

$$\left[Q^a_R(t), Q^b_R(t)\right] = i f^{abc} Q^c_R(t), \tag{4.31}$$

$$\left[Q^a_L(t), Q^b_R(t)\right] = 0, \tag{4.32}$$

where f^{abc} are the $SU(3)$ structure constants. On the other hand, the corresponding relations for the vector and axial charges are:

$$\left[Q^a(t), Q^b(t)\right] = if^{abc}Q^c(t), \tag{4.33}$$

$$\left[Q_5^a(t), Q_5^b(t)\right] = if^{abc}Q^c(t), \tag{4.34}$$

$$\left[Q^a(t), Q_5^b(t)\right] = if^{abc}Q_5^c(t). \tag{4.35}$$

Clearly, Eq. (4.34) shows the nonclosure of the axial-charge commutation relations, meaning the axial charges do not form a group.

The invariance of the theory under axial transformation implies that the axial charge commutes with the QCD Hamiltonian:

$$[H_{QCD}, Q_5^a] = 0. \tag{4.36}$$

Let $|h,+\rangle$ be an eigenstate of the QCD Hamiltonian corresponding to a positive-parity hadron at rest; the corresponding eigenvalue is the hadron mass:

$$H_{QCD}|h,+\rangle = M_h|h,+\rangle. \tag{4.37}$$

Since Q_5^a is the symmetry transformation generator, one should expect the existence, in the spectrum of H_{QCD}, of a state

$$Q_5^a|h,+\rangle \sim |h,-\rangle \tag{4.38}$$

which has opposite parity and is degenerate to $|h,+\rangle$,

$$H_{QCD}\left(Q_5^a|h,+\rangle\right) = M_h\left(Q_5^a|h,+\rangle\right). \tag{4.39}$$

This is the Wigner-Weyl realization of the corresponding symmetry. Therefore, if the approximate chiral symmetry was to be realized in the Wigner-Weyl way, for every hadron multiplet there should exist an almost degenerate multiplet with the opposite parity. But such a pattern is not observed in the hadronic spectrum.

However, there is another way for a symmetry to be realized, the Nambu-Goldstone way, in which despite the invariance of the Hamiltonian under the transformation, the ground state may not be invariant—the interaction breaks the symmetry dinammicaly. In fact, the operator corresponding to the axial charge does not annihilate the vacuum of the theory, which invalidates the Wigner-Weyl mode. Two consequences of the Nambu-Goldstone realization of the chiral symmetry are: the quarks acquire an effective mass of value of the order of Λ_{QCD}, and there appear massless bosons in the spectrum with the quantum numbers of the symmetry generator that is dynamically broken (in this case, pseudoscalar ones). Since the vacuum is not invariant under the chiral transformation, the vacuum expectation value of the quark scalar density, $\langle \bar{\psi}_f \psi_f \rangle$, is nonzero; this vacuum expectation value is the quark condensate discussed in the Introduction. This mass generation mechanism allows us to make contact with the phenomenological quark models of the pre-QCD era discussed above, in that the quark masses used in those models are in close correspondence with the effective masses generated by this symmetry-breaking phenomenon. The masses appearing in the Hamiltonian are commonly named *current quark masses* and those arising through DCSB *constituent quark masses* . In the real-world hadronic spectrum, if we consider the u and d quarks as light, we see that the pions have the desired quantum numbers and small masses (not expected to be exactly zero because the symmetry is only approximate), whilst if we consider also the strange quark as light, we get the pseudoscaler meson octet from Fig. (4.2), where the ones that are formed by strange quarks have higher masses. This may be an evidence of a manifestation of the approximate chiral symmetry breaking in nature. As with any other dynamical symmetry breaking, the chiral symmetry is a nonperturbative phenomenon. As such, it's difficult to analyze it any further. In the next chapter, we present effective models that realize dynamical chiral symmetry breaking and are analytically amenable.

To conclude, we note that the Lagrangian in Eq. (4.26) is also invariant under $U(1)$ transformations, in particular under an axial $U(1)_A$ transformation (generated by the γ_5 matrix). But this symmetry, although a symmetry of the classical Lagrangian, is not a symmetry in the quantum theory—this is the axial anomaly [23]. We will not discuss this problem in the dissertation.

Chapter 5

Field Theoretic Chiral Quark Models

As we have seen in the previous chapter, there are QCD features that are nonperturbative and therefore difficult to treat. The most prominent phenomena are color confinement and dynamical chiral symmetry breaking, the latter being the subject of our interest in this dissertation. In this chapter, we discuss two models that can reproduce such features: the Nambu–Jona-Lasinio (NJL) and the Coulomb gauge quark Hamiltonian (CGQH). The NJL model has a contact interaction that realizes dynamical chiral symmetry breaking (DCSB) but does not confine color. The CGQH model realizes DCSB and color confinement through finite-range interactions that contain ultraviolet runnings mimicking asymptotic freedom.

5.1 The Nambu–Jona-Lasinio Model

The first model that we consider is the one named after Nambu and Jona-Lasinio (NJL). It was proposed originally by them in 1961 [19], before the development of quantum chromodynamics. They wanted a non-trivial theory illustrating how one could understand the smallness of the pion mass through a dynamical symmetry breaking mechanism, in the Goldstone way. That could be formulated in terms of a fundamental bosonic field or of a fermionic field with non-linear interactions. They have chosen the latter as they could include nucleon (baryon) number conservation and explain the nucleon mass generation within the same model. They noted that the respective symmetries are defined by the invariance of the theory under the transformations on the fields:

$$
\begin{aligned}
\psi &\rightarrow e^{i\alpha}\psi, \\
\psi &\rightarrow e^{i\alpha\gamma_5}\psi.
\end{aligned}
\tag{5.1}
$$

Any Lorentz construction with the Dirac bilinears involving $\bar{\psi}$ and ψ is invariant under the first transformation, but not necessarily under the second. In particular, a scalar bilinear transforms as:

$$\bar{\psi}\psi \to \bar{\psi}\psi \cos 2\alpha + \bar{\psi} i\gamma_5 \psi \sin 2\alpha, \tag{5.2}$$

and a pseudoscalar as:

$$\bar{\psi} i\gamma_5 \psi \to \bar{\psi} i\gamma_5 \psi \cos 2\alpha - \bar{\psi}\psi \sin 2\alpha \tag{5.3}$$

so that the simplest non-trivial interaction that has the chiral symmetry is constructet by squaring a scalar and a pseudoscalar and adding them up. Motivated by that, they have written the Lagrangian (in the chiral limit, with zero nucleon mass):

$$\mathcal{L}_{NJL} = i\bar{\psi}\partial\!\!\!/\psi + G\left[(\bar{\psi}\psi)^2 + (\bar{\psi} i\gamma_5 \psi)^2\right]. \tag{5.4}$$

This model already could reproduce the chiral symmetry breaking and idealized pions as the Goldstone bosons, as well as some other physical quantities after fixing the coupling and the theory scale.

With the advent of QCD, the fermion field was reinterpreted as an effective quark field and the model was changed in order to reproduce the same symmetries as we have stated for QCD, so that it's now in the fundamental representations of the $SU(N_c)$ and $SU(N_f)$ symmetry groups. For $N_f = 2$, it can be written as [34]:

$$\mathcal{L}_{NJL} = i\bar{\psi}\partial\!\!\!/\psi + G\left[(\bar{\psi}\psi)^2 + (\bar{\psi} i\gamma_5 \tau^a \psi)^2\right], \tag{5.5}$$

where now the fields have color and flavor indices in the fundamental representation of the respective groups that were omitted and τ^a are the Pauli matrices in the flavor space.

In addition, one can incorporate the $U(1)_A$ axial anomaly in the NJL model by adding a flavor mixing term similar to what was proposed by 't Hooft in Ref. [68]:

$$\mathcal{L}_{det} = -K\left[\det\bar{\psi}(1+\gamma_5)\psi + \det\bar{\psi}(1-\gamma_5)\psi\right], \tag{5.6}$$

where the determinant is taken in the flavor indices, so it is a $2N_f$ fermion interaction term. As already mentioned, although the classical Hamiltonian is invariant under $U(1)_A$ transformation, the quantum Hamiltonian is not invariant. Although potentially interesting, we do not explore in this dissertation the interplay between this $U(1)_A$ nonconservation and quantum entanglement in the DCSB.

The NJL model has its shortcomings. First, a four-fermion contact interaction is nonrenormalizable, so any regularization used to control ultraviolet divergences cannot not be removed and regularization parameters become part of the model. We use a noncovariant momentum cutoff Λ (other equivalent regularization schemes are described in Ref. [34]). Second, it does not confine color. Another missing QCD feature in the model is asymptotic freedom. Despite such shortcomings, the model has the unique advantage of being analytically solvable in the mean field approximation, a feature that allowed us to gain deep insights on this key QCD phenomenon. Much of what one presently knows about DCSB in QCD comes from the NJL model.

5.1.1 DCSB in the NJL model

For our purposes, it it convenient to discuss DCSB with a BCS-like approach. For that, we follow Ref. [34] closely. Such an approach is convenient because it allows us to treat the DCSB phenomenon in terms of an explicit construction of the vacuum state in terms of a quark-antiquark condensate, allowing us to define a density matrix for that state and thereby access the quantum entanglement driven by DCSB.

First, we write down the NJL Hamiltonian density for the $SU(2)$ model in the chiral limit:

$$\mathcal{H}_{NJL} = -i\bar{\psi}\gamma^i\partial_i\psi - G\left[(\bar{\psi}\psi)^2 + (\bar{\psi}i\gamma_5\tau^a\psi)^2\right]. \tag{5.7}$$

To motivate the BCS approach to the DCSB problem, we start with the most direct (and traditional) way to implement the mean field approximation, namely: one factorizes the four-fermion product of quark operators as

$$(\bar{\psi}\psi)^2 \rightarrow 2\langle\bar{\psi}\psi\rangle\bar{\psi}\psi, \tag{5.8}$$

where the factor of 2 comes from the two possible ways of contracting the fields. The meaning of this should be clear: the two-particle scattering is replaced by a two-particle propagation in a mean field. The γ_5 term does not contribute in this approximation as we have:

$$\langle\bar{\psi}i\gamma_5\tau^a\psi\rangle \sim \mathrm{Tr}(\tau^a) = 0. \tag{5.9}$$

Then, the Hamiltonian density becomes:

$$\mathcal{H}_{NJL}^{(MF)} = \bar{\psi} \left(-i\gamma^i \partial_i - 2G\langle\bar{\psi}\psi\rangle \right) \psi. \tag{5.10}$$

Clearly, if the term $\langle\bar{\psi}\psi\rangle$ turns out to be nonzero, the original $SU(2)_L \otimes SU(2)_R$ symmetry of the Hamiltonian is broken, as this term can be seen as a mass term:

$$\langle\bar{\psi}\psi\rangle \equiv -\frac{m}{2G}. \tag{5.11}$$

To decide if $\langle\bar{\psi}\psi\rangle \neq 0$, one must verify if the vacuum energy is lowered by this symmetry breaking. We will discuss this in the context of the BCS approach in the following.

As a remark, looking at the Hamiltonian in the mean field approximation of Eq. (5.10), we see that a current quark mass m_0 breaking the chiral symmetry explicitly would have precisely the same effect as in the case where $\langle\bar{\psi}\psi\rangle \neq 0$, so that we would just have $m \to m + m_0$. Because of this, we will work only in the chiral limit for the NJL model and restore the current mass in a next model, as its behavior will be less trivial.

Next, we expand the quark field operator in terms of the massless plane-wave solutions $u(\mathbf{p}, s)$ and $v(\mathbf{p}, s)$ of the Dirac Hamiltonian:

$$\psi(\mathbf{x}, 0) = \sum_s \int \frac{d^3p}{(2\pi)^3} \left(b(\mathbf{p}, s)u(\mathbf{p}, s) + d^\dagger(-\mathbf{p}, s)v(-\mathbf{p}, s) \right) e^{i\mathbf{p}\cdot\mathbf{x}}, \tag{5.12}$$

where we have omitted the flavor and color indices, and

$$u(\mathbf{p}, s) = \frac{1}{\sqrt{2}} \begin{pmatrix} 1 \\ \sigma \cdot \hat{\mathbf{p}} \end{pmatrix} \chi_s, \quad v(-\mathbf{p}, s) = \frac{1}{\sqrt{2}} \begin{pmatrix} -\sigma \cdot \hat{\mathbf{p}} \\ 1 \end{pmatrix} \chi_s, \tag{5.13}$$

with σ^i being the Pauli matrices and χ_s being the Pauli spinors:

$$\chi_1 = \begin{pmatrix} 1 \\ 0 \end{pmatrix}, \quad \chi_{-1} = \begin{pmatrix} 0 \\ 1 \end{pmatrix}. \tag{5.14}$$

The quark and antiquark creation and annihilation operators $b^\dagger$, $d^\dagger$, b, d obey the canonical anticommutation relations for fermions with the normalization:

$$\{b(\mathbf{p}, s), b^\dagger(\mathbf{p}', s')\} = \{d(\mathbf{p}, s), d^\dagger(\mathbf{p}', s')\} = (2\pi)^3\delta^3(\mathbf{p} - \mathbf{p}')\delta_{ss'}. \tag{5.15}$$

In Eq. (5.13), we have normalized the u and v spinors as:

$$u^\dagger(\mathbf{p},s)u(\mathbf{p},s') = v^\dagger(\mathbf{p},s)v(\mathbf{p},s') = \delta_{ss'}, \tag{5.16}$$

and their orthogonality can be stated as:

$$u^\dagger(\mathbf{p},s)v(-\mathbf{p},s') = v^\dagger(-\mathbf{p},s)u(\mathbf{p},s') = 0. \tag{5.17}$$

We will also use the identities:

$$\begin{aligned} \sum_s u(\mathbf{p},s)u^\dagger(\mathbf{p},s) &= \frac{1}{2}\left(1 - \frac{\gamma^i \cdot p_i \gamma^0}{p}\right), \\ s\gamma^0 u(\mathbf{p},s) &= v(-\mathbf{p},s). \end{aligned} \tag{5.18}$$

Then, the kinetic term of the Hamiltonian becomes (here we need to reinsert flavor and color indices)

$$\int d^3x\, \bar{\psi}\gamma^i\partial_i\psi = \sum_{sfc}\int \frac{d^3p}{(2\pi)^3} E_p \left[b^\dagger_{fc}(\mathbf{p},s)b_{fc}(\mathbf{p},s) + d_{fc}(-\mathbf{p},s)d^\dagger_{fc}(-\mathbf{p},s)\right], \tag{5.19}$$

where $E_p = p$. Likewise, the interaction term in the mean field form becomes:

$$\begin{aligned} -2G\langle\bar{\psi}\psi\rangle \int d^3x\, \bar{\psi}\psi &= 2G\langle\bar{\psi}\psi\rangle \sum_{sfc} s \int \frac{d^3p}{(2\pi)^3}\Big[b^\dagger_{fc}(\mathbf{p},s)d^\dagger_{fc}(-\mathbf{p},s) \\ &\qquad - d_{fc}(-\mathbf{p},s)b_{fc}(\mathbf{p},s)\Big]. \end{aligned} \tag{5.20}$$

Adding the two terms, one sees that the resulting expression for the Hamiltonian is BCS-like, that is, it is of the same form of the two-fermion toy Hamiltonian in Eq. (3.59). In order to diagonalize it, we make a Bogoliubov-Valatin transformation similar to the one made for that toy model, namely:

$$\begin{aligned} B(\mathbf{p},s) &= \cos\theta(\mathbf{p})b(\mathbf{p},s) - s\sin\theta(\mathbf{p})d^\dagger(-\mathbf{p},s), \\ D(-\mathbf{p},s) &= \cos\theta(\mathbf{p})d(-\mathbf{p},s) + s\sin\theta(-\mathbf{p})b^\dagger(\mathbf{p},s), \end{aligned} \tag{5.21}$$

such that the anticommutation relations are kept for the new operators $B(\mathbf{p},s)$ and

$D(-\mathbf{p},s)$. As we have the relations for a generic function F:

$$\left[b(\mathbf{p},s),F[b^\dagger(\mathbf{p}',s')d^\dagger(-\mathbf{p}',s')]\right] = \frac{\delta}{\delta b^\dagger(\mathbf{p},s)}F[b^\dagger(\mathbf{p}',s')d^\dagger(-\mathbf{p}',s')], \tag{5.22}$$

$$\left[d(\mathbf{p},s),F[b^\dagger(\mathbf{p}',s')d^\dagger(-\mathbf{p}',s')]\right] = \frac{\delta}{\delta d^\dagger(\mathbf{p},s)}F[b^\dagger(\mathbf{p}',s')d^\dagger(-\mathbf{p}',s')], \tag{5.23}$$

where the functional derivatives are taken from the left, with, for example:

$$\frac{\delta}{\delta d^\dagger(\mathbf{p},s)}b^\dagger(\mathbf{p}',s')d^\dagger(-\mathbf{p}',s') = -(2\pi)^3\delta^3(\mathbf{p}+\mathbf{p}')\delta_{ss'}b^\dagger(\mathbf{p}',s'), \tag{5.24}$$

the (normalized) state that $B(\mathbf{p},s)$ and $D(-\mathbf{p},s)$ annihilate can be constructed from the trivial vacuum $|0\rangle$, defined as $b(\mathbf{p},s)|0\rangle = d(-\mathbf{p},s)|0\rangle = 0$, as[1] :

$$|\mathrm{vac}\rangle = \prod_{\mathbf{p},sfc}\left(\cos\theta(\mathbf{p}) - s\sin\theta(\mathbf{p})b^\dagger_{cf}(\mathbf{p},s)d^\dagger_{cf}(-\mathbf{p},s)\right)|0\rangle. \tag{5.25}$$

We see, then, that the vacuum $|\mathrm{vac}\rangle$, for $\sin\theta(\mathbf{p}) \neq 0$, is populated with quark-antiquark pairs, correlated in momentum and spin projection. Each pair has zero momentum and zero spin, therefore, the quark and the antiquark in a pair have opposite momenta and spin projections. For example, if the quark in the pair has momentum $\mathbf{p}$ and spin projection -1/2, the corresponding antiquark has moment $-\mathbf{p}$ and spin +1/2. This is very similar to the Cooper pairs in the context of the superconductivity (see, e.g., Ref. [21]), but with pairs of a particle and its antiparticle, emphasizing the presence of a quark condensate that makes $\langle\bar{\psi}\psi\rangle \neq 0$ and breaks the chiral symmetry.

Next, we expand the quark fields in the new operators B and D as:

$$\psi(\mathbf{x},0) = \sum_s \int \frac{d^3p}{(2\pi^3)}\left(B(\mathbf{p},s)U(\mathbf{p},s) + D^\dagger(-\mathbf{p},s)V(-\mathbf{p},s)\right)e^{i\mathbf{p}\cdot\mathbf{x}} \tag{5.26}$$

with the new variational spinors U and V keeping the orthogonality and normal-

[1] We note that when changing back and forth between continuum and discrete momenta, volume factors get implicitly absorbed in the change from the Dirac delta to the Kronecker delta in the anticommutation relations.

ization and being related to the former u and v spinors as:

$$
\begin{aligned}
U(\mathbf{p},s) &= \cos\theta(\mathbf{p})u(\mathbf{p},s) - s\sin\theta(\mathbf{p})v(-\mathbf{p},s), \\
V(-\mathbf{p},s) &= \cos\theta(\mathbf{p})v(-\mathbf{p},s) + s\sin\theta(\mathbf{p})u(\mathbf{p},s).
\end{aligned} \tag{5.27}
$$

It now becomes easy to evaluate the total energy per volume; it is given by:

$$
\begin{aligned}
E[\theta] &\equiv \frac{1}{V}\int d^3x\,\langle \mathrm{vac}|\mathcal{H}_{NJL}|\mathrm{vac}\rangle \\
&= -2N\int \frac{d^3p}{(2\pi)^3}\,p\cos 2\theta(\mathbf{p}) - 4GN^2\left(\int \frac{d^3p}{(2\pi)^3}\,\sin 2\theta(\mathbf{p})\right)^2,
\end{aligned} \tag{5.28}
$$

where V is the total volume of the space and $N = N_f N_c = 2\times 3 = 6$. The first term comes from the kinetic part of $\mathcal{H}_{NJL}$ and the second comes from the $(\bar\psi\psi)^2 \to 2\langle\bar\psi\psi\rangle\bar\psi\psi$ interaction, as the γ_5 term vanishes as we stated earlier.

The problem of deciding if $\langle\bar\psi\psi\rangle \neq 0$ is solved by minimizing $E[\theta]$ with respect to θ to find the ground state of the model. Doing that, we obtain the gap equation:

$$
p\tan 2\theta(\mathbf{p}) = 4GN\int \frac{d^3q}{(2\pi)^3}\sin 2\theta(\mathbf{q}). \tag{5.29}
$$

Also, one can evaluate the condensate $\langle\bar\psi\psi\rangle$ as a functional of θ:

$$
\langle\bar\psi\psi\rangle = \langle\bar\psi_u\psi_u\rangle + \langle\bar\psi_d\psi_d\rangle = -2N\int \frac{d^3q}{(2\pi)^3}\sin 2\theta(\mathbf{q}). \tag{5.30}
$$

The gap equation is a nonlinear equation for $\theta(\mathbf{p})$. Clearly, $\theta(\mathbf{p}) = 0$ is a solution; but we are interested in knowing if there exist $\theta(\mathbf{p}) \neq 0$ solutions, so that $\langle\bar\psi\psi\rangle \neq 0$.

Recalling the definition of m in Eq. (5.11), Eq. (5.29) becomes:

$$
\tan 2\theta(p) = \frac{m}{p}, \tag{5.31}
$$

which, when plugging it back in the integrand of Eq. (5.29), gives us the gap equation in terms of m:

$$
m = 4GN\int \frac{d^3p}{(2\pi)^3}\frac{m}{\sqrt{p^2+m^2}} = \frac{2GN}{\pi^2}\int_0^{\Lambda} dp\,p^2\frac{m}{\sqrt{p^2+m^2}}. \tag{5.32}
$$

Here, we have introduced a cutoff Λ in the momentum as the integral is UV divergent. Since the the model is nonrenormalizable, Λ cannot be removed and becomes a parameter of the model.

As mentioned above, the gap equation has a trivial solution, $m = 0$. Such a solution maintains the $SU(2)_L \otimes SU(2)_R$ chiral symmetry of the vacuum. It implies $\sin\theta = 0$, so Eq. (5.25) gives $\langle 0|\bar{\psi}\psi|0\rangle = 0$ and $|\text{vac}\rangle = |0\rangle$. That is, the symmetry-preserving solution does not lead to a vacuum populated with momentum-correlated quark-antiquark pairs. However, if we look for a $m \neq 0$ solution, we can perform the integral to obtain the NJL condition [19]:

$$\frac{\pi^2}{NG_\Lambda} = \left(1 + m_\Lambda^2\right)^{1/2} - m_\Lambda^2 \sinh^{-1}\left(\frac{1}{m_\Lambda}\right), \tag{5.33}$$

where we have defined the dimensionless quantities:

$$G_\Lambda \equiv G\Lambda^2, \;\; m_\Lambda \equiv m/\Lambda. \tag{5.34}$$

The behavior of m_Λ in terms of G_Λ is represented graphically in the Fig.(5.1):

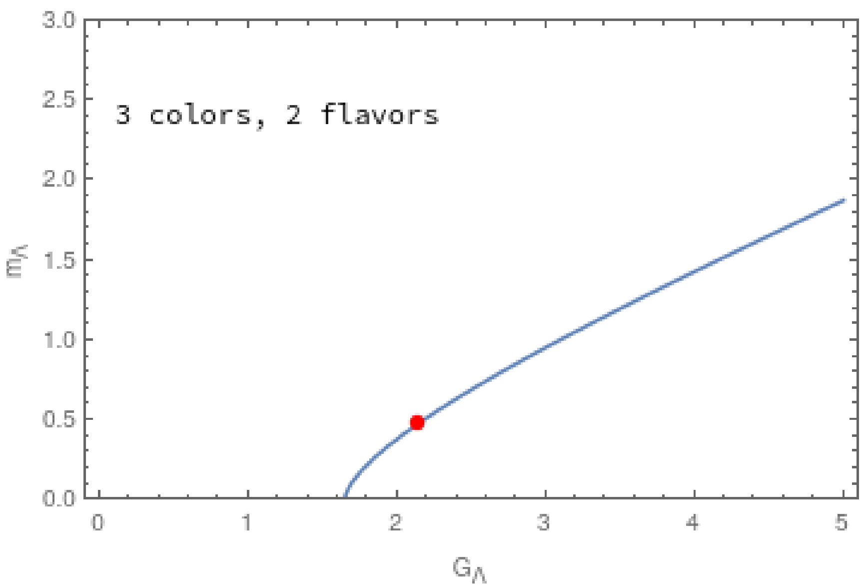

Figure 5.1: Constituent quark mass (rescaled by Λ) as a function of the dimensionless coupling $G\Lambda^2$, for $N = N_c N_f = 6$. The red dot mark identifies the value of m_Λ obtained by fitting the parameters G and Λ to observables (see subsection 5.1.2).

As we can see from Fig. (5.1), there is a critical value for G_Λ above which there is a nontrivial solution for the gap equation. For $N = N_c N_f = 6$, the critical value is given by $G_c\Lambda^2 = \pi^2/N$. Moreover, the symmetry-breaking vacuum has a lower energy than the symmetry-preserving vacuum, as:

$$\begin{aligned} E[\theta] - E[0] &= -4GN^2 \left(\int^{\Lambda} \frac{d^3p}{(2\pi)^3} \sin 2\theta(\mathbf{p}) \right)^2 \\ &= -4GN^2 \left(\int^{\Lambda} \frac{d^3p}{(2\pi)^3} \frac{m}{\sqrt{p^2+m^2}} \right)^2 < 0. \end{aligned} \tag{5.35}$$

Therefore, $\langle\bar{\psi}\psi\rangle$ does not vanish and the $SU(2)_L \otimes SU(2)_R$ chiral symmetry is broken for the ground state, which is populated by momentum-correlated quark-antiquark pairs. In this scenario, m can be interpreted as a constituent quark mass and the $B^\dagger$ and $D^\dagger$ are the operators that create such coinstituent quarks, as well as $U(\mathbf{p}, s)$ and $V(-\mathbf{p}, s)$ being the corresponding massive spinors, as we have:

$$\begin{aligned} \cos\theta(\mathbf{p})u(\mathbf{p},s) - s\sin\theta(\mathbf{p})v(-\mathbf{p},s) &= \sqrt{\frac{E_p+m}{2E_p}} \begin{pmatrix} 1 \\ \frac{\sigma\cdot\mathbf{p}}{E_p+m} \end{pmatrix} \chi_s, \\ \cos\theta(\mathbf{p})v(-\mathbf{p},s) + s\sin\theta(\mathbf{p})u(\mathbf{p},s) &= \sqrt{\frac{E_p+m}{2E_p}} \begin{pmatrix} -\frac{\sigma\cdot\mathbf{p}}{E_p+m} \\ 1 \end{pmatrix} \chi_s, \end{aligned} \tag{5.36}$$

as one can check explicitly by multipling by the left with $u^\dagger(\mathbf{p}, s)$ and $v^\dagger(-\mathbf{p}, s)$ of Eq. (5.13) and substituting the BSC angle $\theta(\mathbf{p})$ of Eq. (5.33). For the ground state to be completely specified, we then just need to fix the free parameters of the model using experimental data, which we will do next.

5.1.2 Fixing the Free Parameters

In the $SU(2)$ NJL model, we have two free parameters: the coupling G and the cutoff Λ. Therefore, we need two experimental pieces of data. We will use the qurak condensate and the pion electroweak decay constant f_π. Eq. (5.33) relates the product $G\Lambda^2$ to the constituent quark mass m. Therefore, we need one experimental quantity depending on m in order to fix $G\Lambda^2$. The quark condensate $\langle\bar{\psi}\psi\rangle$, although not directly accessible in experiments, is a parameter entering in QCD sum rules for hadronic observables, as hadrons masses [69]. Despite the uncertainties in the quark condensate values extracted in such studies, it is common in the literature (e.g., Refs. [70] and [34]) to adopt the value:

$$\langle\bar{\psi}_u\psi_u\rangle \approx \langle\bar{\psi}_d\psi_d\rangle \approx -(250\,\mathrm{MeV})^3. \tag{5.37}$$

This value is in reasonable agreement with with the values extracted in lattice QCD simulations [26]. In order to evaluate f_π in the NJL model, one needs to study the pion as a bound state of constituent quarks. We will not do this here and will simply quote the expression of f_π in the chiral limit [34]:

$$f_\pi^2 = N_c m^2 \int \frac{d^3p}{(2\pi)^3} \frac{1}{(p^2+m^2)^{3/2}}. \tag{5.38}$$

The value of f_π is very well determined expermentally, and we will follow Ref. [34] and take it as 93 MeV for the chiral limit. Given these values for $\langle\bar\psi\psi\rangle$ and f_π, one obtains $\Lambda \approx 653$MeV and $G\Lambda^2 \approx 2.14$, which leads to $m \approx 313$ MeV. This value is shown by the red dot marked on the curve in Fig. (5.1).

As seen, the NJL model brings a clear picture of the DCSB in QCD. As we show in the next section, it allows us to understand some features of the DCSB driven quark-antiquark entanglement. However, since it lacks asymptotic freedom, it fails to describe the ultraviolet behavior of the quark-antiquark pair-momentum entanglement in the vaccum. Such a feature is captured by the CGQH model which we discuss in the next section.

5.2 The Coulomb Gauge Quark Hamiltonian Model

The CGQH model builds on the QCD Hamiltonian in Coulomb gauge [32]. The Coulomb gauge QCD Hamiltonian comprises only dynamical degrees of freedom, quarks and transverse gluons. The Coulomb gauge fixing eliminates nondynamical degrees of freedom but creates an instantaneous interaction, the analogous to the Coulomb potential in electromagnetism. An attractive feature of this gauge is that it allows, in principle, to construct a Fock space to study hadron spectroscopy employing traditional many-body approaches. In particular, it allows us to construct phenomenological models based on the same degrees of freedom of the fundamental Hamiltonian. One of such models is our CGQH model, in that the effects of transverse-gluon degrees of freedom are modeled by an effective static potential that, among other features, includes an ultraviolet running that mimics asymptotic freedom. Moreover, the model Coulomb potential leads to color confinement, in that only color singlet states are finite-energy eigenstates of the Hamiltonian.

DCSB with such an Hamiltonian can be studied using the BCS-like approach discussed above for the NJL model. This approach as been used with similar models continuously since the 1980's, a selected set of references is provided by Refs. [71, 72, 73, 74, 75, 76, 77, 78, 79, 80, 81, 82, 83, 84, 85]. We employ the model discussed in Ref. [86]. We take from that reference only the pieces we need for our study here. The Hamiltonian of that model, including an explicit symmetry breaking quark-mass term, is given by:

$$
\begin{aligned}
H &= \int d^3x\, \bar{\psi}(\mathbf{x})(-i\gamma^i\partial_i + m_0)\psi(\mathbf{x}) - \frac{1}{2}\int d^3x d^3y\, \rho^a(\mathbf{x})V_c(|\mathbf{x}-\mathbf{y}|)\rho^a(\mathbf{y}) \\
&+ \frac{1}{2}\int d^3x d^3y\, J_i^a(\mathbf{x})D^{ij}(|\mathbf{x}-\mathbf{y}|)J_j^a(\mathbf{y}),
\end{aligned}
\tag{5.39}
$$

where m_0 is a diagonal matrix in the flavor space:

$$
m_0 = \mathrm{diag}(m_u, m_d, m_s, m_c, m_b), \tag{5.40}
$$

ρ^a is the color charge density:

$$
\rho^a(\mathbf{x}) = \psi^\dagger(\mathbf{x})T^a\psi(\mathbf{x}), \tag{5.41}
$$

with $T^a = \lambda^a/2$ as introduced earlier, and J_i^a is the color current density:

$$
J_i^a(\mathbf{x}) = \psi^\dagger(\mathbf{x})T^a\gamma_i\psi(\mathbf{x}). \tag{5.42}
$$

In Eq. (5.39), V_c models the QCD Coulomb potential and D^{ij} models the transverse gluon interactions:

$$
D^{ij}(|\mathbf{x}-\mathbf{y}|) = \left(\delta^{ij} - \frac{\partial^i\partial^j}{\partial^2}\right) D(|\mathbf{x}-\mathbf{y}|) \tag{5.43}
$$

where $D(|\mathbf{x}-\mathbf{y}|)$ is a scalar function.

Next, we proceed with the Bogoliubov-Valatin transformation of Hamiltonian, in a manner similar to that used in the NJL model. Ref. [86] does not perform the mean-field approximation at the level of the Hamiltonian, it simply writes the Bogoliubov-Valatin transformed Hamiltonian in Wick-contracted form and reads off the diagonal part of the Hamiltonian. When applied to the NJL model, this leads to the same result as that discussed in the previous section—for details, see Ref. [86].

Since now we have an explicit quark-mass symmetry breaking term in the

Hamiltonian, we need to take its effect into account in the Bogoliubov-Valatin transformation. The u and v spinors written in terms of massive Dirac plane-waves are given by:

$$u(\mathbf{p},s)=\sqrt{\frac{E_p+m_0}{2E_p}}\begin{pmatrix}1\\ \frac{\sigma\cdot\mathbf{p}}{E_p+m_0}\end{pmatrix}\chi_s,\quad v(-\mathbf{p},s)=\sqrt{\frac{E_p+m_0}{2E_p}}\begin{pmatrix}-\frac{\sigma\cdot\mathbf{p}}{E_p+m_0}\\ 1\end{pmatrix}\chi_s, \tag{5.44}$$

where $E_p=\sqrt{p^2+m_0^2}$, and we still have the normalization as:

$$u^\dagger(\mathbf{p},s)u(\mathbf{p},s')=v^\dagger(-\mathbf{p},s)v(-\mathbf{p},s')=\delta_{ss'}, \tag{5.45}$$

and the completeness relations:

$$\begin{aligned}\sum_s u(\mathbf{p},s)\bar{u}(\mathbf{p},s) &= \frac{1}{2E_p}(\not{p}+m_0),\\ \sum_s v(\mathbf{p},s)\bar{v}(\mathbf{p},s) &= \frac{1}{2E_p}(\not{p}-m_0).\end{aligned} \tag{5.46}$$

These reduce to Eq. (5.18) in the chiral limit. Next, we will again introduce the variational spinors with a Bogoliubov-Valatin transformation:

$$\begin{aligned}U(\mathbf{p},s) &= \cos\theta(\mathbf{p})u(\mathbf{p},s)-s\sin\theta(\mathbf{p})v(-\mathbf{p},s),\\ V(-\mathbf{p},s) &= \cos\theta(\mathbf{p})v(-\mathbf{p},s)+s\sin\theta(\mathbf{p})u(\mathbf{p},s),\end{aligned} \tag{5.47}$$

so that the quark fields can be written in the same way as Eq. (5.26), with the constituent quark operators given by Eq. (5.21). However, when dealing with a massive theory, it is convenient reparametrize the variational spinors by introducing the chiral angle $\phi(\mathbf{p})$ as in Ref. [87]:

$$\begin{aligned}U(\mathbf{p},s) &\equiv \frac{1}{\sqrt{2}}\begin{pmatrix}\sqrt{1+\sin\phi(\mathbf{p})}\\ \sqrt{1-\sin\phi(\mathbf{p})}\sigma\cdot\hat{\mathbf{p}}\end{pmatrix}\chi_s\\ V(-\mathbf{p},s) &\equiv \frac{1}{\sqrt{2}}\begin{pmatrix}-\sqrt{1-\sin\phi(\mathbf{p})}\sigma\cdot\hat{\mathbf{p}}\\ \sqrt{1+\sin\phi(\mathbf{p})}\end{pmatrix}\chi_s,\end{aligned} \tag{5.48}$$

so that it is related to the BCS angle $\theta(\mathbf{p})$ as:

$$\begin{aligned} \sin\phi(\mathbf{p}) &= \frac{m_0}{E_p}\cos 2\theta(\mathbf{p}) + \frac{p}{E_p}\sin 2\theta(\mathbf{p}), \\ \cos\phi(\mathbf{p}) &= \frac{p}{E_p}\cos 2\theta(\mathbf{p}) - \frac{m_0}{E_p}\sin 2\theta(\mathbf{p}). \end{aligned} \tag{5.49}$$

Note that, in the chiral limit, we have just $\phi(\mathbf{p}) = 2\theta(\mathbf{p})$ and this new parametrization gets somewhat trivial, and that's why we have worked just with $\theta(\mathbf{p})$ in the NJL model, but as long as $m_0 \neq 0$, some expressions, like the gap equation, get simpler with $\phi(\mathbf{p})$.

The momentum correlated vacuum state is still the one annihilated by all the constituent quark annihilation operators B and D, but now the BCS angle $\theta(\mathbf{p})$ depends on the current mass m_0. Since there is no flavor mixing in the CGQH model, the vacuum is given by

$$|\mathrm{vac}\rangle = \bigotimes_{f=1}^{N_f} |\mathrm{vac}\rangle_f, \tag{5.50}$$

with

$$|\mathrm{vac}\rangle_f = \prod_{\mathbf{p},s} \Big(\cos\theta_f(\mathbf{p}) - s\sin\theta_f(\mathbf{p}) b_f^\dagger(\mathbf{p},s) d_f^\dagger(-\mathbf{p},s)\Big)\, |0\rangle_f, \tag{5.51}$$

where we have still omitted the (trivial) color index. From now on, we will also omit the flavor index, keeping in mind that all the equations are for each flavor.

The Hamiltonian written in terms of the creation and annihilation constituent quark operators $B^\dagger(\mathbf{p},s)$, $D^\dagger(\mathbf{p},s)$, $B(\mathbf{p},s)$, and $D(\mathbf{p},s)$ can be split into a sum of three parts [86]:

$$H = E_0 + H_2 + H_4, \tag{5.52}$$

where E_0 is the vacuum energy and H_2 and H_4 are normal ordered operators quadratic and quartic in the B and D, respectively. We need here E_0 only; H_2 and H_4 are not needed because their vacuum expectation values vanish (they contribute to hadron bound states and scattering processes). The ground state is determined by minimizing E_0 with respect to $\theta(\mathbf{p})$, as we did in the NJL, which leads to a gap equation. As in the NJL model, we can express the gap equation either in terms of $\theta(\mathbf{p})$ (or $\phi(\mathbf{p})$) or in terms of a constituent quark mass function.

In the present case, because of the finite-range nature of the interaction, the constituent quark mass depends on the momentum. Specifically, the relationship is given by [83]

$$\sin\phi(\mathbf{p}) = \frac{M(\mathbf{p})}{\mathcal{E}(\mathbf{p})}, \tag{5.53}$$

where $\mathcal{E}(\mathbf{p}) = \sqrt{M^2(\mathbf{p}) + p^2}$, and the corresponding spinors are given by

$$\begin{aligned} U(\mathbf{p},s) &\equiv \sqrt{\frac{\mathcal{E}(\mathbf{p}) + M(\mathbf{p})}{2\mathcal{E}(\mathbf{p})}} \begin{pmatrix} 1 \\ \frac{\sigma\cdot\mathbf{p}}{\mathcal{E}(\mathbf{p})+M(\mathbf{p})} \end{pmatrix} \chi_s, \\ V(-\mathbf{p},s) &\equiv \sqrt{\frac{\mathcal{E}(\mathbf{p}) + M(\mathbf{p})}{2\mathcal{E}(\mathbf{p})}} \begin{pmatrix} -\frac{\sigma\cdot\mathbf{p}}{\mathcal{E}(\mathbf{p})+M(\mathbf{p})} \\ 1 \end{pmatrix} \chi_s. \end{aligned} \tag{5.54}$$

The gap equation for $M(\mathbf{p})$ is given by

$$M(\mathbf{p}) = m_0 + \frac{2}{3}\int \frac{d^3k}{(2\pi)^3}\Big[F_1(\mathbf{p},\mathbf{k})V_c(|\mathbf{p}-\mathbf{k}|) + 2G_1(\mathbf{p},\mathbf{k})D(|\mathbf{p}-\mathbf{k}|)\Big], \tag{5.55}$$

where $V_c(|\mathbf{p}-\mathbf{k}|)$ and $D(|\mathbf{p}-\mathbf{k}|)$ are the Fourier transforms of $V_c(|\mathbf{x}-\mathbf{y}|)$ and $D(|\mathbf{x}-\mathbf{y}|)$, and with the definitions:

$$\begin{aligned} F_1(\mathbf{p},\mathbf{k}) &= \frac{M(\mathbf{k})}{\mathcal{E}(\mathbf{k})} - \frac{M(\mathbf{p})}{\mathcal{E}(\mathbf{k})}\frac{k}{p}\hat{\mathbf{p}}\cdot\hat{\mathbf{k}} \\ G_1(\mathbf{p},\mathbf{k}) &= \frac{M(\mathbf{k})}{\mathcal{E}(\mathbf{k})} + \frac{M(\mathbf{p})}{\mathcal{E}(\mathbf{k})}\frac{k}{p}\frac{(\mathbf{p}\cdot\mathbf{k}-p^2)(\mathbf{p}\cdot\mathbf{k}-k^2)}{pk|\mathbf{p}-\mathbf{k}|^2}. \end{aligned} \tag{5.56}$$

To obtain explicit results, we have to specify the potentials V_c and D. For V_c, we will use the Model 2 from Ref. [86], that was also used in Ref. [88] to fit the spectrum of idealistic gluelump states and in Ref. [89] to model heavy quarkonia. It consists of a Coulomb long-range part V_l and a short-range part V_s:

$$V_c = V_l + V_s, \tag{5.57}$$

that are given by, in the momentum space:

$$V_l(p) = \frac{8\pi\sigma}{p^4}, \quad V_s(p) = \frac{4\pi\alpha(p)}{p^2}, \tag{5.58}$$

with the definition:

$$\alpha(p) \equiv \frac{4\pi Z}{\left[\beta \log(c + p^2/\Lambda_{QCD}^2)\right]^{3/2}}. \tag{5.59}$$

The parameters of the model were fitted in lattice calculations and are $\Lambda_{QCD} =$ 250MeV, $Z = 5.94$, $c = 40.68$ and $\beta = 10.08$. For the transverse potential D, Ref. [86] chooses:

$$D(p) = \frac{-4\pi\alpha_T}{(p^2 + m_g^2/4)\log^{1.42}(\tau + p^2/m_g^2)}, \tag{5.60}$$

with $m_g = 550\,\text{MeV}$, $\alpha_T = 0.5$ and $\tau = 1.05$. The Yukawa-like part of $D(p)$ was introduced as the Model 4 in Ref. [90] as the potential due to the exchange of a constituent gluon with mass m_g, and was used to study hyperfine splittings in the mesonic spectrum, whilst the log part mimics QCD's asymptotic freedom. Another feature of these potentials is that, when calculating expectation values of the normal ordered part of the Hamiltonian with hadronic states, we get infrared divergences for color nonsinglet states, realizing in this way color confinement [86]. Both $V_s(p)$ and $D(p)$ are asymptotically free. However, their ultraviolet runnings, $1/p^2(\log p^2)^{3/2}$ and $1/p^2(\log p^2)^{1.42}$ respectively, are different from that of QCD. For such runnings the gap equation is finite even for $m_0 \neq 0$, which is not the case in QCD. Therefore, the gap equation does not require renormalization. As such, the mass function in the ultraviolet behaves differently than in QCD, namely $M(p) \to m_0$ with log corrections. We recall that in QCD, the mass function runs as $M(p^2) \to \hat{m}/(\log p^2)^d$, where $\hat{m}$ is a renormalization group invariant mass and $d = 12/(33 - 2N_f)$ [91]. This is the reason why we say the CGQH model mimics, instead of reproduces, QCD's asymptotic freedom.

For our study, it suffices to solve the mass gap equation in Eq. (5.55) for the given potentials to investigate the chiral symmetry breaking, which can be done numerically by iteration. However, the long-range part of the potential, V_l, has a sharp IR peak, which, although cancelled exactly at $p = 0$ so that the integral converges, can be a problem to numerical methods. There are many ways to avoid this problem, and Ref. [86] chooses to modify the equation by adding a convenient zero:

$$M(\mathbf{p}) \to M(\mathbf{p}) - \int \frac{d^3k}{(2\pi^3)} \frac{1}{|\mathbf{p} - \mathbf{k}|^4} \frac{M(\mathbf{p})}{\mathcal{E}(\mathbf{p})} \frac{1}{p} \hat{\mathbf{p}} \cdot (\mathbf{p} - \mathbf{k}), \tag{5.61}$$

so that the function that multiplies the potential in the mass gap equation can be written as:

$$F_1(\mathbf{p},\mathbf{k}) \to \left(\frac{M(\mathbf{k})}{\mathcal{E}(\mathbf{k})} - \frac{M(\mathbf{p})}{\mathcal{E}(\mathbf{k})}\right) - \left(\frac{k}{p}\hat{\mathbf{p}}\cdot\hat{\mathbf{k}} - 1\right)\left(\frac{M(\mathbf{p})}{\mathcal{E}(\mathbf{k})} - \frac{M(\mathbf{p})}{\mathcal{E}(\mathbf{p})}\right) \tag{5.62}$$

and the peak is softened so it becomes numerically tractable.

Figure (5.2) displays results for the quark mass function for values of m_0 in correspondence with those of the PDG for the light (u,d,s) and heavy (c, b). The figure also displays the resulys for $m_0 = 0$, the chiral limit. As we can see, the net

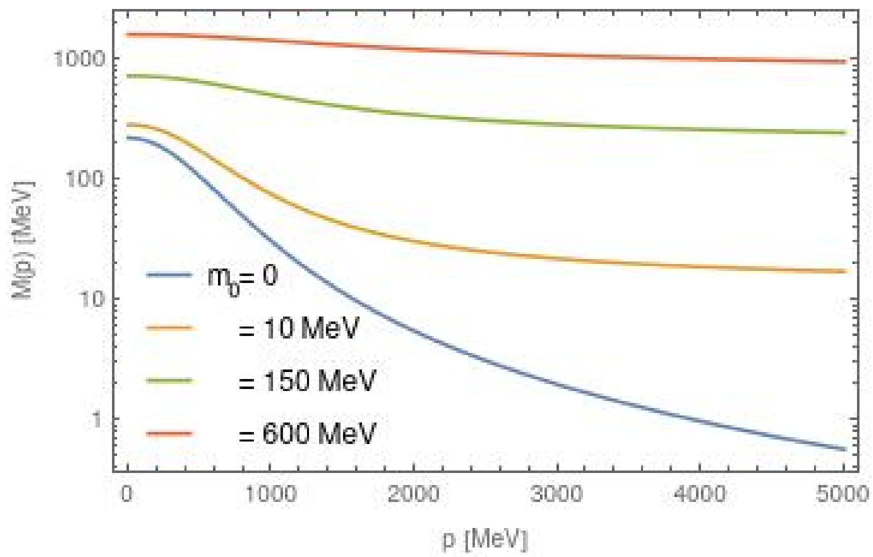

Figure 5.2: Constituent quark masses as a function of momentum.

dressing effect $M(p \sim 0) - m_0$ in the infrared region (low momenta) increases with m_0, but its relative value, $M(p \sim 0)/m_0$, gets smaller for heavier quarks. Moreover, we see that we recover the current masses in the ultraviolet region (large momenta), which is due to the model's asymptotic freedom. Note that, despite the large value of charm current mass, the dressing effect is still substantial; for example, at $p = 5\,\text{GeV}$, the constituent mass for $m_0 = 600\,\text{MeV}$ is still around $1\,\text{GeV}$. But again, the relative values, as we can see by the infrared to ultraviolet drop of the mass function, are more relevant for lighter quarks. For the bottom quark, the dressing effect is quite small and therefore not worthwhile to discuss it further for this quark flavor. These features have a direct impact on the entanglement of the quark-antiquark pair-momentum in the vacuum, as we discuss in the next chapter.

Chapter 6

DCSB and Entanglement in the NJL and CGQH Models

We apply the coherent-state formalism to compute entanglement measures of the quark-antiquark momentum modes in the vaccum of the models described in Chapter 5. In the first part of the chapter, we use the NJL model to set up the coherent state formalism of Chapter 3 to compute vacuum density matrices of the models. We compute the constituent-quark mass dependence of those entropies and introduce a new criterion for determining the physical vacuum state. The criterion is based on the entropy to energy ratio. In the second part of the chapter we apply the coherent-state formalism to the CGQH model. We study the role played by a momentum-dependent quark mass function on the entanglement entropy. In addition, we study the role played by the current quark-mass explicit symmetry breaking on the entanglement entropy.

6.1 DCSB and Entaglement in the NJL Model

In this section, we will apply the formalism we have built in Chapter 3 for the NJL model, using the construction in the Section 5.1.1 that is similar to the examples with two oscillators. We start by writing the variational vacuum in the exponential form so that it becomes similar to Eq. (3.69), which is, up to a normalization constant:

$$|\text{vac}\rangle = \prod_{\mathbf{p},s,f,c} \exp\{-\alpha(\mathbf{p},s)P^{\dagger}_{fc}(\mathbf{p},s)\}|0\rangle, \tag{6.1}$$

with the pair creation operator defined as:

$$P^{\dagger}_{fc}(\mathbf{p},s) = b^{\dagger}_{fc}(\mathbf{p},s)d^{\dagger}_{fc}(-\mathbf{p},s), \tag{6.2}$$

with $\mathbf{p}$ being the 3-dimensional momentum, $s = \pm 1$ being the helicity, f being the flavor and c the color. $|0\rangle$ is defined such that, as usual:

$$b_{fc}(\mathbf{p}, s)|0\rangle = d_{fc}(\mathbf{p}, s)|0\rangle = 0. \tag{6.3}$$

From now on, the flavor and color indices will be ommited. This construction differs only by a constant from Eq. (5.25) for the parametrization:

$$\alpha(\mathbf{p}, s) = s \tan\theta(\mathbf{p}). \tag{6.4}$$

As the exponent in Eq. (6.1) commutes with itself for any $(\mathbf{p}, s)$, we can exchange the productory for an exponential of a sum and write the corresponding density matrix as:

$$\rho = \mathcal{N} \exp\left\{-\sum_{\mathbf{p},s} s \tan\theta(\mathbf{p}) P^{\dagger}(\mathbf{p}, s)\right\}|0\rangle\langle 0| \exp\left\{-\sum_{\mathbf{p},s} s \tan\theta(\mathbf{p}) P(\mathbf{p}, s)\right\}, \tag{6.5}$$

with $P(\mathbf{p}, s)$ being the corresponding pair annihilation operator:

$$P(\mathbf{p}, s) = d(-\mathbf{p}, s) b(\mathbf{p}, s). \tag{6.6}$$

The infinite volume limit (the thermodynamic limit) is taken at the end of the calculation.

Now we are ready to construct the reduced density matrix for a given subspace. We define the total Fock space $\mathcal{F}$ as the span of all possible quark and antiquark single-particle states defined by the quark and antiquark $b^{\dagger}(\mathbf{p}, s)$ and $d^{\dagger}(\mathbf{p}, s)$ creation operators. Therefore, $\mathcal{F}$ can be written in terms of the tensor product of the quark $\mathcal{F}_b$ and antiquark $\mathcal{F}_d$ Fock subspaces:

$$\mathcal{F} = \mathcal{F}_b \otimes \mathcal{F}_d. \tag{6.7}$$

Therefore, one can define the coherent states $|z\rangle$ as:

$$|z\rangle = |z_b\rangle \otimes |z_d\rangle, \tag{6.8}$$

with

$$b(\mathbf{p}, s)|z_b\rangle = z_b(\mathbf{p}, s)|z_b\rangle, \quad d(\mathbf{p}, s)|z_d\rangle = z_d(\mathbf{p}, s)|z_d\rangle, \tag{6.9}$$

where the z's are Grassmann numbers that commute with the operators. Then, we obtain the reduced density matrix for the quarks by tracing out the antiquarks:

$$\rho_b = \mathrm{Tr}_d \rho = \mathcal{N}_b \int Dz_d^* Dz_d \, e^{-z_d^* \cdot z_d} \langle -z_d^* | \rho | z_d \rangle, \tag{6.10}$$

where

$$Dz_d^* Dz_d = \prod_{\mathbf{p},s} dz_d^*(\mathbf{p},s) dz_d(\mathbf{p},s), \;\; z_d^* \cdot z_d = \sum_{\mathbf{p},s} z_d^*(\mathbf{p},s) z_d(\mathbf{p},s). \tag{6.11}$$

The matrix element inside the functional integral gives:

$$\begin{aligned} \langle -z_d^* | \rho | z_d \rangle = & \quad \exp\left\{ -\sum_{\mathbf{p},s} \alpha(\mathbf{p},s) z_d^*(-\mathbf{p},s) b^\dagger(\mathbf{p},\mathbf{s}) \right\} |0\rangle\langle 0| \\ \times & \quad \exp\left\{ \sum_{\mathbf{p},s} \alpha(\mathbf{p},s) b^\dagger(\mathbf{p},\mathbf{s}) z_d(-\mathbf{p},s) \right\}. \end{aligned} \tag{6.12}$$

Next, we are going to work with the matrix elements of the reduced density matrix in the representation of the coherent states, that is:

$$\rho_b(z_b^*, z_b') \equiv \langle z_b^* | \rho_b | z_b' \rangle. \tag{6.13}$$

With this definition, the Eq. (6.10) becomes a Gaussian integral with Grassmanian sources:

$$\rho_b(z_b^*, z_b') = \mathcal{N}_b \int Dz_d^* Dz_d \, e^{-S}, \tag{6.14}$$

with S being defined as:

$$S = z_d^* \cdot z_d + \sum_{\mathbf{p},s} \alpha(\mathbf{p},s) z_b^*(\mathbf{p},s) z_d^*(-\mathbf{p},s) - \sum_{\mathbf{p},s} \alpha(\mathbf{p},s) z_d(-\mathbf{p},s) z_b'(\mathbf{p},s). \tag{6.15}$$

We have, then, up to a normalization constant, $\rho_b(z_b^*, z_b')$ written in the form of the integral I_5 in the Appendix B with:

$$\bar{\eta} = \alpha(\mathbf{p},s) z_b'(\mathbf{p},s), \;\; \eta = -\alpha(\mathbf{p},s) z_b^*(\mathbf{p},s), \;\; M = \mathbb{1}, \tag{6.16}$$

where we have used the symmetry of exchanging $\mathbf{p}$ for $-\mathbf{p}$ within the sums. Performing the integral, writing $\alpha(\mathbf{p},s)$ in terms of $\theta(\mathbf{p})$ and using $s^2 = 1$, we obtain:

$$\rho_b(z_b^*, z_b') = \mathcal{N}_b \exp\left\{ \sum_{\mathbf{p},s} \tan^2\theta(\mathbf{p}) z_b^*(\mathbf{p},s) z_b'(\mathbf{p},s) \right\}. \tag{6.17}$$

The normalization constant can be obtained by imposing $\mathrm{Tr}_b \rho_b = 1$, that is:

$$\mathcal{N}_b^{-1} = \int Dz_b^* Dz_b \, e^{-z_b^* \cdot z_b} \exp\left\{ -\sum_{\mathbf{p},s} \tan^2\theta(\mathbf{p}) z_b^*(\mathbf{p},s) z_b(\mathbf{p},s) \right\}, \tag{6.18}$$

which is the integral I_4 in the Appendix B in which (restoring the flavor and color indices):

$$M^{ff';cc'}_{\mathbf{p}\mathbf{p}';ss'} = \left(1 + \tan^2\theta(\mathbf{p})\right) \delta_{\mathbf{p}\mathbf{p}'} \delta_{ss'} \delta^{ff'} \delta^{cc'}. \tag{6.19}$$

As M is a diagonal matrix, the normalization constant $\mathcal{N}_b^{-1}$ becomes:

$$\mathcal{N}_b^{-1} = \exp\left\{ 2N_c N_f \sum_{\mathbf{p}} \log\left(1 + \tan^2\theta(\mathbf{p})\right) \right\} \tag{6.20}$$

with N_f being the number of flavors and N_c the number of colors.

Now that we have obtained the reduced density matrix for the quarks in the coherent states representation, we can proceed to evaluate the purity $P = \mathrm{Tr}\, \rho_b^2$ as an entanglement measure. First, we note that:

$$\rho_b^2(z_b^*, z_b') = \langle z_b^* | \rho_b \cdot \mathbb{1}_b \cdot \rho_b | z_b' \rangle, \tag{6.21}$$

where $\mathbb{1}_b$ is the identity operator in the quark subspace. Second, we use the resolution of this identity as:

$$\mathbb{1}_b = \int D\bar{z}_b^* D\bar{z}_b \, e^{-\bar{z}_b^* \cdot \bar{z}_b} |\bar{z}_b\rangle \langle \bar{z}_b^*|, \tag{6.22}$$

so that we have:

$$\rho_b^2(z_b^*, z_b') = \int D\bar{z}_b^* D\bar{z}_b \, e^{-\bar{z}_b^* \cdot \bar{z}_b} \rho_b(z_b^*, \bar{z}_b) \rho_b(\bar{z}_b^*, z_b'). \tag{6.23}$$

Therefore, the purity is obtained as:

$$P = Tr_b \rho_b^2 = \int Dz_b^* Dz_b \, e^{-z_b^* \cdot z_b} \rho_b^2(-z_b^*, z_b). \tag{6.24}$$

Third, we note that:

$$\rho_b^2(-z_b^*, z_b) = \mathcal{N}_b^2 \int D\bar{z}_b^* D\bar{z}_b \exp\left\{-\bar{z}_b^* \cdot \bar{z}_b - \sum_{\mathbf{p},s} \tan^2\theta(\mathbf{p}) z_b^*(\mathbf{p},s)\bar{z}_b(\mathbf{p},s)\right\} \\ \times \exp\left\{\sum_{\mathbf{p},s} \tan^2\theta(\mathbf{p})\bar{z}_b^*(\mathbf{p},s) z_b(\mathbf{p},s)\right\}, \quad (6.25)$$

wich is again the integral I_5 from Appendix B with:

$$\bar{\eta} = \tan^2(\theta(\mathbf{p}))z_b^*(\mathbf{p},s), \quad \eta = -\tan^2(\theta(\mathbf{p}))z_b(\mathbf{p},s), \quad M = \mathbb{1}. \quad (6.26)$$

Therefore:

$$\rho_b^2(-z_b^*, z_b) = \mathcal{N}_b^2 \exp\left\{-\sum_{\mathbf{p},s} \tan^4\theta(\mathbf{p}) z_b^*(\mathbf{p},s) z_b(\mathbf{p},s)\right\}. \quad (6.27)$$

Plugging Eq. (6.27) in Eq. (6.24), we obtain:

$$\begin{aligned} P &= \mathcal{N}_b^2 \int Dz_b^* Dz_b \, \exp\left\{-\sum_{\mathbf{p},s} z_b^*(\mathbf{p},s)\left(1+\tan^4(\theta(\mathbf{p})\right) z_b(\mathbf{p},s)\right\} \\ &= \mathcal{N}_b^2 \det\left\{\left[1+\tan^4\theta(\mathbf{p})\right] \mathbb{1}_{\mathbf{p},s}\mathbb{1}_{f,c}\right\}. \end{aligned} \quad (6.28)$$

where we restored again the flavor and color indices. Fourth, using Eq. (6.20) and the identity

$$\det M = \exp\{\mathrm{Tr} \log M\}, \quad (6.29)$$

the purity becomes:

$$P = \frac{\exp\left\{2N_c N_f \sum_{\mathbf{p}} \log\left[1+\tan^4\theta(\mathbf{p})\right]\right\}}{\exp\left\{4N_c N_f \sum_{\mathbf{p}} \log\left[1+\tan^2\theta(\mathbf{p})\right]\right\}}. \quad (6.30)$$

Finally, one can now take infinite-volume limit in Eq. (6.30) in 3 dimensions by using

$$\sum_{\mathbf{p}} \to \frac{V}{(2\pi)^3} \int d^3\mathbf{p}, \quad (6.31)$$

and the fact that $\theta(\mathbf{p}) = \theta(|\mathbf{p}|) = \theta(p)$, which gives a factor of 4π for the integral over the solid angles, so that one obtains the final expression for the purity:

$$P = \frac{\exp\left\{\frac{V}{\pi^2}N_c N_f \int_0^\Lambda dp p^2 \log\left[1+\tan^4\theta(p)\right]\right\}}{\exp\left\{\frac{2V}{\pi^2}N_c N_f \int_0^\Lambda dp p^2 \log\left[1+\tan^2\theta(p))\right]\right\}}, \tag{6.32}$$

in which we reintroduced the cutoff Λ, as required by the nonrenormalizability of the NJL model.

Having obtained the result for the purity, we can evaluate the second Rényi entropy, given by:

$$S_2 = -\log P \tag{6.33}$$

which scales with the volume of the space. Defining the corresponding density as:

$$s_2 \equiv \frac{S_2}{V}, \tag{6.34}$$

we obtain:

$$s_2 = \frac{N_c N_f}{\pi^2}\int_0^\Lambda dp p^2 \left\{\log\left[1+\tan^4\theta(p)\right] - 2\log\left[1+\tan^2\theta(p)\right]\right\}. \tag{6.35}$$

We can also compute the n^{th} Rényi entropy. It can be done by noting that:

$$\rho_b^n(z_b^*, z_b') = \langle z_b^*|\rho_b \cdot \mathbb{1}_b \cdot \rho_b \cdot \mathbb{1}_b \cdots \rho_b|z_b'\rangle, \tag{6.36}$$

where we have put $n-1$ resolutions of the identity between the n density matrices. It becomes:

$$\begin{aligned}\rho_b^n(z_b^*, z_b') &= \int D\bar{z}_{1b}^* D\bar{z}_{1b} \cdots D\bar{z}_{(n-1)b}^* D\bar{z}_{(n-1)b}\, e^{-\sum_{i=1}^{n-1}\bar{z}_{ib}^*\cdot\bar{z}_{ib}}\, \rho_b(z_b^*, \bar{z}_{1b}) \\ &\quad \times \rho_b(\bar{z}_{1b}^*, \bar{z}_{2b}) \cdots \rho_b(\bar{z}_{(n-1)b}^*, z_b'),\end{aligned} \tag{6.37}$$

where the product of the density matrices in the coherent states representation gives:

$$\begin{aligned}\rho_b(z_b^*, \bar{z}_{1b}) \cdots \rho_b(\bar{z}_{(n-1)b}^*, z_b') &= \mathcal{N}_b^n \exp\left\{\sum_{\mathbf{p},s}\tan^2\theta(\mathbf{p}) z_b^*(\mathbf{p},s)\bar{z}_{1b}(\mathbf{p},s)\right\} \\ \times \exp\left\{\sum_{\mathbf{p},s}\tan^2\theta(\mathbf{p})\left[\bar{z}_{1b}^*(\mathbf{p},s)\bar{z}_{2b}(\mathbf{p},s) + \cdots + \bar{z}_{(n-1)b}^*(\mathbf{p},s) z_b'(\mathbf{p},s)\right]\right\}&.\end{aligned} \tag{6.38}$$

Equation (6.37) can be performed as $n-1$ chained Gaussian integrals with sources. The term in the exponent that contributes to the integral over $D\bar{z}^*_{1b}D\bar{z}_{1b}$ is:

$$\sum_{\mathbf{p},s}\left[-\bar{z}^*_{1b}(\mathbf{p},s)\bar{z}_{1b}(\mathbf{p},s)+\tan^2\theta(\mathbf{p})\left(z^*_b(\mathbf{p},s)\bar{z}_{1b}(\mathbf{p},s)+\bar{z}^*_{1b}(\mathbf{p},s)\bar{z}_{2b}(\mathbf{p},s)\right)\right], \tag{6.39}$$

which by doing the integral is replaced by the product of the sources, namely:

$$\sum_{\mathbf{p},s}\tan^4\theta(\mathbf{p})z^*_b(\mathbf{p},s)\bar{z}_{2b}(\mathbf{p},s). \tag{6.40}$$

Therefore, the new term in the exponent for the integral over $D\bar{z}^*_{2b}D\bar{z}_{2b}$ becomes:

$$\begin{aligned}\sum_{\mathbf{p},s}\Big[&\bar{z}_{2b}(\mathbf{p},s)\bar{z}_{2b}(\mathbf{p},s)\\&+\tan^2\theta(\mathbf{p})\left(\tan^2\theta(\mathbf{p})z^*_b(\mathbf{p},s)\bar{z}_{2b}(\mathbf{p},s)+\bar{z}^*_{2b}(\mathbf{p},s)\bar{z}_{3b}(\mathbf{p},s)\right)\Big],\end{aligned} \tag{6.41}$$

so that each integral raises the power of $\tan\theta(\mathbf{p})$ by 2 because of this chain relation. Therefore, the remaining term in the exponent for the integral over $D\bar{z}^*_{(n-1)b}D\bar{z}_{(n-1)b}$ is:

$$\begin{aligned}\sum_{\mathbf{p},s}\Big[&-\bar{z}_{(n-1)b}(\mathbf{p},s)\bar{z}_{(n-1)b}(\mathbf{p},s)\\&+\tan^2\theta(\mathbf{p})\left(\tan^{2(n-1)}\theta(\mathbf{p})z^*_b(\mathbf{p},s)\bar{z}_{(n-1)b}(\mathbf{p},s)+\bar{z}^*_{(n-1)b}(\mathbf{p},s)z'_b(\mathbf{p},s)\right)\Big],\end{aligned} \tag{6.42}$$

and we get that, performing all $n-1$ chained integrals, the exponent becomes

$$\sum_{\mathbf{p},s}\tan^{2n}\theta(\mathbf{p})z^*_b(\mathbf{p},s)z'_b(\mathbf{p},s). \tag{6.43}$$

Then we can take the trace by doing:

$$\mathrm{Tr}\rho^n_b=\int Dz^*_bDz_b\,e^{-z^*_b\cdot z_b}\,\rho^n_b(-z^*_b,z_b). \tag{6.44}$$

The n^{th} Rényi entropy density follows from the formula:

$$s_n=\frac{1}{V(1-n)}\log\mathrm{Tr}\rho^n_b, \tag{6.45}$$

namely:

$$s_n = \frac{N_c N_f}{\pi^2(1-n)} \int_0^{\Lambda} dp p^2 \Big[\log(1+\tan^{2n}\theta(p)) - n\log(1+\tan^2\theta(p))\Big]. \quad (6.46)$$

From the n^{th} Rényi, we can evaluate the entanglement entropy density using the relation:

$$s_E = \lim_{n\to 1} s_n. \quad (6.47)$$

As it gives $0/0$, we can use L'Hospital's rule and obtain:

$$s_E = -\frac{N_c N_f}{\pi^2} \lim_{n\to 1} \frac{\partial}{\partial n} \int_0^{\Lambda} dp p^2 \Big[\log(1+\tan^{2n}\theta(p)) - n\log(1+\tan^2\theta(p)\Big], \quad (6.48)$$

which results in:

$$s_E = \frac{N_c N_f}{\pi^2} \int_0^{\Lambda} dp p^2 \left[\log(1+\tan^2\theta(p)) - \frac{\tan^2\theta(p)\log(\tan^2\theta(p))}{1+\tan^2\theta(p)}\right]. \quad (6.49)$$

Then, we can use Eq. (5.31) to express the entropies as a function of the mass of the constituent quarks, as it implies:

$$\tan\theta(p) = \frac{E_p - p}{m}, \quad (6.50)$$

and work with the dimensionless quantities:

$$p_\Lambda = p/\Lambda, \;\; m_\Lambda = m/\Lambda, \quad (6.51)$$

so the dimensionless entropy densities become:

$$\begin{aligned} \Lambda^{-3} s_n(m_\Lambda) \;\; &= \;\; \frac{N_c N_f}{\pi^2(1-n)} \int_0^1 dp_\Lambda p_\Lambda^2 \left\{ \log\left[1 + \left(\frac{E_{p_\Lambda} - p_\Lambda}{m_\Lambda}\right)^{2n}\right] \right. \\ &- \;\; \left. n\log\left[1 + \left(\frac{E_{p_\Lambda} - p_\Lambda}{m_\Lambda}\right)^{2}\right] \right\}, \end{aligned} \quad (6.52)$$

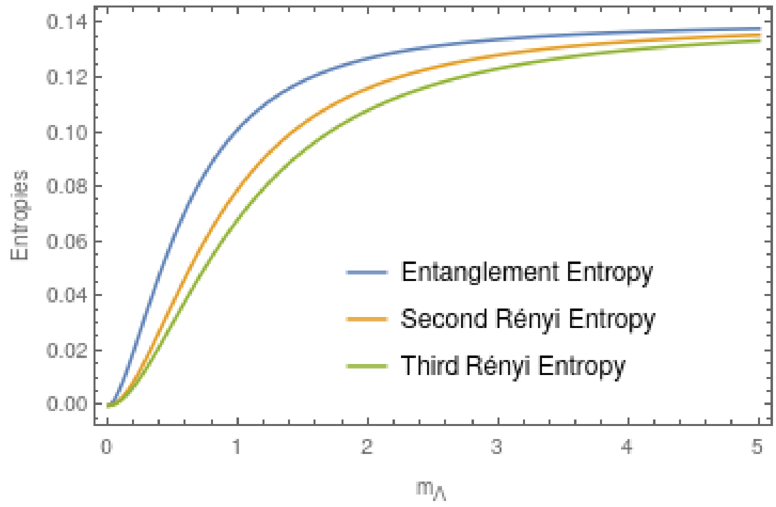

Figure 6.1: Dimnesionless Rényi and entanglement entropies as a function of the dimensionless constituent quark mass for the $SU(2)$ NJL model.

$$\begin{aligned}\Lambda^{-3}s_E(m_\Lambda) \quad &= \quad \frac{N_cN_f}{\pi^2}\int_0^1 dp_\Lambda p_\Lambda^2\left\{\log\left[1+\left(\frac{E_{p_\Lambda}-p_\Lambda}{m_\Lambda}\right)^2\right]\right. \\ &- \left.\frac{(E_{p_\Lambda}-p_\Lambda)^2\log\left[\left(\frac{E_{p_\Lambda}-p_\Lambda}{m_\Lambda}\right)^2\right]}{m^2+(E_p-p)^2}\right\}. \end{aligned} \tag{6.53}$$

Figure (6.1) shows the results for the different entropies we have computed. DCSB induces entanglement in the quark-antiquark momentum correlations, with the entanglement increasing with the strength of the symmetry breaking. The result is in qualitative agreement with our physical expectations outlined in the Introduction. Quantitatively, one should keep in mind that the NJL constituent quark mass is a constant and therefore misses the momentum running of the mass function. The mass function momentum running affects the momentum dependence of the quark-antiquark pairing through $\tan\theta(p)$ and affects the ultraviolet behavior of entanglement entropy. This we explore next with the CGQH model.

Next, we look into the entanglement per energy ratio. In order to do that, we write down the vacuum energy density of Eq. (5.28) as a function of the dimensionless constituent quark mass:

$$\Lambda^{-4}E(m_\Lambda) = -\frac{N_cN_f}{\pi^2}\int_0^1 \frac{dp_\Lambda p_\Lambda^3}{\sqrt{m_\Lambda^2+p_\Lambda^2}} - \frac{m_\Lambda^2 N_cN_f}{4G_\Lambda}, \tag{6.54}$$

where G_Λ is also specified for a given m_Λ using Eq. (5.33). With this in hand, we can plot the dimensionless ratio of the entanglement entropy and the vacuum energy density as a function of the constituent quark mass.

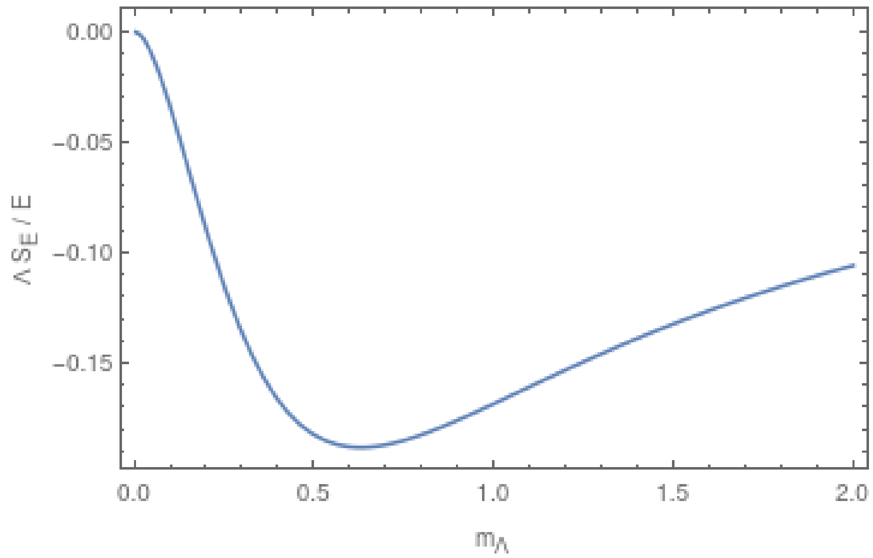

Figure 6.2: Dimensionless ratio of entanglement entropy and vacuum energy densities as a function of the constituent quark mass for the NJL $SU(2)$ model.

We see in Fig. (6.2) that there is an absolute minimum (as the sign of the energy is always negative for a state that has less energy than the trivial vacuum) for this ratio around $m_\Lambda = 0.628$. If we set this value as the physical for the dimensionless constituent quark mass, in order to get the right value for the pion decay constant, using Eq. (5.38), we need to set $\Lambda \approx 602\,\text{MeV}$. Then, the NJL condition of Eq. (5.33) implies $G_\Lambda \approx 2.38$. Using these values on Eq. (5.11), we get:

$$\langle \bar{\psi}_u \psi_u \rangle \approx -(243\,\text{MeV})^3, \tag{6.55}$$

which is compatible with the value in Eq. (5.37). This might indicate a criterion to constrain the physical vacuum, namely as the one generating the most quark-antiquark pair-momentum entanglement with the less energy gap. Such a criterion would be in line with the maximal entanglement conjecture presented in, e.g., Ref. [11] in a different context. Of course, such a conjecture is based on a simplified model and needs closer scrutiny.

6.2 DCSB and entanglement in the CGQH Model

In this section, we explore the consequences of having a momentum running of the quark mass function on the entanglement. We also study the role played by explicit symmetry breaking current quark masses on the quark-antiquark momentum correlations induced by the symmetry breaking. We compute the entanglement entropy for two different vacuum setups in the context of the CGHQ model described in Section 5.2. In the first vacuum setup, the induced quark-antiquark momentum correlations contain both explicit and dynamical symmetry breaking. In the second vacuum setup, we attempt to remove from the entanglement entropy the entanglement induced by the explicit symmetry breaking and so access the dynamical entanglement induced by the interaction.

6.2.1 Explicit and dynamical symmetry breaking

Since we have used for the CGQH in Section 5.2 the same procedure as for the NJL model to diagonalize the Hamiltonian, it becomes straightforward to generalize our entanglement entropy calculations. Indeed, as the variational vacuum is of the form of Eq. (5.25) for each flavor, the entanglement entropy of Eq. (6.49) is also valid and all we need to do is specify the BCS angle $\theta(\mathbf{p})$. This can be done by inverting Eq. (5.49) as:

$$\sin 2\theta(\mathbf{p}) = \frac{p}{E_p}\sin\phi(\mathbf{p}) - \frac{m_0}{E_p}\cos\phi(\mathbf{p}), \tag{6.56}$$

$$\cos 2\theta(\mathbf{p}) = \frac{p}{E_p}\cos\phi(\mathbf{p}) + \frac{m_0}{E_p}\sin\phi(\mathbf{p}), \tag{6.57}$$

and using Eq. (5.53) to obtain $\tan\theta(\mathbf{p})$ in terms of the effective mass $M(\mathbf{p})$ and the current mass m_0 as:

$$\tan\theta(\mathbf{p}) = \frac{1-\cos 2\theta(\mathbf{p})}{\sin 2\theta(\mathbf{p})} = \frac{E_p\mathcal{E}(\mathbf{p}) - p^2 - m_0 M(\mathbf{p})}{p(M(\mathbf{p}) - m_0)}. \tag{6.58}$$

As seen in the previous chapter, the explicit symmetry breaking current-quark mass entails different values of $M(\mathbf{p})$ and $\tan\theta(\mathbf{p})$ for different values of m_0. Of course, this fact does not change the way the entanglement entropy is derived, as the there is no flavor mixing in variational vacuum and the reduced density matrix of the quarks subspace becomes a product of density matrices for each flavor. Therefore, we can proceed with the calculations in the same way as for the NJL and compute the entanglement entropy. As in the NJL model, the entanglement total entropy density is given by the sum of the entropy densities for each flavor, that is:

$$s_E = \sum_{f=1}^{N_f} s_E^f(m_0), \tag{6.59}$$

where again we labeled the flavors with numbers from 1 to N_f. We then import the expression we had for the NJL model:

$$s_E^f(m_0) = \frac{N_c}{\pi^2} \int dpp^2 \left(\log(1 + \tan^2\theta_f(p)) - \frac{\tan^2\theta_f(p)\log(\tan^2\theta_f(p))}{1+\tan^2\theta_f(p)} \right). \tag{6.60}$$

The momentum running of the mass function affects the ultraviolet behavior of the integrand in Eq. (6.60). As for a QCD running mass, the CHQH running mass function makes that integral divergent, just the same way as the quark condensate is divergent. Therefore, one needs to specify a momentum scale μ for which one intends to quote a value for the entanglement entropy. In the same way one computes the μ-dependence of the quark condensate, one would need to evaluate the integral up to some large momentum Λ and then run the result to the intended μ with the use of renormalization group equations. In the present case, this would not be different. However, for the purpose of getting insight into the DCSB induced entanglement, we can simplify the analysis. The divergence is very mild because $\theta(p)$ decreases logarithmically with p; from Eq. (6.58) we have that, for $p \to \infty$:

$$\tan\theta(p) \approx \frac{M(p) - m_0}{2p} - \frac{M(p)^3 - m_0^3 + m_0 M(p)^2 - m_0^2 M(p)}{8p^3} + \cdots . \tag{6.61}$$

Since $M(p) - m_0$ decreases logarithmically with p, so does $\tan\theta(p)$. Now, since the DCSB is an infrared effect, the integrand in Eq. (6.60) grows at low momenta and then decays logarithmically for large p. Therefore, one can grasp the DCSB effect on the entanglement entropy by computing $s_E^f(m_0)$ up to some large momentum and then perform, e.g., the ratio of $s_E^f(0)$, the entanglement entropy in the chiral limit, with $s_E^f(m_0)$ for $m_0 \neq 0$.

Before we proceed with the numerical analyses, we notice that we have an important prediction here, namely: the entanglement entropy associated with the quark-antiquark momentum correlations induced by DCSB in the vacuum runs with the renormalization group scale μ determined by ultraviolet running of the mass function. Therefore, in the chiral limit the entanglement entropy is finite since the mass function runs as $M(p) \sim 1/p^2(\log p^2/\Lambda^2_{QCD})^{d-1}$ [91].

Using the numerical results from Section 5.2 for $M(p)$, we then obtain the entanglement entropy density as a function of m_0 up to a very large momentum (in the present case, up to $p \simeq 2.5 \times 10^6$ MeV). We present the results in Fig. (6.3), in which we plot the m_0 dependence of the ratio of $s^f_E(m_0)$ for $m_0 = 0$ and $m_0 \neq 0$.

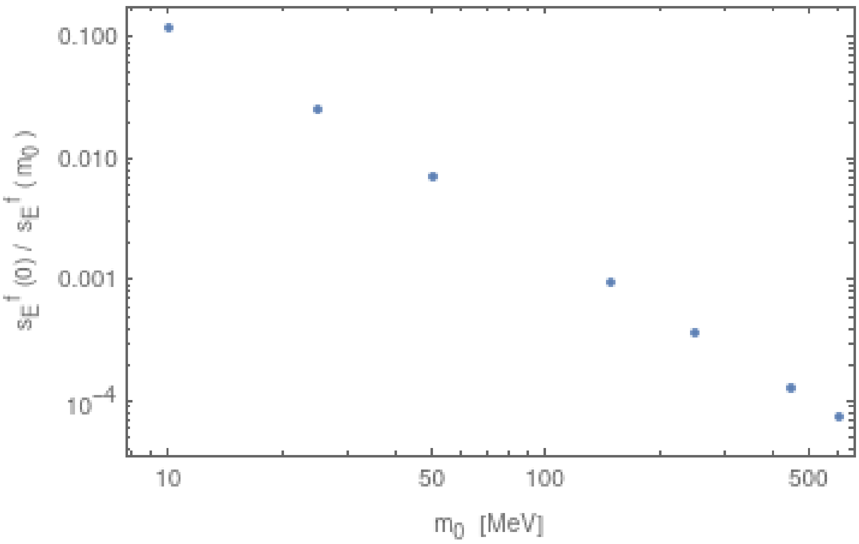

Figure 6.3: Entanglement entropy ratios in the $m_0 = 0$ chiral limit and for $m_0 \neq 0$.

Figure 6.3 reveals that the entanglement entropy $s^f_E(m_0)$ grows with m_0 (as the ratio descreases with m_0). This happens because the dressing effect at low energies, $M(p \approx 0) - m_0$, grows with m_0, despite its value relative to m_0 gets smaller, as discussed in the previous chapter. This is due to the way we have defined our Fock space partition, as the quark and antiquark creation and annihilation operators already take the current mass into account. In the next subsection we reformulate the problem by constructing the entangled vacuum from a chirally symmetric vacuum.

6.2.2 Removal of Explicit Chiral Symmetry Breaking

We reformulate the Bogoliubov-Valatin setup of the quark-antiquark pair-momentum entangled vacuum. Specifically, we start from the chiral vacuum and expand the quark fields in massless Dirac plane-waves:

$$\psi(\mathbf{x},0) = \sum_s \int \frac{d^3p}{(2\pi^3)} \left(b_{ch}(\mathbf{p},s) u_{ch}(\mathbf{p},s) + d^\dagger_{ch}(-\mathbf{p},s) v_{ch}(-\mathbf{p},s) \right) e^{i\mathbf{p}\cdot\mathbf{x}}, \tag{6.62}$$

with the spinors given by:

$$u_{ch}(\mathbf{p},s) = \frac{1}{\sqrt{2}} \begin{pmatrix} 1 \\ \sigma\cdot\hat{\mathbf{p}} \end{pmatrix} \chi_s, \quad v_{ch}(-\mathbf{p},s) = \frac{1}{\sqrt{2}} \begin{pmatrix} -\sigma\cdot\hat{\mathbf{p}} \\ 1 \end{pmatrix} \chi_s. \tag{6.63}$$

Then, we can make a Bogoliubov-Valatin transformation that takes the chiral spinors straight to the constituent spinors, that is:

$$\begin{aligned} U(\mathbf{p},s) &= \cos\theta(\mathbf{p}) u_{ch}(\mathbf{p},s) - s\sin\theta(\mathbf{p}) v_{ch}(-\mathbf{p},s) \\ &\equiv \sqrt{\frac{\mathcal{E}(\mathbf{p}) + M(\mathbf{p})}{2\mathcal{E}(\mathbf{p})}} \begin{pmatrix} 1 \\ \frac{\sigma\cdot\mathbf{p}}{\mathcal{E}(\mathbf{p})+M(\mathbf{p})} \end{pmatrix} \chi_s, \end{aligned} \tag{6.64}$$

$$\begin{aligned} V(-\mathbf{p},s) &= \cos\theta(\mathbf{p}) v_{ch}(-\mathbf{p},s) + s\sin\theta(\mathbf{p}) u_{ch}(\mathbf{p},s) \\ &\equiv \sqrt{\frac{\mathcal{E}(\mathbf{p}) + M(\mathbf{p})}{2\mathcal{E}(\mathbf{p})}} \begin{pmatrix} -\frac{\sigma\cdot\mathbf{p}}{\mathcal{E}(\mathbf{p})+M(\mathbf{p})} \\ 1 \end{pmatrix} \chi_s, \end{aligned} \tag{6.65}$$

so that we get $\cos\theta(\mathbf{p})$ and $\sin\theta(\mathbf{p})$ by multiplying, e.g., Eq.(6.64) respectively by $u^\dagger_{ch}(\mathbf{p},s)$ and $sv^\dagger_{ch}(-\mathbf{p},s)$ by the left, which imples:

$$\tan\theta(\mathbf{p}) = \frac{\mathcal{E}(\mathbf{p}) - p}{M(\mathbf{p})}. \tag{6.66}$$

The basis transformation is of the same kind as the one made previously and therefore the single-flavor entanglement entropy is given by Eq. (6.60). But the ultraviolet behavior of $\tan\theta(p)$ is different in the present case, namely: for $p \to \infty$ we have that, up to log corrections:

$$\tan\theta(\mathbf{p}) \approx \frac{m_0}{2p}. \tag{6.67}$$

As in the previous subsection, this makes the entanglement divergent, albeit with a different log behavior.

To extract from the full entanglement entropy the contribution from the explicit chiral symmetry breaking, we perform another Bogoliubov-Valatin transformation parametrized by an angle $\theta_0(p)$ that brings the chiral spinors to the ones with current quark masses m_0:

$$\begin{aligned} U_0(\mathbf{p}, s) &= \cos\theta_0(\mathbf{p}) u_{ch}(\mathbf{p}, s) - s\sin\theta_0(\mathbf{p}) v_{ch}(-\mathbf{p}, s) \\ &\equiv \sqrt{\frac{E_p + m_0}{2E_p}} \begin{pmatrix} 1 \\ \frac{\sigma\cdot\mathbf{p}}{E_p+m_0} \end{pmatrix} \chi_s, \end{aligned} \tag{6.68}$$

$$\begin{aligned} V_0(-\mathbf{p}, s) &= \cos\theta_0(\mathbf{p}) v_{ch}(-\mathbf{p}, s) + s\sin\theta_0(\mathbf{p}) u_{ch}(\mathbf{p}, s) \\ &\equiv \sqrt{\frac{E_p + m_0}{2E_p}} \begin{pmatrix} -\frac{\sigma\cdot\mathbf{p}}{E_p+m_0} \\ 1 \end{pmatrix} \chi_s, \end{aligned} \tag{6.69}$$

so that we obtain:

$$\tan\theta_0(p) = \frac{E_p - p}{m_0}. \tag{6.70}$$

The corresponding entanglement entropy is given by:

$$s_0^f = \frac{N_c}{\pi^2}\int dp p^2 \left(\log(1+\tan^2\theta_0(p)) - \frac{\tan^2\theta_0(p)\log(\tan^2\theta_0(p))}{1+\tan^2\theta_0(p)}\right). \tag{6.71}$$

The noninteracting chiral vacuum refers to the vacuum annihilated by quark and antiquark annihilation operators with well defined chirality. In the new vacuum with explicit chiral symmetry breaking, left-handed and right-handed quarks get mixed or momentum-correlated due to the mass term in the Hamiltonian. The entropy in Eq. (6.71) refers to this mixing or correlation induced by the explicit breaking. But our interest is in the correlation induced by the interaction and so we aim to extract, so to say, the trivial entropy from the full entropy.

Let us consider the ratio

$$s_R^f(m_0, \Lambda) \equiv \frac{s_E^f(m_0, \Lambda)}{s_0^f(m_0, \Lambda)}, \tag{6.72}$$

where Λ is the momentum up to which the integrals of the entropies are calculated (this Λ should not be confused with the NJL cutoff). As $\Lambda \to \infty$ limit, $s_R^f(m_0, \Lambda) \to 1$. Therefore, by varying Λ from the infrared to the ultraviolet, one would reveal the effect of the interaction on the entanglement, as shown Fig. (6.4).

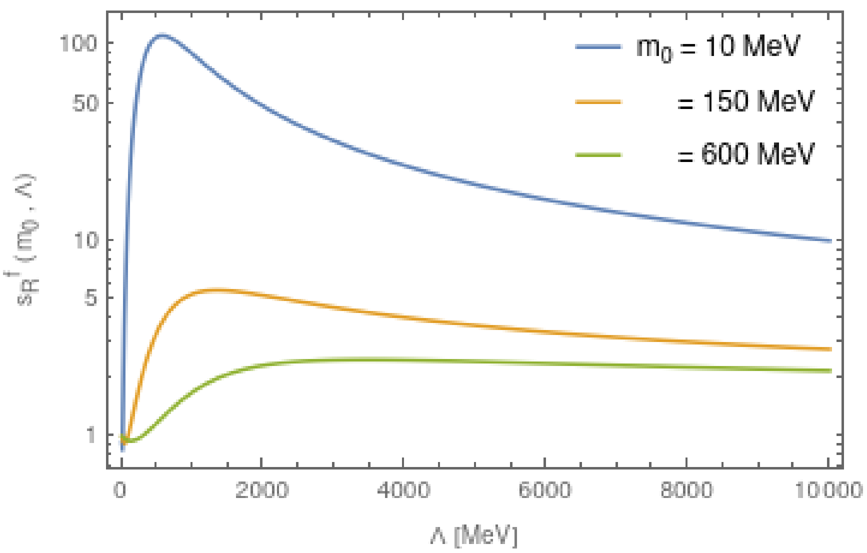

Figure 6.4: The ratio $s_R^f(m_0, \Lambda)$ of entanglement entropies defined in Eq. (6.72) as a function of Λ, the upper limit of the integrals determining the entanglement entropies.

The physics behind the result shown in the figure should be clear: the interaction induced entanglement dominates by far in the infrared, whereas the m_0 induced entanglement is more effective in the ultraviolet. The result reiterates in a more dramatic way what we have have already seen in Section 5.2 that dynamical chiral symmetry breaking gets less important for heavier quarks but still not neglegible for the c quark.

As we have seen in all the cases we have discussed, entanglement measures bring complementary information on the DCSB phenomenon. Although our study is limited to the two models we considered, there is room for optimism that some of the qualitative results will survive further scrutiny with more sophisticated models or even lattice QCD simulations. For example, the prediction that the entanglement entropy runs with the renormalization group scale μ determined by the ultraviolet running of the mass function should be testable with lattice simulations. If confirmed, this would be a major advancement in our understanding of DCSB in QCD.

Chapter 7

Conclusions and Perspectives

The primary goal of this study was to set up a formalism to quantify quantum entanglement of quark-antiquark momentum correlations due to the dynamical chiral symmetry breaking (DCSB) in quantum chromodynamics (QCD). DCSB entails the existence of a vacuum condensate of momentum-correlated quark-antiquark pairs. The access to the amount of quantum entanglement in such correlations brings new insight into DCSB, complementary to that brought by the traditional field-theoretic functional and lattice methods. The formalism builds on the coherent state representation of Fock-space states and can be used to compute entanglement entropies in any theory dealing with an explicit Fock-space representation of multi-particle states.

In Chapter 2 we reviewed the most basic quantum information theory concepts relevant for our purposes in the dissertation. Then, in Chapter 3, we reviewed the formalism of coherent states to compute density matrices defined in a Fock space. We applied the formalism to two toy models involving two-bosonic and two-fermionic degrees of freedom. The models neatly illustrate the way one can compute the entanglement between, e.g., momentum modes. We obtained the relevant density matrices in the coherent state representation for a variational vacuum defined through a Bogoliubov-Valatin transformation. This transformation allows to obtain the vacuum of the model Hamiltonian as a coherent state of pair-correlated particles built on the top of the vacuum of the nointeracting part of the Hamiltonian. The calculation of the corresponding entanglement measures amounted to perform Gaussian integrals. We could relate the entanglement measures to the strength of the interaction and to the energy of the respective states. We have obtained that, for both models, the entanglement increases as we increase the interaction parameter, but only for the fermionic system it saturates to a finite value. However, the energy grows faster than the entropy for both cases. The lessons learnt from these models were invaluable for the computation of density matrices and partial traces in the much more complicated QCD models.

In Chapter 4 we presented the basic phenomenology of the strong interactions that lead to the establishment of QCD. Then, in Chapter 5, we detailed the models for the QCD vacuum we used to study DCSB driven quantum entanglement: the Nambu–Jona-Lasion model (NJL) and the model defined by a Hamiltonian inspired on the Coulomb gauge QCD Hamiltonian (CGQH). For both models, we showed how the Bogoliubov-Valatin transformation leads to an explicit construction of the vacuum state as a momentum-correlated quark-antiquark condensate.

Chapter 6 presented our results for the NJL and CGQH models. We used the NJL model mainly to present the details of the implementation of the coherent state formalism discussed in Chapter 3 to a field theoretic setting. We have evaluated the n-th Rényi entropy and used the replica trick to obtain the entanglement entropy between the momentum-correlated quarks and antiquarks in a generalization of the procedure used for the simple model of two coupled fermionic oscillators. We then expressed the entanglement entropy as a function of the constituent quark mass in the chiral limit, which, in a sense, is a measure of by how much the chiral symmetry is dynamically broken. We found that the entanglement grows with the constituent quark mass. We also considered the ratio of the entanglement entropy to the energy and examined its dependence on the constituent quark mass. The minimum of that ratio leads to parameter values of the model that reproduce the physical quantities, a feature that is in line with the conjecture of extremizing entanglement criteria discussed in different contexts [11, 12, 13].

Next, we have considered the CGQH model [86], a model featuring a momentum-dependent mass function, color confinement and asymptotic freedom. We have introduced a current quark mass m_0 and studied its effect on the entanglement entropy. We found that the entanglement entropy increases with m_0. To access the entanglement induced by the interaction, we considered two Bogoliubov-Valatin transformations, one taking the noninteracting chiral vacuum to the dynamically broken vacuum, and another taking the noninteracting chiral vacuum to the nointeracting explicitly broken vacuum. Then, we computed the ratio of the entanglement entropies associated with the two vacua, with the entropies computed up to some momentum Λ. The ratio goes to unity as $\Lambda \to \infty$. By changing Λ, we could see that the interaction induced entanglement dominates in the infrared, whereas the m_0 induced entanglement dominates in the ultraviolet, features that evince the fact that interaction-induced DCSB gets less important as m_0 increases.

We also found that the explicit symmetry-breaking mass also determines whether the expression for the entanglement entropy, Eq. (6.60), diverges or not. Based on our model study, we predicted that the quark mass momentum running in QCD entails that the entanglement entropy is finite in the chiral limit and therefore scale independent. For $m_0 \neq 0$, it acquires a scale dependence determined by the ultraviolet running of the mass function. This prediction should be testable with lattice simulations. A confirmation of the prediction would be a major advancement in our understanding of DCSB in QCD.

We conclude by restating that our study was a first attempt to quantify the amount of entanglement in the quark-antiquark momentum correlations induced by DCSB in the vacuum. Although our results and conclusions were obtained within two models of the QCD vacuum, we conjecture that their qualitative features will survive further studies with more sophisticated methods. We envisage progress by considering different entanglement measures, like the concurrence [92], that can signal a critical behavior due to symmetry breaking [93].

Appendix A

Notations and Conventions

Unless stated otherwise, in this work, we are using the convention of sum over repeated indices. Also, when in Minkowski space, our metric convention is:

$$\eta = \mathrm{diag}(1, -1, -1, -1). \tag{A.1}$$

When using a representation for spinors, we choose the Dirac basis, which is the one that diagonalizes γ^0, given by:

$$\gamma^0 = \sigma^3 \otimes \mathbb{1}, \;\; \gamma^i = i\sigma^2 \otimes \sigma^i, \;\; \gamma_5 = \sigma^1 \otimes \mathbb{1}. \tag{A.2}$$

where $\mathbb{1}$ is the 2x2 identity, with σ^i being the Pauli matrices:

$$\sigma^1 = \begin{pmatrix} 0 & 1 \\ 1 & 0 \end{pmatrix}, \;\; \sigma^2 = \begin{pmatrix} 0 & -i \\ i & 0 \end{pmatrix}, \;\; \sigma^3 = \begin{pmatrix} 1 & 0 \\ 0 & -1 \end{pmatrix}. \tag{A.3}$$

Also, we are using the slashed symbol to scalar product with gamma matrices:

$$\not{a} \equiv \gamma^\mu a_\mu \tag{A.4}$$

We are denoting representations of a group by their multiplicity, so that it becomes easier to talk about multiplets. For example, the fundamental representation of $SU(3)$ will be denoted by **3**, whilst the adjoint will be **8**. When the representation is not real, the conjugate is denoted with a bar. For example, the antifundamental representation of $SU(3)$ will be $\bar{\mathbf{3}}$.

In this dissertation, we are using the natural system of units, that is, $\hbar = c = 1$.

Appendix B

Gaussian Integrals

In this appendix we derive some results for Gaussian integrations that are very recurrent during entanglement calculations in a wide variety of systems.

B.1 Bosonic Functional Integrals

We start by evaluating a Gaussian integral for real variables x_i without sources:

$$I_1 = \int Dx \, e^{-\frac{1}{2}x \cdot M \cdot x} \tag{B.1}$$

for a symmetric matrix M, with:

$$Dx \equiv \prod_{i=1}^{N} \frac{dx_i}{\sqrt{2\pi}}. \tag{B.2}$$

In order to evaluate the integral, we use that M can be diagonalized by an orthogonal transformation matrix $O^T = O^{-1}$:

$$O^T \cdot M \cdot O = D, \;\; D = \mathrm{diag}(\{\lambda_i\}), \tag{B.3}$$

with $\{\lambda_i\}$ being the eigenvalues of M. As O is orthogonal, this transformation can be performed by the change of variables $x \to O \cdot x$, which has jacobian $\mathbb{1}$, so that we obtain:

$$I_1 = \int Dx \;\exp\left\{-\frac{1}{2}\sum_i x_i \lambda_i x_i\right\} = \prod_i \int \frac{dx_i}{\sqrt{2\pi}} \exp\left\{-\frac{1}{2}\lambda_i x_i^2\right\}, \tag{B.4}$$

which is now written in terms of one-dimensional Gaussian integrals of the form:

$$\int dx \exp\left\{-\frac{1}{2}ax^2\right\} = \sqrt{\frac{2\pi}{a}}, \tag{B.5}$$

and we get that:

$$I_1 = \prod_i \lambda_i^{-\frac{1}{2}} = (\det[M])^{-\frac{1}{2}}. \tag{B.6}$$

Now we proceed for the integration with sources:

$$I_2 = \int Dx e^{-\frac{1}{2}x \cdot M \cdot x - J \cdot x} \equiv \int Dx e^{-S_2} \tag{B.7}$$

In order to solve this, we'll be doing a procedure similar to what's done in Ref. [48]. First, we seek for the critical set of variables x_c that extremizes S_2:

$$\partial_x S_2(x = x_c) = 0, \tag{B.8}$$

which results on the equation:

$$\frac{1}{2} M_{ij} \left(\delta_{ik}(x_c)_j + \delta_{jk}(x_c)_i \right) + J_k = 0, \tag{B.9}$$

with sum over repeated indices. Using that M can be taken to be a symmetric matrix (if it had an antisymmetric part, it would vanish in Eq. (B.7)), we obtain that critical coordinates are given by:

$$x_c = -M^{-1} \cdot J \tag{B.10}$$

Then, we expand S around x_c. As it's quadratic and the linear term vanishes by construction, we obtain:

$$S_2(x) = S_2(x_c) + \frac{1}{2}(x - x_c) \cdot M \cdot (x - x_c). \tag{B.11}$$

Now we perform a constant shift on the integrated coordinates $x \to x - x_c$, which has jacobian $\mathbb{1}$, so we get a constant $e^{-S_2(x_c)}$ outsite of the integral and what remains is just the case without sources (I_1). We note that:

$$S_2(x_c) = -\frac{1}{2} J \cdot M^{-1} \cdot J, \tag{B.12}$$

so we finally obtain the result:

$$I_2[J] = I_2[J = 0] \;\; e^{\frac{1}{2} J \cdot M^{-1} \cdot J}. \tag{B.13}$$

Now suppose we want to generalize it to the case where x is a set of complex variables and solve the integral:

$$\int Dx^* Dx \, e^{-x^* \cdot M \cdot x + \bar{J} \cdot x + x^* \cdot J}, \tag{B.14}$$

for some complex source vector J and the matrix M being Hermitian, and the integration measure defined as:

$$Dx^* Dx \equiv \prod_{k=1}^{N} \left(\frac{dx_k^* dx_k}{2\pi i} \right). \tag{B.15}$$

In order to perform the calculation, we rewrite x in terms of its real and imaginary components, $x = x_1 + ix_2$, as well as the vector $J = J_1 + iJ_2$. Then, we redefine the integration measure as:

$$\prod_{k=1}^{N} \left(\frac{dx_k^* dx_k}{2\pi i} \right) = \prod_{k=1}^{N} \left(\frac{dx_{1k} dx_{2k}}{2\pi} \right) \equiv Dx_1 Dx_2, \tag{B.16}$$

and note that the exponent in Eq. (B.14) can be written as:

$$- x^* \cdot M \cdot x + \bar{J} \cdot x + x^* \cdot J = -x_1 \cdot M \cdot x_1 - x_2 \cdot M \cdot x_2 + x_1 \cdot J_1 + x_2 \cdot J_2, \tag{B.17}$$

so that Eq. (B.14) can be broken into an integral of the form of Eq. (B.13) for x_1 and J_1 multiplied by another one for x_2 and J_2, so that it becomes:

$$I_3[J] = \frac{e^{J_1 \cdot M^{-1} \cdot J_1} e^{J_2 \cdot M^{-1} \cdot J_2}}{\det[M]}. \tag{B.18}$$

However, for M Hermitian, we have:

$$J_1 \cdot M^{-1} \cdot J_1 + J_2 \cdot M^{-1} \cdot J_2 = \bar{J} \cdot M^{-1} \cdot J, \tag{B.19}$$

so that, finally:

$$I_3[J] = \frac{e^{\bar{J} \cdot M^{-1} \cdot J}}{\det[M]} \tag{B.20}$$

B.2 Fermionic Functional Integrals

In fermionic calculations, we frequently integrate over Grassmanian numbers that obey the anticommutation relation:

$$z_1 z_2 = -z_2 z_1 \tag{B.21}$$

and commute with c-numbers. Next, we are going to solve the integral:

$$I_4 = \int Dz^* Dz \, e^{-z^* \cdot M \cdot z} \tag{B.22}$$

with:

$$Dz^* Dz = \prod_{i=1}^{N} dz_i^* dz_i \tag{B.23}$$

The procedure we are going to use is similar to what is done in Ref. [31]. We start by making a variation in the integral with respect to the matrix M:

$$\delta_M I_4 = -\int Dz^* Dz \, z^* \cdot \delta M \cdot z \, e^{-z^* \cdot M \cdot z}. \tag{B.24}$$

However, using the definition of the Grassmanian derivative by the left, we have the identity:

$$\frac{\partial}{\partial z^*} e^{-z^* \cdot M \cdot z} = -M \cdot z \, e^{-z^* \cdot M \cdot z}. \tag{B.25}$$

Multiplying by M^{-1} by the left, it becomes:

$$M^{-1} \cdot \frac{\partial}{\partial z^*} e^{-z^* \cdot M \cdot z} = -z \, e^{-z^* \cdot M \cdot z}, \tag{B.26}$$

then we can replace it as it appears in Eq. (B.24) to obtain:

$$\delta_M I_4 = \int Dz^* Dz \, z^* \cdot \delta M \cdot M^{-1} \cdot \frac{\partial}{\partial z^*} e^{-z^* \cdot M \cdot z}. \tag{B.27}$$

The next step is doing an integration by parts. To do that, we define the product rule by making a variation with respect to z^* and anticommuting δz^* all the way to the left, that is:

$$\begin{aligned}\delta[z_i^* F(z^*)] &= (\delta z_i^*) F(z^*) + z_i^* (\delta z_j^*) \frac{\partial}{\partial z_j^*} F(z^*) \\ &= (\delta z_j^*) \left(\delta_{ij} - z_i^* \frac{\partial}{\partial z_j^*} \right) F(z^*). \end{aligned} \tag{B.28}$$

On the other hand, as the variation is with respect to z^*, we have:

$$\delta[z_i^* F(z^*)] = (\delta z_j^*) z_i^* \frac{\partial}{\partial z_j^*} F(z^*), \tag{B.29}$$

so that, as an integral of a derivative of a Grassmanian variable vanishes, we can replace under the integration:

$$z_i^* \frac{\partial}{\partial z_j^*} F(z^*) \to \delta_{ij} F(z^*). \tag{B.30}$$

Taking the exponential that appears in $\delta_M I_4$ as our $F(z^*)$, it becomes:

$$\begin{aligned}\delta_M I_4 &= \int Dz^* Dz\ \delta_{ik} (\delta M)_{ij} (M^{-1})_{jk}\ e^{-z^* \cdot M \cdot z} \\ &= \mathrm{Tr}(\delta M \cdot M^{-1}) I_4, \end{aligned} \tag{B.31}$$

so we have the relation:

$$\frac{\delta_M I_4}{I_4} = \mathrm{Tr}(\delta M \cdot M^{-1}), \tag{B.32}$$

which, as we have $I_4(M = \mathbb{1}) = 1$ (check Eq. (3.46)), imples:

$$I_4 = \det[M]. \tag{B.33}$$

Then, we can add Grassmanian sources to I_4 and solve the integral:

$$I_5 = \int Dz^* Dz\ e^{-z^* \cdot M \cdot z - z^* \cdot \eta - \bar{\eta} \cdot z} \equiv \int Dz^* Dz\ e^{-S_5} \tag{B.34}$$

following the same steps as in the bosonic case taking care of the anticommutation rules. By defining our critical point taking derivatives by the left:

$$\frac{\partial S_5}{\partial z^*}(z^* = z_c^*) = \frac{\partial S_5}{\partial z}(z = z_c) = 0 \tag{B.35}$$

we obtain:

$$z_c = -M^{-1} \cdot \eta, \;\; z_c^* = -\bar{\eta} \cdot M^{-1}. \tag{B.36}$$

As in the bosonic case, we have:

$$S_5(z^*, z) = (z^* - z_c^*) \cdot M \cdot (z - z_c) + S_5(z_c^*, z_c), \tag{B.37}$$

with:

$$S(z_c^*, z_c) = -\bar{\eta} \cdot M^{-1} \cdot \eta \tag{B.38}$$

Taking $e^{-S_5(z_c^*, z_c)}$ out of the integral and doing a shift on the integration measure, it becomes, finally:

$$I_5[\bar{\eta}, \eta] = I_5[\bar{\eta} = 0, \eta = 0] \; e^{\bar{\eta} \cdot M^{-1} \cdot \eta}. \tag{B.39}$$

Bibliography

[1] M. V. Fedorov and N. I. Miklin, "Schmidt Modes and Entanglement," *Contemporary Physics*, vol. 55, pp. 94–109, 2014.

[2] M. A. Nielsen and I. L. Chuang, *Quantum Computation and Quantum Information*. Cambridge University Press, 2010.

[3] J. Preskill, "Quantum computing and the entanglement frontier," 3 2012.

[4] F. Arute *et al.*, "Quantum Supremacy Using a Programmable Superconducting Processor," *Nature*, pp. 505–510, 2019.

[5] R. Horodecki *et al.*, "Quantum Entanglement," *Rev. Mod. Phys.*, vol. 81, pp. 865–942, Jun 2009.

[6] C. H. Bennett *et al.*, "Teleporting an Unknown Quantum State via Dual Classical and Einstein-Podolsky-Rosen Channels," *Phys. Rev. Lett.*, vol. 70, pp. 1895–1899, Mar 1993.

[7] M. Le Bellac, *Quantum Physics*. Cambridge University Press, 2006.

[8] G. Vidal *et al.*, "Entanglement in Quantum Critical Phenomena," *Phys. Rev. Lett.*, vol. 90, p. 227902, Jun 2003.

[9] C. K. Law, "Quantum Entanglement as an Interpretation of Bosonic Character in Composite Two-Particle Systems," *Phys. Rev. A*, vol. 71, p. 034306, 2005.

[10] C. Chudzicki *et al.*, "Entanglement and Composite Bosons," *Phys. Rev. Lett.*, vol. 104, p. 070402, 2010.

[11] A. Cervera-Lierta *et al.*, "Maximal Entanglement in High Energy Physics," *SciPost Phys.*, vol. 3, no. 5, p. 036, 2017.

[12] S. R. Beane *et al.*, "Entanglement Suppression and Emergent Symmetries of Strong Interactions," *Phys. Rev. Lett.*, vol. 122, p. 102001, Mar 2019.

[13] I. Low and T. Mehen, "Symmetry from Entanglement Suppression," 4 2021.

[14] H. Fritzsch, M. Gell-Mann, and H. Leutwyler, "Advantages of the Color Octet Gluon Picture," *Phys. Lett. B*, vol. 47, pp. 365–368, 1973.

[15] T. Muta, *Foundations of Quantum Chromodynamics: An Introduction to Perturbative Methods in Gauge Theories, (3rd ed.)*, vol. 78 of *World scientific Lecture Notes in Physics*. Hackensack, N.J.: World Scientific, 3rd ed., 2010.

[16] D. J. Gross and F. Wilczek, "Ultraviolet Behavior of Nonabelian Gauge Theories," *Phys. Rev. Lett.*, vol. 30, pp. 1343–1346, 1973.

[17] H. D. Politzer, "Reliable Perturbative Results for Strong Interactions?," *Phys. Rev. Lett.*, vol. 30, pp. 1346–1349, 1973.

[18] Y. Nambu, "Axial vector current conservation in weak interactions," *Phys. Rev. Lett.*, vol. 4, pp. 380–382, 1960.

[19] Y. Nambu and G. Jona-Lasinio, "Dynamical Model of Elementary Particles Based on an Analogy with Superconductivity I," *Phys. Rev.*, vol. 122, pp. 345–358, Apr 1961.

[20] Y. Nambu and G. Jona-Lasinio, "Dynamical Model of Elementary Particles Based on an Analogy with Superconductivity II," *Phys. Rev.*, vol. 124, pp. 246–261, 1961.

[21] J. F. Annett, *Superconductivity, Superfluids and Condensates*. Oxford University Press, 2003.

[22] P. W. Anderson, "Higgs, Anderson and all that," *Nature Physics*, vol. 11, pp. 93–93, 2015.

[23] J. F. Donoghue, E. Golowich, and B. R. Holstein, *Dynamics of the standard model*, vol. 2. CUP, 2014.

[24] T. Horn and C. D. Roberts, "The pion: an enigma within the Standard Model," *J. Phys. G*, vol. 43, no. 7, p. 073001, 2016.

[25] I. Montvay and G. Munster, *Quantum fields on a lattice*. Cambridge Monographs on Mathematical Physics, Cambridge University Press, 3 1997.

[26] C. Gattringer and C. B. Lang, *Quantum chromodynamics on the lattice*, vol. 788. Berlin: Springer, 2010.

[27] R. Alkofer and L. von Smekal, "The Infrared behavior of QCD Green's functions: Confinement dynamical symmetry breaking, and hadrons as relativistic bound states," *Phys. Rept.*, vol. 353, p. 281, 2001.

[28] H. Gies, "Introduction to the functional RG and applications to gauge theo-

ries," *Lect. Notes Phys.*, vol. 852, pp. 287–348, 2012.

[29] I. C. Cloet and C. D. Roberts, "Explanation and Prediction of Observables using Continuum Strong QCD," *Prog. Part. Nucl. Phys.*, vol. 77, pp. 1–69, 2014.

[30] A. C. Aguilar, D. Binosi, and J. Papavassiliou, "The Gluon Mass Generation Mechanism: A Concise Primer," *Front. Phys.(Beijing)*, vol. 11, no. 2, p. 111203, 2016.

[31] L. S. Brown, *Quantum Field Theory*. Cambridge University Press, 1992.

[32] T. D. Lee, *Particle Physics and Introduction to Field Theory*, vol. 1 of *Contemoray Concepts in Physics*. New York, N.Y.: Harwood Academic, 1981.

[33] U. Vogl and W. Weise, "The Nambu and Jona Lasinio model: Its implications for hadrons and nuclei," *Prog. Part. Nucl. Phys.*, vol. 27, pp. 195–272, 1991.

[34] S. P. Klevansky, "The Nambu–Jona-Lasinio Model of Quantum Chromodynamics," *Rev. Mod. Phys.*, vol. 64, pp. 649–708, 1992.

[35] T. Hatsuda and T. Kunihiro, "QCD phenomenology based on a chiral effective Lagrangian," *Phys. Rept.*, vol. 247, pp. 221–367, 1994.

[36] M. Buballa, "NJL model analysis of quark matter at large density," *Phys. Rept.*, vol. 407, pp. 205–376, 2005.

[37] A. P. Szczepaniak and E. S. Swanson, "Chiral extrapolation, renormalization, and the viability of the quark model," *Phys. Rev. Lett.*, vol. 87, p. 072001, 2001.

[38] F. J. Llanes-Estrada, S. R. Cotanch, A. P. Szczepaniak, and E. S. Swanson, "Hyperfine meson splittings: Chiral symmetry versus transverse gluon exchange," *Phys. Rev. C*, vol. 70, p. 035202, 2004.

[39] P. Bicudo, J. E. Ribeiro, and J. Rodrigues, "K-N S channel I=1, 0 phase shifts as a direct measure of chiral condensation," *Phys. Rev. C*, vol. 52, pp. 2144–2157, 1995.

[40] C. E. Fontoura, G. Krein, and V. E. Vizcarra, "$\bar{D}$N interaction in a color-confining chiral quark model," *Phys. Rev. C*, vol. 87, no. 2, p. 025206, 2013.

[41] J. Bardeen, L. N. Cooper, and J. R. Schrieffer, "Microscopic theory of superconductivity," *Phys. Rev.*, vol. 106, p. 162, 1957.

[42] W. Thirring *et al.*, "Entanglement or Separability: the Choice of How to Factorize the Algebra of a Density Matrix," *The European Physical Journal D*,

pp. 181–196, 2011.

[43] K. Zyczkowski, "Rényi Extrapolation of Shannon Entropy," *Open Sys. & Information Dyn.*, pp. 297–310, 2003.

[44] A. Rényi, "On Measures of Entropy and Information," January 1961.

[45] M. Srednicki, "Entropy and Area," *Phys. Rev. Lett.*, pp. 666–669, 1993.

[46] T. Nishioka, "Entanglement Entropy: Holography and Renormalization Group," *Rev. Mod. Phys.*, vol. 90, p. 035007, 2018.

[47] T. Prokopec, M. G. Schmidt, and J. Weenink, "The Gaussian Entropy of Fermionic Systems," *Annals of Physics*, vol. 327, no. 12, pp. 3138–3169, 2012.

[48] J. Ambjørn and J. L. Petersen, *Quantum Field Theory (Lecture Notes)*. University of Copenhagen, January 1998.

[49] V. Vedral, "Entanglement in the Second Quantization Formalism," *Central European Journal of Physics*, vol. 2, pp. 289–306, 2003.

[50] J. Chadwick, "Possible Existence of a Neutron," *Nature*, vol. 129, p. 312, 1932.

[51] W. Heisenberg, "On the Structure of Atomic Nuclei," *Z. Phys.*, vol. 77, pp. 1–11, 1932.

[52] H. Yukawa, "On the Interaction of Elementary Particles. I," *Proceedings of the Physico-Mathematical Society of Japan. 3rd Series*, vol. 17, pp. 48–57, 1935.

[53] C. Lattes, "Observations on the Tracks of Slow Mesons in Photographic Emulsions," *Nature*, vol. 160, pp. 453–456, 1947.

[54] M. Gell-Mann, "The Eightfold Way: a Theory of Strong Interaction Symmetry," 1961.

[55] Y. Ne'eman, "Derivation of Strong Interactions from a Gauge Invariance," *Nucl. Phys.*, vol. 26, pp. 222–229, 1961.

[56] V. E. Barnes *et al.*, "Observation of a Hyperon with Strangeness Minus Three," *Phys. Rev. Lett.*, vol. 12, pp. 204–206, Feb 1964.

[57] M. Gell-Mann, "A Schematic Model of Baryons and Mesons," *Physics Letters*, vol. 8, no. 3, pp. 214–215, 1964.

[58] T.-P. Cheng and L.-F. Li, *Gauge Theory of Elementary Particle Physics*. Clarendon Press, 1982.

[59] C. Quigg and J. L. Rosner, "Quarkonium Level Spacings," *Physics Letters B*, vol. 71, no. 1, pp. 153–157, 1977.

[60] A. Martin, "A Fit of Upsilon and Charmonium Spectra," *Physics Letters B*, vol. 93, no. 3, pp. 338–342, 1980.

[61] X.-t. Song and H.-f. Lin, "A New Potential Model for Heavy Quarkonium," *Z. Phys. C*, vol. 34, p. 223, 1987.

[62] O. W. Greenberg, "Spin and Unitary Spin Independence in a Paraquark Model of Baryons and Mesons," *Phys. Rev. Lett.*, vol. 13, pp. 598–602, 1964.

[63] H. Nastase, *Introduction to Quantum Field Theory*. Cambridge University Press, 2020.

[64] P. Zyla *et al.*, "Review of Particle Physics," *PTEP*, vol. 2020, no. 8, p. 083C01, 2020.

[65] G. Krein, A. W. Thomas, and K. Tsushima, "Nuclear-bound quarkonia and heavy-flavor hadrons," *Prog. Part. Nucl. Phys.*, vol. 100, pp. 161–210, 2018.

[66] J. Collins, *Foundations of perturbative QCD*, vol. 32. Cambridge University Press, 11 2013.

[67] T. Appelquist and J. Carazzone, "Infrared singularities and massive fields," *Phys. Rev. D*, vol. 11, pp. 2856–2861, May 1975.

[68] G. 't Hooft, "Symmetry Breaking through Bell-Jackiw Anomalies," *Phys. Rev. Lett.*, vol. 37, pp. 8–11, Jul 1976.

[69] L. Reinders, H. Rubinstein, and S. Yazaki, "Hadron Properties from QCD Sum Rules," *Physics Reports*, vol. 127, no. 1, pp. 1–97, 1985.

[70] V. Bernard, "Remarks on Dynamical Breaking of Chiral Symmetry and Pion Properties in the Nambu and Jona-Lasinio Model," *Phys. Rev. D*, vol. 34, pp. 1601–1605, Sep 1986.

[71] J. R. Finger and J. E. Mandula, "Quark Pair Condensation and Chiral Symmetry Breaking in QCD," *Nucl. Phys. B*, vol. 199, p. 168, 1982.

[72] A. Amer, A. Le Yaouanc, L. Oliver, O. Pene, and J. c. Raynal, "INSTABILITY OF THE CHIRAL INVARIANT VACUUM FOR A CONFINING POTENTIAL," *Phys. Rev. Lett.*, vol. 50, pp. 87–90, 1983.

[73] A. Le Yaouanc, L. Oliver, O. Pene, and J. C. Raynal, "Chiral Noninvariant

Solutions of the Gap Equation for a Confining Potential," *Phys. Lett. B*, vol. 134, p. 249, 1984.

[74] A. Le Yaouanc, L. Oliver, O. Pene, and J. C. Raynal, "Spontaneous Breaking of Chiral Symmetry for Confining Potentials," *Phys. Rev. D*, vol. 29, pp. 1233–1257, 1984.

[75] A. Le Yaouanc, L. Oliver, S. Ono, O. Pene, and J. C. Raynal, "A Quark Model of Light Mesons with Dynamically Broken Chiral Symmetry," *Phys. Rev. D*, vol. 31, pp. 137–159, 1985.

[76] S. L. Adler and A. C. Davis, "Chiral Symmetry Breaking in Coulomb Gauge QCD," *Nucl. Phys. B*, vol. 244, p. 469, 1984.

[77] A. Kocic, "Chiral Symmetry Restoration at Finite Densities in Coulomb Gauge QCD," *Phys. Rev. D*, vol. 33, p. 1785, 1986.

[78] P. J. d. A. Bicudo and J. E. F. T. Ribeiro, "Current Quark Model in a p Wave Triplet Condensed Vacuum. 1. The Dynamical Breaking of Chiral Symmetry," *Phys. Rev. D*, vol. 42, pp. 1611–1624, 1990.

[79] H. Mishra and S. P. Misra, "Chiral symmetry breaking and pion wave function," *Phys. Rev. D*, vol. 48, pp. 5376–5381, 1993.

[80] A. Mishra, H. Mishra, V. Sheel, S. P. Misra, and P. K. Panda, "Vacuum structure in QCD with quark and gluon condensates," *Int. J. Mod. Phys. E*, vol. 5, pp. 93–106, 1996.

[81] F. J. Llanes-Estrada and S. R. Cotanch, "Meson structure in a relativistic many body approach," *Phys. Rev. Lett.*, vol. 84, pp. 1102–1105, 2000.

[82] P. J. A. Bicudo, G. Krein, and J. E. F. T. Ribeiro, "Chiral corrections to baryon properties with composite pions," *Phys. Rev. C*, vol. 64, p. 025202, 2001.

[83] F. J. Llanes-Estrada and S. R. Cotanch, "Relativistic many body Hamiltonian approach to mesons," *Nucl. Phys. A*, vol. 697, pp. 303–337, 2002.

[84] N. Ligterink and E. S. Swanson, "A Coulomb gauge model of mesons," *Phys. Rev. C*, vol. 69, p. 025204, 2004.

[85] R. F. Wagenbrunn and L. Y. Glozman, "Chiral symmetry patterns of excited mesons with the Coulomb-like linear confinement," *Phys. Rev. D*, vol. 75, p. 036007, 2007.

[86] C. E. Fontoura, G. Krein, and V. E. Vizcarra, "$\bar{D}N$ Interaction in a Color-Confining Chiral Quark Model," *Phys. Rev. C*, vol. 87, p. 025206, Feb 2013.

[87] F. J. Llanes-Estrada and S. R. Cotanch, "Relativistic Many-Body Hamiltonian Approach to Mesons," *Nuclear Physics A*, vol. 697, no. 1, pp. 303–337, 2002.

[88] P. Guo *et al.*, "Gluelump Spectrum from Coulomb Gauge QCD," *Phys. Rev. D*, vol. 77, p. 056005, Mar 2008.

[89] P. Guo *et al.*, "Heavy Quarkonium Hybrids from Coulomb Gauge QCD," *Phys. Rev. D*, vol. 78, p. 056003, Sep 2008.

[90] F. J. Llanes-Estrada, S. R. Cotanch, A. P. Szczepaniak, and E. S. Swanson, "Hyperfine Meson Splittings: Chiral Symmetry Versus Transverse Gluon Exchange," *Phys. Rev. C*, vol. 70, p. 035202, Sep 2004.

[91] A. G. Williams, G. Krein, and C. D. Roberts, "Quark Propagator in an Ansatz Approach to QCD," *Annals Phys.*, vol. 210, pp. 464–485, 1991.

[92] W. K. Wootters, "Entanglement of formation of an arbitrary state of two qubits," *Phys. Rev. Lett.*, vol. 80, pp. 2245–2248, Mar 1998.

[93] L.-A. Wu, M. S. Sarandy, and D. A. Lidar, "Quantum phase transitions and bipartite entanglement," *Phys. Rev. Lett.*, vol. 93, p. 250404, Dec 2004.